Università degli Studi di Palermo
AREA QUALITÀ, PROGRAMMAZIONE E SUPPORTO STRATEGICO
SETTORE STRATEGIA PER LA RICERCA
U. O. DOTTORATI

University of Palermo

Department of Health Promotion, Maternal and Child, Internal Medicine, and Specialist Excellence "G. D'Alessandro" (PROMISE)

Doctoral Program in Molecular and Clinical Medicine

# HLA-E-restricted SARS-CoV-2 epitopes drive CD8$^+$ T cell memory in convalescent and vaccinated individuals: implications for the design of next-generation vaccines and Immunotherapeutics

Doctoral Dissertation of:
**MAHSA RAFIEIYAN**

The Chair of the Doctoral Program:
**PROF. ANTONINO TUTTOLOMONDO**

Supervisor:
**PROF. NADIA CACCAMO**

Cycle XXXVIII
2025/2026

# Abstract

Human leukocyte antigen-E (HLA-E) is a non-polymorphic, non-classical HLA class I molecule that presents signal peptides from classical HLA class Ia molecules to natural killer (NK) cell receptors. Emerging evidence suggests that HLA-E also presents viral peptides to $CD8^+$ T cells, potentially influencing the control of viral infections. However, $CD8^+$ T cell responses to viral epitopes presented by HLA-E remain largely unexplored. This study investigates the potential of SARS-CoV-2-derived peptides presented by HLA-E to elicit $CD8^+$ T cell responses and to identify T cell-mediated immunity in SARS-CoV-2 infection. We describe seven peptides from SARS-CoV-2 that display substantial conservation among the predominant strains from December 2021 to February 2025. These peptides fit within the HLA-E pocket and elicit HLA-E-restricted $CD8^+$ T cell responses by producing cytokines. HLA-E/SARS-CoV-2-restricted $CD8^+$ T cells were identified in the blood of convalescent patients, predominantly expressing TNF-α, with lower levels of IFN-γ and IL-2, in response to predicted immunogenic epitopes. These cytokines were detected at higher frequencies in convalescent patients but were nearly absent in hospitalized patients with severe COVID-19. HLA-E/SARS-CoV-2-restricted $CD8^+$ T cells were induced after BNT162b2 mRNA vaccination, with their frequencies increasing with more vaccine doses. Furthermore, they were significantly elicited in vaccinated individuals after SARS-CoV-2 infection. Conserved immunogenic peptides from SARS-CoV-2 can activate HLA-E-restricted T cells, suggesting their potential as universal targets for enhancing T cell-mediated immunity in controlling infection.

# Acknowledgement

At the end of this thesis, I am compelled to dedicate a few lines to the people who have accompanied me throughout this educational, scientific, professional, and, above all, human journey.

This thesis would not have been possible without the support, patience, experience, and expertise of many people.

I would like to first thank my supervisors, Professor Nadia Caccamo and Professor Francesco Dieli, for giving me the opportunity to passionately explore the world of research, guiding me through every stage of this project, and helping me complete this thesis.

Special thanks are also extended to Dr. Marco La Manna and Dr. Davide Badami for their dedication and expertise throughout this process. I would also like to sincerely thank all my colleagues and the technical and administrative staff of the CLADIBIOR Unit at the Paolo Giaccone University Hospital.

My sincere thanks go to the coordinator of the PhD program in Molecular and Clinical Medicine, Professor Antonino Tuttolomondo, and Professor Domenico Di Raimondo.

I would like to thank my beloved husband, dearest parents, most precious sister, and sweetest friends for their continuous support.

# Table of Contents

## List of Figures



## List of Tables

# Abbreviations

| | |
|---|---|
| AIDS | Acquired Immunodeficiency Syndrome |
| ALF | Acute Liver Failure |
| ANN | Artificial neural network |
| APC | Antigen-Presenting Cell |
| BCG | Bacillus Calmette–Guérin (TB vaccine) |
| BNT162b2 | Pfizer/BioNTech mRNA COVID-19 vaccine |
| CHB | Chronic Hepatitis B |
| CMV | Cytomegalovirus |
| COVID-19 | Coronavirus Disease 2019 |
| DMSO | Dimethyl sulfoxide |
| DPBS | Dulbecco's Phosphate-Buffered Saline |
| EBV | Epstein–Barr Virus |
| FBS | Fetal bovine serum |
| HBV | Hepatitis B Virus |
| HBV-ALF | HBV-associated Acute Liver Failure |
| HCC | Hepatocellular Carcinoma |
| HCMV | Human Cytomegalovirus |
| HCV | Hepatitis C Virus |
| HIV | Human Immunodeficiency Virus |
| HIV-1 | Human Immunodeficiency Virus Type 1 |
| HLA | Human Leukocyte Antigen |
| HLA-E | Non-classical HLA class Ib molecule |
| HLA-Ia | Classical HLA class I molecules (e.g., HLA-A, -B, -C) |
| ICS | Intracellular cytokine staining |
| IEDB | Immune Epitope Database |
| IFN-γ | Interferon- gamma |
| IL | Interleukin |
| JN.1 | a subvariant of the Omicron variant |
| LIR-1 | Leukocyte Immunoglobulin-like Receptor 1 |
| mAb(s) | Monoclonal antibody(ies) |
| MFI | Mean fluorescence intensity |
| MHC | Major Histocompatibility Complex |
| MT020880 | Reference GenBank accession for SARS-CoV-2 strain |
| NCBI | National Center for Biotechnology Information |
| NHP | Non-Human Primate |
| NK | Natural Killer |
| ORF | Open reading frame |
| ORF1ab | Polyprotein-encoding SARS-CoV-2 ORF |
| PBMC | Peripheral Blood Mononuclear Cells |
| PBS | Phosphate-buffered saline |
| PD-1 | Programmed Death-1 |
| PepTivator | Commercial SARS-CoV-2 peptide pool (Miltenyi Biotec) |
| PRC | Pentameric Receptor Complex |
| RBM/RBD | Receptor-binding motif/domain (Spike) |
| RhCMV | Rhesus cytomegalovirus |
| RMA-S | TAP-deficient murine lymphoma cell line |
| SARS-CoV-2 | Severe Acute Respiratory Syndrome Coronavirus 2 |
| SB/WB | Strong binder / Weak binder (peptide affinity classes) |
| SIV | Simian Immunodeficiency Virus |
| Spike (S) | SARS-CoV-2 spike glycoprotein |
| TAP | Transporter Associated with Antigen Processing |
| TB | Tuberculosis |
| TCR | T Cell Receptor |
| TGF | Transforming Growth Factor |
| TLR | Toll-like Receptor |
| TNF-α | Tumor Necrosis Factor-alpha |
| VL9 | Canonical HLA-I leader nonamer (VMAPRTLVL) |

# Chapter 1. Background

## 1.1 Introduction

T cell receptors (TCRs) expressed by $CD8^+$ T lymphocytes recognize specific endogenous peptides presented by major histocompatibility complex (MHC)-class I molecules on the cell surface. The specificity of the interaction between the MHC-class I and TCRs has been exploited in immunotherapeutic applications, particularly in the development of innovative vaccines. However, TCR-based biologics targeting infectious antigens encounter limitations in clinical applications due to the diverse MHC-class Ia. Classical MHC class-Ia molecules (in humans, Human Leukocyte Antigen-la) can bind and present a vast array of peptides to T cells and activate them, yet they exhibit substantial genetic variation [1–3]. In fact, HLA molecules display remarkable polymorphism, with 28,409 classical HLA-class I (HLA class Ia) alleles identified as of January 15, 2025 [4–8].

In contrast, non-classical HLA class Ib molecules like HLA-E exhibit limited polymorphism and are relatively more conserved [9]. The HLA-E molecule is represented by only two functional alleles, HLA-E*01:03 and HLA-E*01:01. These alleles are translated into proteins that differ by a single amino acid at position 107, where HLA-E*01:03 has glycine (Gly) and HLA-E*01:01 has arginine (Arg); this difference is located outside the peptide-binding groove [4,5,10]. This indicates that both alleles have a similar range of peptide-binding capabilities, although cell surface stability and peptide affinity slightly differ [11]. The conventional function of HLA-E in regulating the innate immune response has been indicated by substantial research [12]. The primary function of HLA-E is to present a highly conserved nonameric signal peptide, VMAPRTLVL (VL9-peptides), which is derived from the leader sequence of classical HLA-class Ia molecules such as HLA-A, -B, -C, and -G. This presentation inhibits natural killer (NK) cells by interacting with the inhibitory receptor NKG2A-CD94 [13,14].

A growing body of research has recently demonstrated that various pathogen-derived peptides presented by HLA-E molecules can evoke HLA-E-restricted cytotoxic T-cell responses and directly kill the infected cells [15]. For example, in *Mycobacterium tuberculosi*s (*M. tuberculosis*) infection, HLA-E is an essential mediator for activating $CD8^+$ T cells by presenting multiple mycobacterial peptides to the TCR of these cells [16,17]. Furthermore, a series of studies have shown that in cytomegalovirus (CMV)-seropositive individuals, a proportion of $CD8^+$ T cells are HLA-E restricted [18–21]. Another study suggested that $CD8^+$

T cells can recognize HIV-Gag peptides bound to HLA-E and suppress the replication of HIV-1 *in vitro* [22].

During infection with severe acute respiratory syndrome coronavirus 2 (SARS-CoV-2), the SP1 peptide derived from Spike stabilizes the expression of HLA-E on lung epithelial cells [23]. In severe to moderate COVID-19 patients, HLA-E is upregulated in the lung epithelium [24]. Hammer et al. showed that a SARS-CoV-2 peptide derived from the non-structural protein (Nsp) 13 can be presented by human HLA-E, leading to the activation of NK cells that express NKG2A in individuals with COVID-19, and the effective restriction of SARS-CoV-2 replication in infected lung epithelial cells *in vitro* [25]. Genetic variations in the NKG2C/HLA-E axis also affect the severity of SARS-CoV-2 infections [26]. A significant study into HLA-E–restricted $CD8^+$ T cell responses in individuals recovering from SARS-CoV-2 infection identified five viral peptides capable of eliciting $CD8^+$ T cell responses restricted by HLA-E [27].

Besides understanding peptide binding and loading mechanisms, it is essential to comprehend and clarify the specifics of TCR recognition of HLA-E/peptide complexes and the resulting $CD8^+$ T cell responses. Thus, recent enhancements in predictive peptide-binding motifs from pathogens and tumors have verified that hydrophobic amino acids at positions 9 and 2 serve as essential anchors for the peptide-binding groove of HLA-E [28–30]. This review highlights the current limited understanding of T cell recognition of HLA-E-presented peptides across various infections and explores how advancing this knowledge could inform the development of future HLA-E-based vaccines and immunotherapies targeting microbial pathogens.

## 1.2 HLA-E in immune evasion and activation

HLA-E was initially identified as a ligand for the CD94/NKG2A or CD94/NKG2C heterodimeric co-receptor complexes, which are expressed on NK cells [12]. These co-receptors recognize HLA-E/VL9-peptide complexes to either inhibit or activate the cytolytic activity of NK cells. CD94/NKG2A is present on around 50% of NK cells and 5% of $CD8^+$ T cells in the peripheral blood of healthy humans, whereas CD94/NKG2C is expressed less frequently on these cells [13]. Notably, the CD94/NKG2A receptor exhibits a higher binding affinity for HLA-E/VL9-peptide complexes compared to CD94/NKG2C, although both receptors recognize the HLA-E/VL9-peptide through a similar structural motif [31,32]. Some viruses have evolved the ability to manipulate HLA surface expression, such as by upregulating

HLA-E, thereby inhibiting the activity of NK cells and escaping immune surveillance. For example, human CMV (HCMV) evades immune response through various proteins. US2 and US11 promote the degradation of HLA class I to prevent the presentation of viral epitopes to $CD8^+$ T cells. US6 disrupts TAP function, blocking peptide transport to HLA-class I, while US3 interferes with tapasin, preventing peptide stabilization in the HLA binding groove. UL94 disrupts the cGAS-MITA-mediated antiviral response, promoting viral replication and decreasing IFN-γ production. UL23 enhances viral resistance to T cell-mediated cytotoxicity by modulating IFN-γ secretion and upregulating programmed death-ligand 1 (PD-L1), ultimately facilitating HCMV's immune evasion and replication. Another important protein associated with HCMV is UL40, which plays an essential role in immune evasion by increasing the HLA-E surface expression independently of TAP; consequently, HLA-E interacts with CD94/NKG2A and effectively prevents NK cell-mediated destruction of infected cells [32–36]. On the contrary, during CMV infection, a subset of NK cells characterized by low CD56 and high NKG2C expression ($CD56^{dim}NKG2C^{bright}$) expands in approximately 50% of individuals and remains stable during the latent infection. This subset can effectively control the virus due to its enhanced cytotoxic activity. $CD56^{dim}NKG2C^{bright}$ NK cells may also express CD57, which indicates maturation and potentially creates an innate 'memory' state for persistent infections such as HCMV [33,37,38].

Over the past two decades, an increasing number of studies have reported the presence of pathogen-specific HLA-E-restricted $CD8^+$ T cells in response to intracellular infections, including several bacterial and viral infections (Figure 1). However, while these analyses highlight the vital role of these $CD8^+$ T cells in host defense, they have not yet characterized these cells in detail [19,39,40].

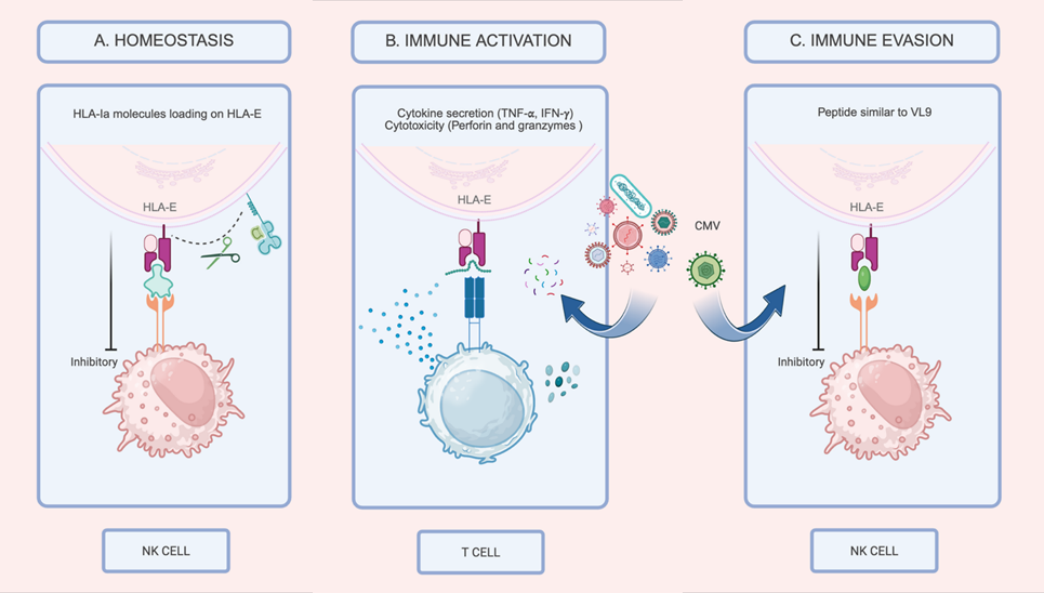


**Figure 1. HLA-E in Immunity: Activation, Homeostasis, and Evasion.**

(A) Homeostasis (NK cell). In the absence of infection, HLA-E predominantly presents peptides derived from the leader sequence of classical HLA-Ia molecules. Engagement of HLA-E by the inhibitory CD94/NKG2A receptor on NK cells transmits an inhibitory signal that restrains NK-cell cytotoxicity and maintains self-tolerance. (B) Immune activation (T cell). During infection, HLA-E can present pathogen-derived peptides to HLA-E–restricted $CD8^+$ T cells. TCR recognition triggers effector functions, including IFN-γ/TNF-α secretion and perforin/granzyme-mediated cytotoxicity. The magnitude of the response depends on factors such as peptide abundance and HLA-E/peptide stability/affinity. (C) Immune evasion (NK cell). Viruses such as CMV provide HLA-E–binding peptides that mimic the HLA-Ia leader sequence (e.g., VL9-like motifs). These identical-structure epitopes are recognized by CD94/NKG2A, reinforcing inhibitory signaling and thereby protecting infected cells from NK-cell–mediated lysis. Figure created with BioRender.com.

## 1.3 HLA-E in viral infection

Viruses reside within host cells because they depend on human hosts to survive. Their proteins are processed and presented by HLA class I molecules, including the non-classical HLA class Ib, to $CD8^+$ cytotoxic T lymphocytes (CTLs), which recognize HLA class I/peptide complexes via the TCR to mediate antiviral responses. HLA-E–restricted T cell responses have been reported in several viral infections, such as cytomegalovirus (CMV), SARS-CoV-2, hepatitis B virus (HBV), and human immunodeficiency virus type 1 (HIV-1). However, the phenotypic and functional characteristics of these HLA-E–restricted T cells have not been thoroughly studied.

### *1.3.1 HLA-E and CMV*

CMV is a double-stranded DNA virus classified within the herpesvirus family that can infect multiple cell types, such as endothelial, epithelial, and immune cells, and causes mononucleosis

and pneumonia associated with CMV [41]. During infection, CMV downregulates HLA-class Ia expression to evade detection by the immune system. The reduced expression of HLA-class Ia molecules results in fewer HLA-class Ia leader sequences available for interaction with HLA-E, thereby increasing NK cell-mediated lysis. To evade immune detection, the CMV-derived UL40 peptide (VMAPRTLIL), which closely resembles leader sequence peptides from classical HLA class Ia molecules, binds to HLA-E. This interaction stabilizes HLA-E expression on the surface of infected cells and presents it to NK cells via interaction with NKG2A/CD94 to prevent lysis [32]; consequently, this results in evasion from NK cells.

Beyond NK cell regulation, this mechanism also impacts HLA-E-restricted $CD8^+$ T cell responses to CMV peptides [42–44]. In fact, peptides derived from the leader sequences of HLA-class Ia molecules exhibit strong binding affinity to HLA-E; hence, any other CMV peptides with sequence homology to the leader sequences of HLA-class Ia molecules, are unlikely to activate HLA-E-restricted $CD8^+$ T cells since these peptides will be identified as "self," thus preventing initiation of a $CD8^+$ T cell response to the CMV UL40 peptide. However, those individuals with HLA-class Ia molecules that possess leader sequences differing from the CMV UL40 peptides generate a strong $CD8^+$ T cell response.

CMV infection can elicit a robust $CD8^+$ T cell response that is specific to the UL40-derived peptide VMAPRTLIL and restricted by HLA-E, particularly in individuals lacking HLA-C alleles with identical leader sequences. In individuals who develop a T cell response against UL40, a specific TCR type (TRBV14) has been found to recognize the HLA-E/VMAPRTLIL peptide complex [43,44]. Structural analysis of the TRBV14 TCR (KK50.4) bound to HLA-E/VMAPRTLIL has revealed both similarities to classical HLA class I recognition and unique features specific to the HLA-E/TCR interaction. The CDR2 loop played a predominant role in the interaction between HLA-E and the TCR. In particular, the TCR made direct contact with *Ile* (Isoleucine) at position 8 of the peptide, which was the only difference from self-peptides [19,45]. A recent study has highlighted an unconventional subset of HLA-E-restricted $CD8^+$ T cells, in addition to the classical HLA-class I-restricted $CD8^+$ T cell responses towards pp65 and IE1, which represent up to 38% of circulating $CD8^+$ T cells in human (H)-CMV-infected hosts. In the study investigating CMV-host interactions during congenital infection, profiling of CMV-derived HLA-E-binding peptides suggested that a mismatch between the $UL40_{15-23}$ peptide and the HLA-class I peptides of mothers and their children may contribute to congenital CMV disease [46]. In research on adaptive NK cells, three unconventional HLA-E-

restricted 15-mer peptides derived from the HCMV pp65 protein were discovered, eliciting NK cell memory responses specific to HCMV [47].

Recent molecular studies suggest that the inhibition of the transporter associated with antigen presentation (TAP) may be critical for the presentation of non-canonical peptides by HLA-E during CMV infection [45]. Although TAP is involved in peptide loading onto classical HLA class I molecules, its blockade does not affect HLA-E surface expression, indicating a potentially distinct pathway. Notably, TAP inhibition appears to play a key role in initiating HLA-E–restricted $CD8^+$ T cell responses in CMV, though the underlying mechanisms remain poorly understood and require further investigation [48].

A vaccine utilizing a modified strain of rhesus CMV (RhCMV68-1) prompted $CD8^+$ T cells to react to antigens presented by MHC-E. The primary distinction between this vaccine strain and the wild-type RhCMV is that it lacks specific genes (Rh157.4, Rh157.5, Rh158, and Rh161) that influence a pentameric receptor complex (PRC). CMV utilizes the PRC to infect non-fibroblast cells, and when these genes were deleted, the $CD8^+$ T cell responses became restricted to MHC-E. However, the exact mechanisms behind the generation of MHC-E-restricted $CD8^+$ T cell responses remain unknown, particularly regarding how the deleted genes and the PRC affect whether T cell responses to either MHC-class Ia or MHC-E [49].

### *1.3.2 HLA-E and SARS-CoV-2*

SARS-CoV-2 is a single positive-stranded, enveloped RNA virus [50] that causes a systemic disease capable of spreading beyond the lungs through blood-based dissemination, affecting multiple organs and leading to fever, upper respiratory symptoms, and potentially multiple organ failure [51]. SARS-CoV-2 infections, which can present with a clinical spectrum ranging from asymptomatic cases to severe illness and fatalities, have led to the global COVID-19 pandemic since December 2019 [52].

Effective vaccines that protect against symptomatic COVID-19 and target the Spike protein have been developed [53,54]. These vaccines focus on antiviral antibody responses [55,56], but the instability of viral genomes could have contributed to the development of variants that led to the escape of the humoral immune response [57]. Meanwhile, T cells appear to play a crucial role in the immune response to COVID-19. Since the start of the pandemic, data has revealed a combination of immune evasion and higher transmissibility in several variants of SARS-CoV-2, including the Alpha (B.1.1.7), Delta (B.1.617.2), and Omicron (B.1.1.529) strains [58–61]. The continuous emergence of mutated variants and their capacity to evade

immune defenses has raised a significant threat to public health and the global economy. A study on SARS-CoV-2 Nsp1 indicates that the downregulation of ligands for the activating NK cell receptor NKG2D (NKG2D-L) facilitates immune evasion. While NK cells are capable of efficiently detecting and eliminating infected cells during early stages of infection, their cytotoxic activity diminishes as viral protein expression increases [62].

Public health records and clinical reports indicate that the susceptibility and severity of SARS-CoV-2 rely on several risk factors, including variations across regions, countries, age, sex, [63] and host genetic background, mainly linked to the high genetic polymorphisms of HLA-class I and II molecules [64]. Host genetic variation significantly influences clinical outcomes following SARS-CoV-2 infection, such as requiring critical care or hospitalization [65–67]. Several HLA-class II alleles, including HLA-DRB1*04, HLA-DRB1*08:02, and HLA-DRB1*09:01, have been associated with the disease severity, suggesting that HLA-class II molecules play a role in modulating the immune response [68–71]. Additionally, HLA-class I alleles, such as HLA-C*04:01, may also influence clinical outcomes and epidemic patterns of SARS-CoV-2, with some alleles linked to severe cases [72].

The immunological mechanisms associated with SARS-CoV-2 infection are not entirely clear. In patients with severe COVID-19, NK cells undergo extensive phenotypic and functional changes. For example, NK cells from critically ill COVID-19 patients are highly activated yet exhausted, exhibiting poor cytotoxic function and cytokine production upon stimulation [73]. Recent studies suggest that HLA-class Ib molecules, including HLA-E, may be involved in SARS-CoV-2 infection. In 2020, a survey of peripheral blood NK cells revealed that NK cells are influenced by the expression of the SARS-CoV-2 Spike 1 protein in lung epithelial cells through the HLA-E/NKG2A interaction, subsequently leading to reduced NK cell degranulation and potential exhaustion. The exhaustion of NK cells, involving the GATA3 transcription factor, may play a role in the immunopathogenesis observed in SARS-CoV-2 infections [74]. Hammer demonstrated that the SARS-CoV-2 Nsp13 contains an HLA-E-restricted peptide ($Nsp13_{232-240}$) that, unlike normal self-peptides, prevents binding to the inhibitory receptor NKG2A. Activated $NKG2A^+$ NK cells, triggered by missing self-recognition, exhibit significant activity in COVID-19 patients, effectively restricting SARS-CoV-2 replication in infected lung epithelial cells *in vitro*. This suggests that the viral peptide interferes with the suppression of $NKG2A^+$ NK cells, leading to enhanced immune detection and response. [75].

A significant study on HLA-E-restricted $CD8^+$ T cell responses in convalescent patients with COVID-19 disease identified five peptides from SARS-CoV-2 that elicit HLA-E-restricted $CD8^+$ T cell responses at similar frequencies as classical HLA-class Ia-restricted $CD8^+$ T cells. Notably, the generated HLA-E–restricted peptide-specific T cell clones, with diverse TCRs, demonstrated the ability to suppress SARS-CoV-2 replication in Calu-3 human lung epithelial cells. In contrast, the downregulation of classical HLA class I molecules occurs upon infection in Calu-3 cells. Therefore, HLA-E-restricted T cell responses may play a role in controlling infection and could be used as a promising vaccine targeting universally presented epitopes [76].

### *1.3.3 HLA-E and HBV*

HBV, a double-stranded DNA virus and a member of the Hepadnaviridae family, is highly contagious through infected blood or body fluids. HBV infection can trigger immune-mediated liver diseases and lead to chronic liver conditions, such as chronic hepatitis, cirrhosis, and hepatocellular carcinoma [77]. According to the WHO, nearly one-third of the global population has been infected with HBV at some stage in their lives. Most infections acquired in infancy or early childhood become chronic hepatitis B (CHB) [78], affecting more than 300 million individuals worldwide in different ways, including complications from persistent infection, liver cirrhosis, and hepatocellular carcinoma (HCC), with around 820,000 annual mortalities [79,80].

Experimental evidence shows that in acute symptomatic hepatitis B, the infection is controlled by HBV-specific $CD4^+$ and $CD8^+$ T cell responses, as well as neutralizing antibodies. HBV-specific $CD8^+$ T cells directly destroy infected hepatocytes and produce cytokines, such as IFN-γ, to eliminate the virus and recruit other immune cells. The memory T cell response has been detectable for decades. In contrast, in chronic patients, the frequency of HBV-specific $CD8^+$ T cells is considerably reduced, and chronic liver inflammation suppresses the ability of HBV-specific T cells to access the infected liver parenchyma [81,82]. Various intrahepatic inhibitory mechanisms help limit liver damage but also reduce T cell function. Specifically, HBV-specific T cells are severely dysfunctional due to several inhibitory mechanisms in the chronically inflamed liver. As a tolerogenic organ, the liver and its non-parenchymal cells contribute to this dysfunction by promoting T cell tolerance rather than activation [83]. Various strategies, such as immune checkpoint receptor inhibitors, Toll-like receptor (TLR) agonists, and therapeutic vaccines, are being pursued to reinvigorate HBV-reactive T cells [84].

Furthermore, T-cell responses are affected by genetic variation in HLA-class I profile and different HBV subtypes across populations. Each viral epitope, from nucleocapsid, envelope, polymerase, and X proteins, can elicit T cell responses differently and vary significantly between individuals and ethnic groups. In individuals with closely related HLA-A2 subtypes, the dominance of various epitopes varied significantly, and even slight variations in HLA-class I molecules can greatly impact the T cell response to HBV [85]. Consequently, the identified universal epitopes that can be presented with HLA-E are crucial for developing effective vaccines that can elicit robust and broad T cell responses capable of combating HBV and preventing the emergence of escape variants. In a recent study, Murugesan et al. identified HLA-E-restricted $CD8^+$ T cells targeting HBV $Env_{371-379}$ (L6I) peptide in the peripheral blood mononuclear cells (PBMC) of individuals with chronic HBV, as well as in HBV-naive subjects, after they were expanded *in vitro* using L6I peptide/HLA-E complexes. This is the first HBV peptide identified as an HLA-E epitope through bioinformatic predictions and verified by biochemical and cellular assays [86]. A study using data from the Gene Expression Omnibus database, including patients with acute liver failure (ALF) caused by HBV infection and healthy controls, indicated that HLA-E is one of the candidate genes associated with the progression of HBV-ALF. HLA-E may influence disease outcomes by regulating NK cell activity [87]. Another study highlights the significant role of HLA-class Ib molecules in determining the outcome of HBV infections by examining genetic polymorphisms in HLA-E and measuring soluble HLA-E levels in 200 patients with chronic HBV infection and 100 individuals who had resolved the infection spontaneously. They found that individuals with an allele in the HLA-G and HLA-E genes had a higher chance of spontaneously clearing the HBV. HBV persistence is associated with elevated levels of soluble HLA-E, highlighting the molecule's potential as a biomarker for disease progression [88].

### *1.3.4. HLA-E and HIV*

HIV is a lentivirus with single-stranded RNA (ssRNA) that belongs to the Retroviridae family. HIV-1 infects humans and causes acquired immunodeficiency syndrome (AIDS), which continues to be a global health burden, with an estimated 1.3 million infections and over 600,000 AIDS-related deaths annually [89,90].

$CD8^+$ T cells are essential for controlling HIV-1 infection by recognizing viral peptides presented by HLA class I molecules, exhibiting a wide range of inhibitory capacity against the virus among individuals [91]. HIV-1 utilizes its Nef protein to selectively downregulate the

expression of HLA-A, -B, and -C molecules on infected cells by modulating intracellular trafficking pathways, thereby promoting the endocytosis and degradation of these molecules [92]. Interestingly, HLA-E is typically spared from this process. This selective modulation impairs the ability of $CD8^+$ T cells to recognize and attack the infected cells and minimizes the activation of NK cells, which are inhibited by HLA-E. La Manna et al. found that HLA-E-restricted $CD8^+$ T cells, which can recognize and respond to *M. tuberculosis*, might provide a protective immune response even in the presence of HIV-1. They showed that in infected patients, the presence of both pathogens led to a decrease in HLA-A2 expression on macrophages, resulting in reduced effectiveness of HLA-A2-restricted $CD8^+$ T cells in killing infected cells and controlling the growth of intracellular *M. tuberculosis*. In contrast, the expression of HLA-E and the activity of HLA-E-restricted $CD8^+$ T cells were not negatively affected by HIV-1 [16]. HLA-class I-associated HIV-1 amino acid polymorphisms lead to immune escape from HLA-class I-restricted $CD8^+$ T cells, either through loss of peptide recognition or through mutations that maintain peptide recognition but result in ineffective T cell responses and dysfunctional T cell phenotypes [93,94]. These mechanisms enable HIV-1 to evade the immune pressure exerted by HLA-class I-restricted $CD8^+$ T cells, a phenomenon referred to as "*viral adaptation*" [95]. Consequently, despite over four decades of research, developing a vaccine for HIV-1 has been challenging due to genetic diversity and the evasion of detection and clearance by the immune system of the host [94,96].

Furthermore, clinical applications are limited because of the high diversity of HLA-class I. One promising approach is to focus on antigen presentation by the nonpolymorphic HLA-E molecule. However, HLA-E-restricted T cells specific to HIV-1 have not been detected in infected individuals. Experiments on virus inhibition demonstrated that TCR mediated the interaction between the RL9 peptide and HLA-E, and that cells infected with HIV-1 displayed the RL9-HIV-1 peptide-HLA-E complex. Yang et al. [22] demonstrated that $CD8^+$ T cells, which recognize a Gag peptide presented by HLA-E, are capable of suppressing HIV-1 replication *in vitro*. They cloned these HLA-E-restricted HIV-1-specific $CD8^+$ T cells and transduced them with their TCRs, effectively suppressing HIV-1 replication in $CD4^+$ T cells *in vitro*.

A recent study has shown that the previously reported HLA-E ligand, $Gag_{275\text{-}283}$ peptide, displayed inconsistent presentation in killing assays, requiring continuous loading of HLA-E molecule with exogenous peptide to elicit consistent T-cell responses. The peptides were assessed for stability and presentation, but no HLA-E-binding HIV peptides were identified by

mass spectrometry in HIV-infected cells [93]. Bansal et al. [94] investigated the biological relevance of HLA-E-restricted $CD8^+$ T cell responses in HIV infection, which had been previously associated with protection in an SIV/rhesus macaque model. They analyzed $CD8^+$ T cells responding to two epitopes: a newly identified subdominant Gag-KL9 and a well-described immunodominant Gag-KF11. They reported that bulk $CD8^+$ T cells from HIV-infected individuals recognized infected cells through HLA-E presentation. Hannoun et al. [95] screened over 400 HIV-1-derived 15-mer peptides and analyzed the cell-surface stabilization of HLA-E01:01 and HLA-E01:03 molecules upon peptide binding. They showed that four novel 9-mer peptides (PM9, RL9, RV9, and TP9) derived from the 15-mer binders specifically stabilized the surface expression of HLA-E*01:03, and five other peptides (EI9, MD9, NR9, QF9, and YG9) showed binding signals. A crystal structural study examining HLA-E in complex with HIV-derived peptides and its interaction with CD94/NKG2 receptors revealed that HLA-E exhibits a broad tolerance for hydrophobic and polar residues within its primary binding pockets, highlighting its adaptability in presenting pathogen-derived antigens. Furthermore, the study revealed that the HIV-derived RL9 peptide, although binding to HLA-E, weakly stabilizes the HLA-E molecule due to a large aromatic residue at P3, which disrupts the peptide's conformation and decreases the stability of the HLA-E-RL9 complex [29]. In early research examining the ability of HLA-E to present a capsid peptide (AISPRTLNA) from HIV-1 and its recognition by NKG2A/CD94, it was shown that NKG2A/$CD94^+$ NK cells provoked prompt responses toward HIV-infected T-cells. This occurred despite high HLA-E expression, and the capsid peptide presented by HLA-E was not recognized by NKG2A/CD94, which enabled NK cells to target the infected cells. The study suggested that *ex vivo*-expanded NKG2A/$CD94^+$ $KIR2DL^-$ NK cells might be beneficial for treating latently HIV-1-infected patients, as they can effectively target HIV-infected cells despite the presence of HLA-E [96]. HIV evades NK cell-mediated cytotoxicity by upregulating HLA-E expression on T cells, using the capsid protein $p24_{14-22}$ peptide to stabilize HLA-E and suppress NK cell responses [97].

A specific subset of NK cells expressing NKG2C receptors, called adaptive NK cells, recognize infected cells via an HLA-E molecule presenting certain HIV peptide fragments [98]. A study on participants during acute infection highlighted that adaptive NK cells are particularly active during peak viral load (VL) in HIV-1 infection, contributing to immune responses by producing significant amounts of IFN-γ that could enhance the activity of $CD8^+$ T cells, which are crucial for fighting viral infections. During early HIV-1 infection, there is an expansion of mature NK cell subsets showing adaptive features ($CD57^+FcεRγ^-NKG2C^+$) and

sustained cytotoxic capacity, followed by the activation of $CD8^+$ T cells [99]. However, the lack of homology between the HIV $p24_{14-22}$ peptide and HLA leader peptide may probably lead to the ligation of CD94-NKG2A to the HLA-E peptide complex. To date, no peptide restricted by HLA-E that can interact with NKG2C has been found for any of these viruses [100].

Despite the challenges in developing an effective HIV-1 vaccine due to the virus's genetic diversity and immune evasion strategies, there is potential in exploring HLA-E. However, understanding the interactions between HIV-derived peptides and HLA-E, as well as the immune responses they elicit, is still under study.

## 1.4 HLA-E in bacterial infection

$CD8^+$ T cells recognize endogenous antigens from intracellular bacteria presented by HLA-class Ib and lyse infected target cells, thereby playing a crucial role in the immune response [101]. Notably, in the absence of HLA class Ia-restricted $CD8^+$ T cells, HLA-E-restricted $CD8^+$ T cells that are capable of recognizing pathogen-derived peptides have been documented for *M. tuberculosis* and *Salmonella* (*S.*) Typhi [16,17,102–106].

### *1.4.1 HLA-E and M. tuberculosis*

*M. tuberculosis* is one of the leading causes of mortality from infectious diseases worldwide, resulting in approximately 10 million new active cases and around 1.5 million deaths each year [107]. While activated $CD8^+$ and $CD4^+$ T cells migrate to the lungs to target infected tissue cells, their ability to control the infection is limited due to *M. tuberculosis* strategies that evade detection and induce T cell exhaustion. Furthermore, the highly conserved antigens of *M. tuberculosis*, which elicit strong T cell responses, may cause tissue damage and promote transmission. All these processes emphasize the necessity of a deeper understanding of the mechanisms of antigen recognition in disease progression [108].

Analysis of *M. tuberculosis*-infected human dendritic cells shows that HLA-E is preferentially enriched in phagosomes compared to classical HLA-A2, with abundant HLA-E/peptide complexes present in these compartments [109] and HLA-E-restricted $CD8^+$ T cells specific for *M. tuberculosis*-derived peptides are detectable in the peripheral blood of individuals with either active tuberculosis or latent *M. tuberculosis* infection [103,110].

Screening of the entire *M. tuberculosis* genome for HLA-E-restricted sequences identified 69 potential candidates using three different prediction algorithms. Most of the 69 tested peptides

elicited the proliferation of $CD8^+$ T-cells in both *M. tuberculosis*-responsive adults and BCG-vaccinated infants. In a peptide competition assay, 36 peptides were found to bind to HLA-E, and 11 of those peptides were able to activate $CD8^+$ T-cell responses through $CD8^+$ T-cell proliferation. These T-cells showed cytotoxicity against *M. bovis*-infected monocytes and exhibited regulatory activities that inhibited T-cell proliferation, partially through membrane-bound TGF-β [111]. However, a more recent study reported that *M. tuberculosis*-specific HLA-E-restricted T cells are not generated after BCG vaccination either in non-human primates or in humans [112]. Further research identified mycobacterial antigenic peptides displayed by HLA-E molecules and targeted by $CD8^+$ T cells with an atypical, multifunctional phenotype. HLA-E-restricted T cells showed reduced production of typical cytokines associated with cytotoxic activity, such as IFN-γ and TNF, but instead produced cytokines linked to a Th2 type of immune response. These T cells performed cytolytic and regulatory activities and activated B cells. This indicates that HLA-E-bound peptides enable $CD8^+$ T cells to respond effectively to *M. tuberculosis*, as well as the responses mediated by classical HLA-class I and II molecules [113].

Caccamo et al. additionally found that HLA-E-restricted $CD8^+$ T cells represent a significant subset of effector cells involved in the immune defense during active *M. tuberculosis* infection. The frequency of these cells is significantly increased in the circulation of active TB patients and their presence in patients with and without HIV co-infection underscores their potential contribution to protective immunity in diverse populations. This HLA-E-restricted $CD8^+$ T cell population expands our knowledge of immune mechanisms in tuberculosis and may inform the development of targeted therapeutics and vaccines [113]. McMurtrey et al. [114] investigated the ligandome presented by HLA-E following infection with *M. tuberculosis* using mass spectrometry. They used an APC line to collect soluble HLA-E-restricted peptides from *M. tuberculosis*. A total of 28 *M. tuberculosis* ligands from 13 different proteins, including members of the Esx family, were identified. After assessing the immunogenicity of these ligands, they discovered that nine of the ligands induced an IFN-γ response, with a robust consensus response observed for peptide $Rv0634A_{19\text{-}29}$ in 14 out of the 16 donors. Further analysis confirmed the HLA-E restriction and identified reactive $CD8^+$ T cells in human blood. Another study revealed that a specific peptide derived from the *M. tuberculosis* protein MPT32, which requires N-terminal O-linked mannosylation for recognition, underscores the importance of post-translational modifications in immune recognition. This finding is

particularly noteworthy as it is the first report detailing a modified *M. tuberculosis*-derived protein antigen that elicits an HLA-E-specific $CD8^+$ T cell response [115].

Voogd et al. [112] conducted a comprehensive analysis of HLA-E-restricted $CD4^+$ and $CD8^+$ T cells specific to *M. tuberculosis* across both bronchoalveolar lavage fluid and peripheral blood in non-human primates (NHPs) and humans. Their investigation included two independent NHP studies and human cohorts vaccinated with BCG via intradermal or mucosal routes. The data revealed that BCG vaccination elicits only a limited activation of HLA-E-restricted *M. tuberculosis*-specific T cells in both species. Interestingly, these T cells were robustly induced following *M. tuberculosis* infection in unvaccinated rhesus macaques, suggesting that natural infection, rather than BCG immunization, is a more potent driver of HLA-E-restricted T cell responses. Furthermore, BCG vaccination followed by *M. tuberculosis* challenge did not significantly alter the frequency of circulating or tissue-resident HLA-E-restricted $CD4^+$ and $CD8^+$ T cells in NHPs, a trend that was similarly observed in vaccinated humans. In contrast, unvaccinated NHPs exhibited a marked expansion of these T cell subsets upon infection, underscoring the differential immunogenicity of BCG *versus* natural exposure in shaping HLA-E-mediated immunity.

In a recent study, Voogd et al. [116] conducted a comprehensive analysis of HLA-E-restricted T cell responses using HLA-E tetramers specific for *M. tuberculosis*. Their investigation included individuals with latent *M. tuberculosis* infection, active tuberculosis, and those co-infected with HIV. The study revealed that HIV co-infection primarily affects the distribution of memory subsets among HLA-E-restricted $CD4^+$ and $CD8^+$ T cells, while their overall frequencies remain consistent across clinical groups. These T cells exhibited expression of markers such as KLRG1, PD-1, and 2B4, similar to the broader T cell population.

The identification of microbial peptides, particularly those derived from *M. tuberculosis*, as ligands for HLA-E has provided important insight into the molecular determinants of peptide–MHC interactions. Structural analyses of HLA-E complexed with peptides from HIV and *M. tuberculosis* reveal that, while canonical anchor residues are generally conserved, these ligands can adopt multiple conformations within the peptide-binding groove. Notably, High-resolution crystal structures of HLA-E demonstrate a broader specificity than previously appreciated, showing notable tolerance for both hydrophobic and polar residues at key anchor positions. For example, the P2 residue of the *M. tuberculosis* peptide (p44) fits well in the B pocket of HLA-E, and substitutions with residues such as glutamine or phenylalanine are well tolerated without

inducing major conformational shifts. Furthermore, even though C-terminal substitutions such as P9-Phe present spatial constraints, HLA-E can still accommodate these variations, illustrating its versatility and potential alternative antigen-presenting functions *in vivo* [29]. Understanding of the specific mechanisms through which pathogen-derived peptides contribute to immune surveillance has benefited from the co-complex crystal structure of a CD8 TCR bound to a *M. tuberculosis* peptide presented by HLA-E [117].

### *1.4.2 HLA-E and S. Typhi*

*S. Typhi* is a rod-shaped, gram-negative bacterium from the Enterobacteriaceae family that can cause gastroenteritis in healthy individuals or result in more severe systemic enteric fever and invasive nontyphoidal Salmonellosis. Multifunctional $CD8^+$ cytotoxic T lymphocytes are essential for preventing the onset of typhoid disease and providing protection after the Ty21a vaccine [118], particularly those cells that target the *S. Typhi* antigen presented by HLA-E.

Salerno Goncalves et al. identified nonameric-derived *S. Typhi* peptides for HLA-E-specific recognition in the PBMC of Ty21a typhoid vaccinees. The binding of these bacterial-derived peptides to HLA-E triggered the activation of $CD8^+$ T cells, leading to enhanced cytotoxic activity and the production of IFN-γ that can effectively eliminate *S. Typhi*-infected cells [106]. Further research has identified HLA-E-restricted $CD8^+$ T cell responses targeting *S. Typhi*, both prior to and following vaccination with the Ty21a strain of typhoid. This study highlights the importance of long-lasting, multifunctional HLA-E-restricted $CD8^+$ responses in adaptive immunity to *S. Typhi*, marking the first demonstration of such cells after immunization in either animals or humans [105]. HLA-E–restricted T cells are associated with delayed disease onset and protection. However, limited pediatric data suggest that younger children may have a reduced capacity to mount protective cell-mediated immune responses post-vaccination. Using mass cytometry analyses and tSNE (t-distributed Stochastic Neighbor Embedding), they identified age-dependent differences in the abundance and function of gut-homing effector memory ($T_{EM}$) and terminally-differentiated ($T_{EMRA}$) T cell subsets, emphasizing the maturation of HLA-E–restricted immunity and its importance for optimizing pediatric vaccine strategies.

## 1.5 HLA-E in immunotherapy and vaccine development for infectious diseases

The HLA-E molecule has traditionally been recognized for its role in regulating NK cell activity through interactions with the inhibitory receptor NKG2A. However, recent research has expanded its functional relevance to the adaptive immune system, particularly in vaccine design and T cell immunotherapy for infectious diseases, given the limited display of polymorphisms (Figure 2).

### *1.5.1 HLA-E–based vaccine and TCR strategies for tuberculosis*

There is an urgent need for new vaccines targeting *M. tuberculosis* due to the limited effectiveness of the BCG vaccine in its current application. HLA-E-restricted and *M. tuberculosis*-specific $CD8^+$ T cells can control the growth of intracellular *M. tuberculosis*; therefore, this unconventional antigen-presenting molecule, HLA-E, represents a promising target for developing a new vaccine.

Donor-unrestricted T cell responses and HLA-E-restricted T cells show promise as vaccine targets. However, identifying HLA-E binding peptides from pathogens has been challenging due to the limited availability of prediction algorithms. A study developed a UV-mediated HLA-E-/peptide binding assay to gather data on various peptides, which was used to train a prediction algorithm by NNAlign for creating binding motifs. These motifs scanned the *M. tuberculosis* genomes to predict peptide sequences that bind to HLA-E. Selected peptides were synthesized and evaluated in binding assays, and the process was repeated three times to improve accuracy. Finally, promising candidates were chosen for T cell recognition assays. In this way, the algorithm for predicting HLA-E binding peptides was improved, leading to the identification of novel *M. tuberculosis*-derived peptides that can activate $CD8^+$ T cells in humans exposed to the bacterium [119].

A study from our group focused on enhancing the immune response using a modified *Bordetella* (*B.*) *pertussis* toxin (CyaA toxoid) to deliver specific *M. tuberculosis* peptides recognized by HLA-E molecule. The results showed that this approach significantly expanded HLA-E-restricted $CD8^+$ T cells, which produced IFN-γ and exhibited cytotoxic activity against infected cells [120].

Paterson et al. outlined a bispecific molecule based on TCR that interacts robustly and specifically with HLA-E when combined with a peptide derived from the inhA gene of *M.*

*tuberculosis*. The TCR-bispecific molecule consists of an affinity-enhanced TCR linked to an anti-CD3-activating domain and effectively induces T cell-mediated responses that can kill *M. tuberculosis*-infected macrophages. They suggested that this donor-unrestricted TCR-based immunotherapeutic could effectively target TB infections, eliminate infected cells, and reduce *M. tuberculosis* growth. Moreover, due to the limited polymorphism of HLA-E, it could be applicable to a broader range of patients, overcoming challenges associated with traditional TCR therapies [121].

### *1.5.2 CMV-vectored vaccines for SIV*

SIV and HIV effectively evade host immunity after establishing an infection. This makes it challenging to control the virus through immunologic mechanisms once it begins to spread. The early stage of disease, before the virus spreads, is a critical period during which the immune system can potentially control the infection.

Hansen et al. examined the efficacy of SIV vaccines using RhCMV vectors to generate long-lasting, high-frequency SIV-specific effector-memory T cell responses in rhesus macaques. This approach improved early control of SIVmac239 infection after mucosal challenge. Protection was linked to the peak SIV-specific $CD8^+$ T cell responses during vaccination and was maintained even after depletion of both $CD4^+$ and $CD8^+$ T lymphocytes, indicating a strong, stable immune response and the potential for viral clearance. These findings emphasize the potential of persistent vectors such as CMV in developing effective HIV/AIDS vaccines [27].

In more detail, the RhCMV/SIV vector stimulates specific $CD8^+$ T cell responses restricted by MHC-E, which are crucial for their effectiveness against SIV challenges in rhesus monkeys. The study found that a genetic rearrangement in RhCMV eliminated the function of several immunomodulatory genes, thereby enhancing these unconventional responses. However, responses produced from repaired genes did not protect against SIV. The results indicate that MHC-E-restricted $CD8^+$ T cell responses play a crucial role in mediating effective anti-SIV immunity [49].

Strain 68–1 of the RhCMV vectors that express SIV antigens provoke the activation of $CD8^+$ T cells that identify epitopes presented by MHC-class II and MHC-E, instead of MHC-class Ia. Specifically, the peptide VMAPRTLLL (VL9) from the RhCMV protein Rh67 enhances MHC-E transport, facilitating the recognition of RhCMV-infected cells by MHC-E-restricted $CD8^+$ T cells. When VL9 was deleted or mutated, the priming of these MHC-E-restricted T

cells was significantly impaired, resulting in an immune response that focused solely on MHC-II-restricted epitopes. Although similar in scale, this response did not provide protection against SIV [122].

Priming of unconventional T cells induced by a CMV vaccine and the control of SIV replication are conserved across different primate species. In rhesus macaques, the RhCMV vector expressing SIV antigens was found to prime MHC-E-restricted $CD8^+$ T cells, which help control SIV replication in about 50% to 60% of vaccinated individuals. However, it was unclear if this immune response was unique to rhesus macaques or the RhCMV itself. When the CyCMV vectors were tested in cynomolgus macaques, a different primate species, it was found that for MHC-E-restricted $CD8^+$ T cells to be activated, the CMV used must match the host species and the RhCMV vector did not trigger this immune response in cynomolgus macaques. Still, when a species-matched CyCMV/SIV vector was used, the cynomolgus macaques produced the necessary $CD8^+$ T cells, and half were able to control SIV replication after challenge. Furthermore, the IL-15 transcriptomic profile associated with SIV protection was observed in cynomolgus monkeys vaccinated with CMV, suggesting that the underlying mechanisms for SIV protection are maintained across various primate species when a suitable CMV vector is utilized [123].

According to the review by Picker et al. [124], CMV has been explored as a vaccine vector for HIV/SIV due to its capacity to elicit broad and unconventional $CD8^+$ T cell responses and effectively boost immune readiness against emerging viral infections. They reported that non-human primate CMVs can be genetically engineered to trigger distinct $CD8^+$ T cell responses that recognize viral peptides through various MHC molecules, including MHC-class Ia, MHC-class II, and MHC-E. Notably, the MHC-E-restricted $CD8^+$ T cell responses demonstrated an unexpected ability to tightly control SIV replication, offering a new perspective on vaccine-induced protection. The review further suggested that similar mechanisms could be applied to HIV-1, with the potential for MHC-E molecules to present universal viral epitopes, thereby addressing the challenge of HIV diversity.

In a recent study, Malouli et al. [125] uncovered a novel immune evasion strategy employed by human cytomegalovirus (HCMV) through its UL18 gene, which selectively inhibits the priming of unconventional $CD8^+$ T cells restricted by HLA-E. Using a rhesus CMV (RhCMV) vector system optimized for MHC-E–restricted responses, they systematically inserted 41 HCMV-specific open reading frames (ORFs) into the RhCMV backbone and found that only

UL18 abolished the induction of MHC-E and MHC-II–restricted $CD8^+$ T cells. UL18, a structural homolog of MHC-I, does not engage T-cell receptors but instead binds with high affinity to the inhibitory receptor LIR-1. This interaction suppresses the stimulation of HLA-E–restricted T cells both *in vitro* and *in vivo*, redirecting immune responses toward classical MHC-Ia restriction. Importantly, UL18 mutants engineered to disrupt LIR-1 binding restored unconventional T-cell priming, confirming that LIR-1 engagement is essential for UL18-mediated inhibition. These findings underscore that disruption of UL18–LIR-1 interactions, in addition to deletion of known inhibitory genes such as UL128, UL130, UL146, and UL147 [123], will be critical for advancing HCMV-based HIV vaccine platforms aimed at eliciting HLA-E–restricted $CD8^+$ T-cell responses [126].

Recent advances in CMV-vectored vaccine design for SIV have highlighted the critical role of MHC-E (HLA-E in humans) in mediating protective $CD8^+$ T-cell responses. The canonical 68-1 RhCMV vector elicits effector memory-biased, MHC-E–restricted $CD8^+$ T cells [127], which are uniquely capable of inducing early and complete replication arrest of SIV in ~60% of vaccinated macaques. However, translating this efficacy to humans requires safer, non-disseminating ("single-cycle") vectors. Earlier attenuation strategies, such as Rh108/UL79 destabilization, disrupted late gene expression and shifted immune responses toward conventional MHC-Ia restriction, leading to a loss of protection. In contrast, a novel approach using glycoprotein L (gL) deletion preserves late gene expression while preventing viral spread. These new ΔgL vectors produced high levels of effector memory-biased, SIV-specific $CD8^+$ T cells, including some that recognized peptides presented by MHC-E, resulting in high efficacy. This was crucial, as these immune responses correlated with preventing SIV replication in 70% of the vaccinated macaques [128].

Another study examined the combination of two immune strategies to enhance SIV protection in rhesus macaques, using a combination of RhCMV/SIV vaccine and neutralizing antibodies (nAbs). Twenty-four macaques were divided into three groups: one received the vaccine with sub-protective neutralizing antibodies (nAb) K11-LS, another with a control antibody, and the last received only nAbs. After a high-dose SIVmac239 challenge, the combination group showed a 44% replication arrest rate, compared to 11% in the vaccine-only group, while the nAb-only group exhibited unexpected protection. These findings support the potential of multimodal vaccine strategies for HIV, as even sub-protective nAbs can reduce initial viral burden when combined with enhanced MHC-E-restricted T cell responses [129].

### *1.5.3 TCR-based therapy for HBV*

A recent study created HLA class I-deficient T cells to evade recognition by the recipient's $CD8^+$ T cells and introduced a modified receptor, dtHLA-E4, to restore tolerance against NK cells. This optimized molecule displayed enhanced surface expression and inhibitory potential against NK cells while minimizing $CD8^+$ T cell recognition through specific mutations. The findings suggest that the engineered dtHLA-E4 can significantly reduce immunogenicity, thereby facilitating the longer-term survival of these T cells in the recipient, which could improve the effectiveness of immunotherapy treatments [130].

Another new therapeutic approach is the so-called Immune Mobilizing Monoclonal T Cell Receptors Against Viruses (ImmTAV®) platform, which targets HBV-positive hepatocytes by redirecting functional T cells, bypassing exhausted ones. Recently, an ImmTAV® molecule has been developed that targets an HLA-A*02:01-restricted HBV Env-derived peptide and has shown promise in selectively eliminating HBsAg-positive hepatocytes *in vitro* [131]. However, the frequency of the HLA-A*02:01 allele is approximately under 30% in chronic HBV infections (CHB); therefore, they focused on HLA-E-restricted $CD8^+$ T cells. Murugesan et al. [86] performed a systematic search for HLA-E binding peptides within the HBV proteome due to the high conservation of the HLA-E molecule, to maximize the potential population coverage. Three common variants of $Env_{371-379}$ (an HLA-E-binding HBsAg peptide) have been characterized using bioinformatics, HLA-E peptide-binding assays, and refolded HLA-E complexes. An ImmTAV molecule was generated with picomolar affinities, enabling the redirection of polyclonal T cells to target and destroy HBV-associated hepatocellular carcinoma (HCC) cells.

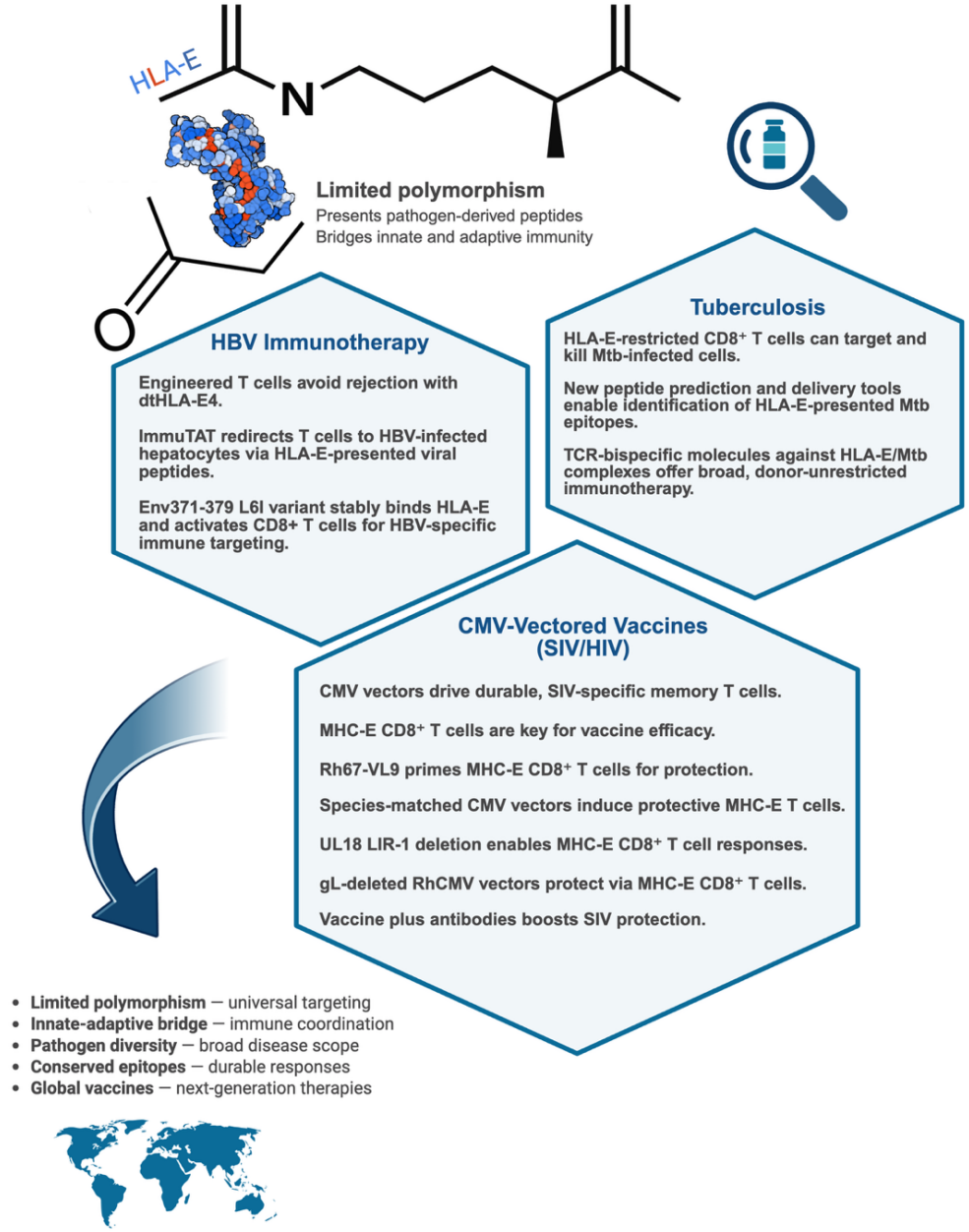


**Figure 2. HLA-E–based immunotherapeutic strategies in infectious diseases.**

The scheme summarizes recent advances in HLA-E-based approaches in immunotherapy and vaccine development for infectious diseases. The figure is divided into three sections, each highlighting a different pathogen (*M. tuberculosis*, SIV/HIV, and HBV) and the corresponding immunotherapeutic or vaccine development. HLA-E, a limited polymorphic molecule, presents conserved epitopes derived from various pathogens to $CD8^+$ T cells, making it a potential universal target for next-generation therapies. Figure created with BioRender.com.

# Chapter 2. Research Project

The COVID-19 pandemic, caused by the severe acute respiratory syndrome coronavirus 2 (SARS-CoV-2), has had a profound impact on global health and economics [132]. Current vaccines primarily aim to stimulate neutralizing antibodies; however, the emergence of SARS-CoV-2 variants may compromise their long-term efficacy. In contrast, most $CD4^+$ and $CD8^+$ T cell responses remain largely intact [133,134]. T cells play a critical role in the immune response to SARS-CoV-2 infection and vaccination [135–137]. Studies have shown that most individuals recovering from COVID-19 develop strong and broad SARS-CoV-2-specific $CD8^+$ T cell responses, suggesting these cells may help reduce disease severity. Patients with mild symptoms tend to exhibit a higher frequency of polyfunctional, multi-epitope classical $CD8^+$ T cell responses compared to those with severe symptoms, which may contribute to controlling infection [138,139]. However, during infection, the expression of classical HLA class I molecules in Calu-3 cells is significantly reduced, while HLA-E expression remains unchanged, enabling recognition by T cells [76].

To date, most studies on SARS-CoV-2-specific $CD8^+$ T cells have focused on pools of predicted or overlapping peptides restricted by classical HLA molecules, such as HLA-A and HLA-B [133,140]. The immunogenic potential of HLA-E-restricted $CD8^+$ T cell epitopes remains largely unexplored, while HLA-E exhibits low polymorphism across human populations, making it an appealing target for broadly applicable vaccine strategies. Moreover, unlike classical HLA molecules, HLA-E resists downregulation by certain viral immune evasion proteins, including HIV Nef and SARS-CoV-2 ORF8 [76,141,142]. Additionally, preclinical studies have shown that rhesus cytomegalovirus (RhCMV) vectors can elicit robust MHC-E–restricted $CD8^+$ T cell responses, capable of controlling simian immunodeficiency virus (SIV) infection in rhesus macaques [126]. This suggests that, while virus-infected cells may evade recognition by HLA-A- and HLA-B-restricted $CD8^+$ T cells, HLA-E-restricted $CD8^+$ T cell responses may remain functional, thereby maintaining immune surveillance in infected individuals [76,126,141].

In this study, we explored the role of HLA-E-restricted $CD8^+$ T cells in the immune response to SARS-CoV-2. Through in silico analysis, we identified seven peptides derived from six distinct SARS-CoV-2 proteins and assessed their binding affinity to the HLA-E molecule. Furthermore, we assessed their ability to elicit antigen-specific HLA-E-restricted $CD8^+$ T cell responses using both in vitro and ex vivo assays. Collectively, our findings underscore the

potential of HLA-E-restricted peptides in mediating T cell responses against SARS-CoV-2, highlighting their relevance in the development of peptide-based vaccines and therapeutic strategies.

# Chapter 3. Materials and methods

## 3.1 Study participants

A total of 89 participants were enrolled and categorized into three groups: convalescent (n = 40), hospitalized (n = 22), and vaccinated (n = 27), according to their COVID-19 status and vaccination history (Table 1). The selection was based on the availability of peripheral blood mononuclear cells (PBMCs) and clinical data. The study adhered to the Declaration of Helsinki and was approved by the Ethical Committee of the A.O.U.P. "Paolo Giaccone" Hospital (protocol code 09/2021). Written informed consent was obtained from all participants. Hospitalized COVID-19 patients were recruited from three medical centers in Palermo, Italy: A.O.U.P. "Paolo Giaccone" University Hospital, A.R.N.A.S. "Civico Di Cristina e Benfratelli" Hospital, and Villa Sofia/Cervello Hospital. Vaccinated individuals were enrolled after receiving two or three doses of the Pfizer/BioNTech BNT162b2 mRNA vaccine.

**Table 1. Subjects enrolled in the study.**

| Characteristic | Hospitalized | Convalescent | Vaccinated |
|---|---|---|---|
| No. of donors | 22 | 40 | 27 |
| Median age, years (range) | 65 (41-92) | 38 (26-66) | 28 (20-60) |
| Sex no. (%) | | | |
| Female | 10 (45,45) | 17 (42,5) | 16 (59,3) |
| Male | 12 (54,55) | 23 (57,5) | 11 (40,7) |

## 3.2 In Silico Peptide Prediction

The SARS-CoV-2 genome (strain 2019-nCoV/USA-WA1-A12/2020; MT020880) was obtained from the NCBI Protein Database. Peptide binding affinities were predicted using NetMHC 4.0 [17], which identified cytotoxic T lymphocyte epitopes across ten viral proteins. Strong binders (%Rank < 0.5) and weak binders (%Rank <2) were selected and filtered for HLA-E specificity via the Immune Epitope Database Analysis Resource (IEDB). NetMHC 4.0 was also used to predict binding affinities for longer peptides and to incorporate structural information from MHC molecules. Sequence homology was assessed using BLAST at an 80% similarity threshold, ensuring specificity and relevance to SARS-CoV-2.

## 3.3 SARS-CoV-2 epitope conservation

The conservation of HLA-E-restricted peptides derived from eight SARS-CoV-2 proteins-Spike, Nucleocapsid, ORF8, 3C-like Protease, RNA-dependent RNA Polymerase, and Exonuclease was assessed using the Los Alamos AnalyzeAlign tool [143]. The analysis was conducted on over 400,000 publicly available SARS-CoV-2 sequences from the GISAID database, collected between June 15, 2021, and February 6, 2025. The tool calculates the frequency of each amino acid and mutation at each position, visualized through sequence logos generated by WebLogo. In these logos, the Y-axis represents residue probability, and the X-axis corresponds to amino acid positions based on the reference genome NC_045512. Stack height indicates overall conservation at each position, while the height of individual symbols reflects the frequency of specific amino acids. A focused analysis was also performed on a subset of over 90,000 sequences from the JN.1 lineage, collected between December 1, 2021, and February 6, 2025. Mutation frequencies and sequence alignments were examined using a reference genome, with data updates from GISAID on February 12, 2025.

## 3.4 HLA-E/Peptide Stabilization Assay

Peptide binding to HLA-E was evaluated using a stabilization assay in RMA-S cells (RRID: CVCL_2180) transfected with HLA-E*01:03 and human β2-microglobulin. The expression index was calculated based on MFI values. Peptides were obtained from Bio-Fab Research (Rome, Italy) at ≥99% purity. They were reconstituted at 5 mg/mL in DMSO, diluted to 1 mg/mL in Dulbecco's Phosphate Buffered Saline (DPBS, Euroclone), and used at a final concentration of 5 μg/mL. RMA-S/HLA-E01:03 cells (TAP2-deficient murine lymphoma cells stably transfected with HLA-E01:03 and human β2-microglobulin; kindly provided by J.E. Coligan, NIAID, USA) were cultured overnight at 37 °C 5% $CO_2$ with test peptides at 37 °C for 24 hours in Iscove's medium supplemented with 1% glutamine, 20 mM HEPES, 100 U/mL penicillin, and 100 μg/mL streptomycin. Peptide binding to HLA-E was assessed by measuring surface HLA-E expression via flow cytometry using a PE-conjugated anti-HLA-E monoclonal antibody (REA1031, Miltenyi Biotec). Data were acquired on a BD FACSAria™ and analyzed with FlowJo software (BD Biosciences). Results were expressed as geometric mean fluorescence intensity (MFI). The VL9 peptide (from the HLA-C leader sequence) and a non-binding control peptide (WNSNNLDSKVGG) were used as positive and negative controls, respectively.

## 3.5 Blood Sampling, PBMC Isolation, and Stimulation

Peripheral blood was collected in heparin tubes (Greiner Bio-One) from convalescent and hospitalized patients (September 2020), and from vaccinated individuals at 6–9 months post-second dose (January 2021) and 12 months after the booster (November 2023). PBMCs were isolated via density gradient centrifugation using Lympholyte-H (CEDARLANE). Unused cells were cryopreserved in TexMACS Medium (Miltenyi Biotec) with FBS and 20% DMSO, pre-chilled at –80 °C, and then stored in liquid nitrogen. Thawed PBMCs were seeded ($4 \times 10^5$ cells/well) into 96-well U-bottom plates. Cells were stimulated with PepTivator® SARS-CoV-2 Prot_S (1 µg/mL/peptide), a pool of HLA-E-restricted peptides, or peptide SP09 (5 µg/mL), and incubated at 37 °C with 5% $CO_2$.

## 3.6 Intracellular cytokine staining

PBMCs were stimulated with peptides for 18 hours, then harvested, washed with PBS (EuroClone), and prepared for intracellular staining. PBMCs were stimulated with peptides for 18 hours, then harvested and washed with PBS (EuroClone) and prepared for intracellular staining procedure. Viability staining was performed using Viobility 405/452 Fixable Dye (Miltenyi Biotec) for 15 minutes at room temperature in the dark. After washing, surface staining was conducted using anti-human CD3 PerCP-Vio 700, CD4 PE-Vio 770, and CD8 APC antibodies (all from Miltenyi Biotec). Cells were fixed with IC Fixation Buffer (eBioscience) and permeabilized twice with Intracellular Staining Permeabilization Wash Buffer (BioLegend). Intracellular cytokine staining was performed using fluorochrome-conjugated antibodies against IFN-γ FITC (REA600), TNF-α PE (REA656), and IL-2 PE-Vio 770 (REA689) (Miltenyi Biotec) in permeabilization buffer. Samples were acquired on a BD FACSLyric and analyzed with FlowJo™ Software v10.9 (BD Biosciences). $CD8^+$ T cells were gated as $CD3^+$ $CD8^+$ $CD4^-$. A positive response was defined as >0.01% cytokine-producing cells; values below this threshold were considered negative and set to zero. The gating strategy is shown in Figure S1.

## 3.7 Blocking antibody experiments

To confirm that cytokine production by $CD8^+$ T cells was specifically mediated through HLA-E-restricted TCR-peptide recognition, PBMCs were incubated with blocking monoclonal antibodies (mAbs) in the presence or absence of synthetic SARS-CoV-2-derived peptides (final

concentration: 5 μg/mL) in 96-well U-bottom plates. The blocking mAbs included anti-HLA-E (clone unconjugated 3D12HLA-E, eBioscience™) and anti-TCR αβ (clone IP26, eBioscience™), each used at a final concentration of 10 μg/mL. Isotype-matched control antibodies were included as negative controls. Blocking antibodies were added to the PBMC cultures 1 hour prior to peptide stimulation. Following 18 hours of incubation at 37 °C with 5% $CO_2$, cells were harvested and stained for surface markers CD3 and CD8, along with viability dyes. Intracellular staining for TNF-α was subsequently performed to assess cytokine production.

## 3.8 Statistical analysis

Statistical analyses were performed in GraphPad Prism (RRID: SCR_002798). The Two-way ANOVA or mixed model and the non-parametric tests, Mann-Whitney and Kruskal-Wallis, were used for unpaired samples. p values less than 0.05 were considered statistically significant.

See Supplementary Table S1 for key resources and Supplementary Table S2 for RRIDs of antibodies.

# Chapter 4. Results

## 4.1 Computational discovery of seven unique SARS-CoV-2 epitopes with exclusive HLA-E binding

We assembled ten essential SARS-CoV-2 protein sequences into a FASTA file and performed peptide–MHC binding affinity predictions using an artificial neural network (ANN) algorithm. The complete reference genome (MT020880) was analyzed across all annotated open reading frames (ORFs), including both structural and non-structural proteins, to identify potential HLA-E-restricted epitopes. Using NetMHC 4.0 [17,144], we predicted a total of 72,572 peptides with the potential to bind to MHC class I molecules. Peptides ranging from 9 to 15 amino acids were evaluated, and 1,261 sequences with predicted binding affinities between 0.5 and 0.08 log (IC50) for HLA-E*01:01 were selected for further analysis (Figure 3A).

To assess specificity, we screened all predicted epitopes against 81 HLA-A, HLA-B, HLA-C, and HLA-E alleles. A substantial proportion of peptides showed cross-reactivity with classical MHC class I molecules, particularly HLA-A (49.9%), followed by HLA-B (39%) and HLA-C (9.8%) (Figure 3B). In contrast, only 1.04% of epitopes were found to have affinity for HLA-E*0101, highlighting the relatively low frequency of HLA-E-restricted SARS-CoV-2 epitopes in the SARS-CoV-2 Predicted Epitope Database (Figure 3B). From this subset, we identified 216 peptides as unique binders to HLA-E*01:01. We then performed homology screening using BLAST with an 80% similarity threshold to exclude peptides with close homologs in other organisms, and we utilized the IEDB for final homology control and epitope selection.

Next, we calculated immunogenicity scores using T-cell epitope prediction tools on the IEDB (21). Peptides were classified as strong binders (SB) or weak binders (WB) based on predicted log (IC50) affinity values (Figure 3C). Finally, we selected seven HLA-E-restricted epitopes that were unique to SARS-CoV-2, distinct in their core sequences, and demonstrated positive immunogenicity scores. These peptides were chosen as candidates for downstream validation and analysis (Table 2; Figure 3D).

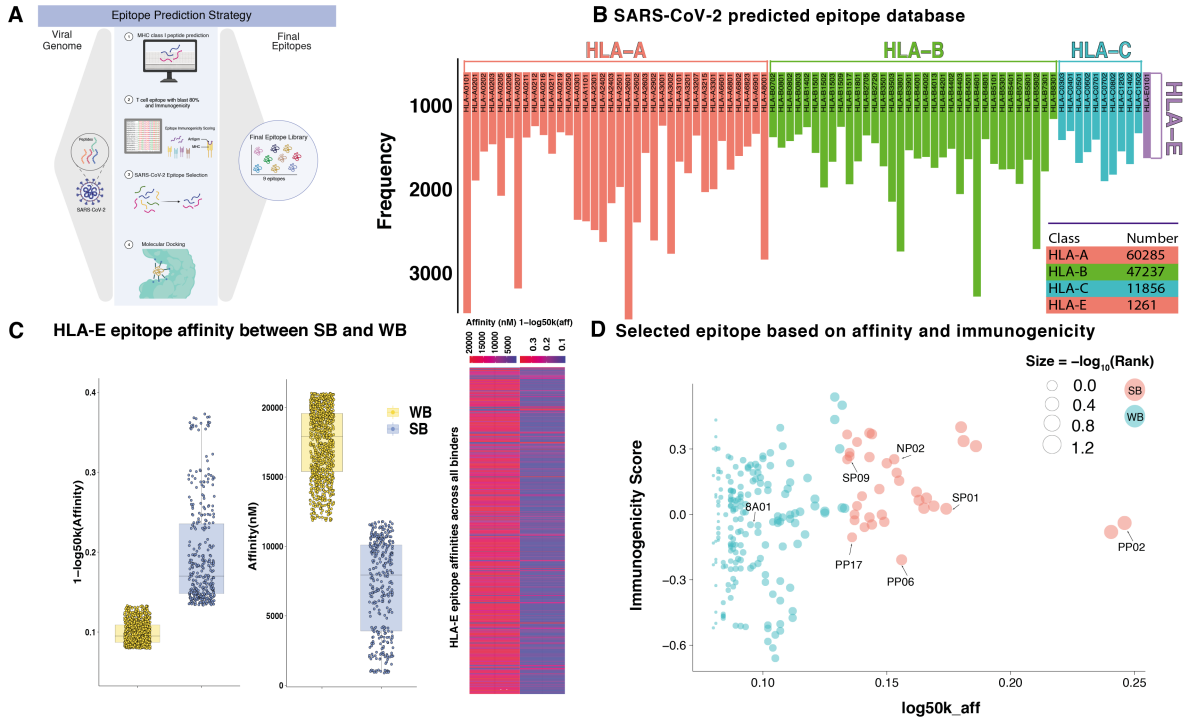


**Figure 3. In silico prediction of unique SARS-CoV-2 epitopes with high affinity for HLA-E*01:03.**

A) Schematic representation of the computational pipeline used to predict HLA-E binding epitopes from SARS-CoV-2 proteins, which included data acquisition, epitope prediction, and affinity analysis. B) Frequency distribution of SARS-CoV-2 epitopes binding to different MHC class I molecules (HLA-A, HLA-B, HLA-C, and HLA-E). The bar chart represents the number of unique epitopes predicted to bind each HLA allele. The total number of epitopes binding to each HLA allele is indicated at the bottom right. C) A total of 120.639 peptides were classified as strong binders (SB) or weak binders (WB) based on their binding affinities, determined using the 1-log50k affinity scale (nM). A heatmap illustrates the predicted binding affinities of the peptides to HLA-E*01:03. D) Scatter plot showing the distinctiveness of selected epitopes based on their uniqueness to SARS-CoV-2 and strong immunogenicity scores, each colored according to their classification as SB or WB. These seven epitopes were prioritized for further analysis due to their potential effective immunogenicity.

**Table 2. Characteristics of predicted HLA-E binding SARS-CoV-2 peptides, stabilization and activation assay.**

| Code | protein | position | Peptide sequence | Lenght | Log ($IC_{50}$) Affinity (core) | Stabilization MFI 24h | Activation[1] |
|---|---|---|---|---|---|---|---|
| SP09 | SPIKE | 320-330 | VQPTESIVRFP | 11 | 0.244 | 5.4 ± 6.5 | 0.18 ± 0.05 |
| SP01 | SPIKE | 503-514 | VGYQPYRVVVLS | 12 | 0.174 | 7.8 ± 3.6 | 0.04 ± 0.04 |
| NP02 | N | 149-159 | RNPANNAAIVL | 11 | 0.156 | -1.27 ± 5.6 | 0.07 ± 0.06 |
| 8A01 | ORF8a | 48-58 | RVGARKSAPLI | 11 | 0.143 | 1.6 ± 2.1 | 0.21 ± 0.08 |
| PP02 | ORF1ab | 106-116 | IQPGQTFSVLA | 11 | 0.136 | 4.4 ± 3.1 | 0.13 ± 0.05 |
| PP06 | ORF1ab | 565-576 | TMTNRQFHQKLL | 12 | 0.134 | 12.3 ± 4.5 | 0.16 ± 0.11 |
| PP17 | ORF1ab | 17-30 | GLHPTQAPTHLSVD | 14 | 0.089 | 1.5 ± 1.5 | 0.08 ± 0.04 |

[1]As a readout of activation, we assessed the overall frequency of $CD8^+$ T lymphocytes producing the cytokines IFN-γ, TNF-α, and IL-2 following 24-hour stimulation of PBMCs with peptide-pulsed or unpulsed RMA-S/HLA-E cells, from seven convalescent individuals.

## 4.2 Stabilization and immunogenicity of SARS-CoV-2 epitopes binding to HLA-E

To experimentally validate peptide binding, we performed stabilization assays using TAP-deficient RMA-S cells expressing HLA-E and β2-microglobulin (RMA-S/HLA-E). Cells were incubated with peptides at 37 °C, and HLA-E surface expression was quantified by flow cytometry after 24-hours incubation. The stabilization data are shown in Table 2, with cumulative results from five independent experiments (each in duplicate). Normalized mean fluorescence intensity (MFI) was calculated as described in the Methods section. Stabilization was defined by an MFI index ≥ 0.1 [17]. There was no evidence of HLA-E expression in the absence of peptide, while the canonical VL9 peptide, used as a positive control, stabilized HLA-E expression (data not shown). All peptides except NP02 promoted HLA-E stabilization on transfected RMA-S cells, with SP01, SP09, and PP06 showing the highest MFI values.

We next evaluated the immunogenicity of the seven peptides by assessing cytokine responses in $CD8^+$ T cells. PBMCs were stimulated with peptide-pulsed or unpulsed RMA-S/HLA-E cells, and intracellular cytokine staining was performed. A response was considered positive if cytokine expression exceeded 0.01% above background in at least 30% of donors [17]. According to these criteria, all seven tested peptides elicited at least one cytokine expression amongst IFN-γ, TNF-α, and IL-2 by $CD8^+$ T cells, although at very different extent. Table 2 shows cumulative data from COVID-19 patients while Figure 4 shows individual data.

Therefore, and as found for other HLA molecules as well, since actual affinities as predicted by computational approaches do not fully correlate HLA-E cell surface stabilization assay and the CD8 T cell responses, in subsequent experiments we decided to use the seven peptides that gave a positive result in either assay.

Blocking TCRαβ or HLA-E significantly reduced $CD8^+$ T cell cytokine responses to SARS-CoV-2 peptides in PBMCs from convalescent and vaccinated donors (see Figure 5), confirming TCRαβ-dependent recognition of HLA-E-bound peptides.

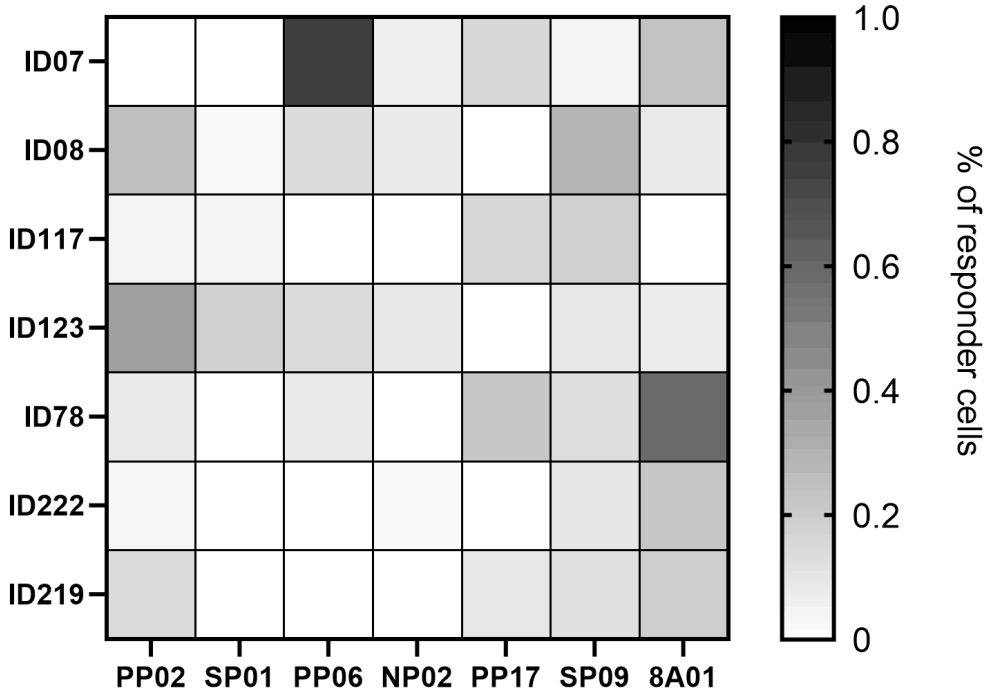


**Figure 4. Representation of the combined cytokine expression results for a discovery cohort of 7 convalescent COVID-19 patients.**

The figure shows the frequency of the $CD8^+$ T cell cytokine (IFN-γ, TNF-α, and IL-2) response to HLA-E-binding SARS-CoV-2 peptides. White boxes, no cytokine response (the total percentage of $cytokine^+$ $CD8^+$ T cells is < 0,01); light gray boxes, the total percentage of $cytokine^+$ $CD8^+$ T cells ranges from 0,01 – 0,2%; gray boxes, the total percentage of $cytokine^+$ $CD8^+$ T cells ranges from 0,4 – 0,6%; dark gray boxes, the total percentage of $cytokine^+$ $CD8^+$ T cells ranges from 0,6 – 0,8% and black boxes, the total percentage of $cytokine^+$ $CD8^+$ T cells ranges from 0,8 –1% or more.

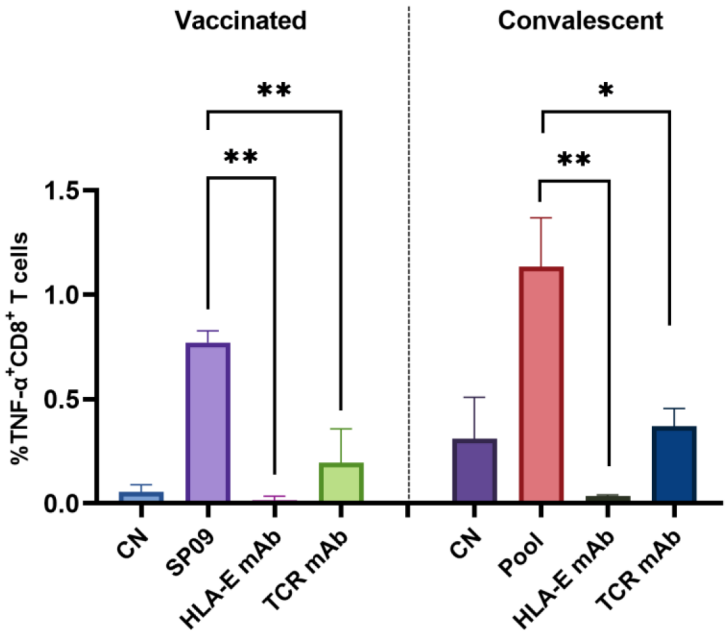


**Figure 5. Recognition requirements of SARS-CoV-2-specific HLA-E-restricted CD8$^+$ T cells.**

PBMCs from vaccinated individuals (left panel) or COVID-19 convalescent (right panel) patients were cultured for 18 hrs with SP09 peptide or with a pool of the 7 HLA-E/SARS-CoV-2 peptides in the presence of blocking mAbs to HLA-E or the TCR ab. Intracellular TNF-α expression by CD8$^+$ T cells was estimated by flow cytometry. Data are shown as mean ± SD and are pooled from two independent experiments, each performed in triplicate. **$p < 0.005$ and *$p<0.05$ when compared to peptide stimulation in the absence of mAbs, using one-way analysis of variance (ANOVA).

## 4.3 SARS-CoV-2 peptides are conserved in the main SARS-CoV-2 strains

The Alamos AnalyseAlign tool was used to assess the conservation of HLA-E-restricted peptides derived from Spike, Nucleocapsid, ORF8, and ORF1ab proteins in over 400,000 SARS-CoV-2 sequences deposited between June 15, 2021, and February 6, 2025. Our analysis showed a high level of sequence conservation across all major SARS-CoV-2 variants, including Alpha (B.1.1.7), Beta (B.1.351), Gamma (P.1), Delta (B.1.617.2), and Omicron (B.1.1.529). Importantly, we also observed substantial sequence conservation within more than 90,000 sequences collected between December 1, 2021, and February 6, 2025, specifically from the JN.1 SARS-CoV-2 lineage, which is a descendant of BA.2.86 and is currently the most prevalent SARS-CoV-2 variant globally.

As detailed in the Data Sheet S1, we observed significant conservation of amino acid sequences across a range of proteins from SARS-CoV-2, with logo frequency by position in the Nucleocapsid, 3C-like protease, RNA-dependent RNA polymerase, and Exonuclease proteins ranging from 98.23% to 99.84%. Furthermore, we noted approximately 96% conservation within the Spike protein, which displayed slightly lower conservation levels in the JN.1 variant. Across all main SARS-CoV-2 variants, amino acid sequence conservation ranged from 87.54% to 97.58% for Spike, and between 96.99% and 99.64% for other peptides. For example, the Logo frequency for amino acid position 116 in the 3C-like protease (IQPGQTFSVLA) was present in A: 99.63% (379341/380754), X: 0.35% (1342/380754), and V: 0.01% (53/380754) of sequences across all variants (see Figure 6A). In the JN.1 variant, it was A: 99.84% (90602/90750), X: 0.16% (142/90750), and V: 0.01% (5/90750) (see Figure 6B).

**A. Alpha (B.1.1.7), Beta (B.1.351), Gamma (P.1), Delta (B.1.617.2), and Omicron (B.1.1.529)**

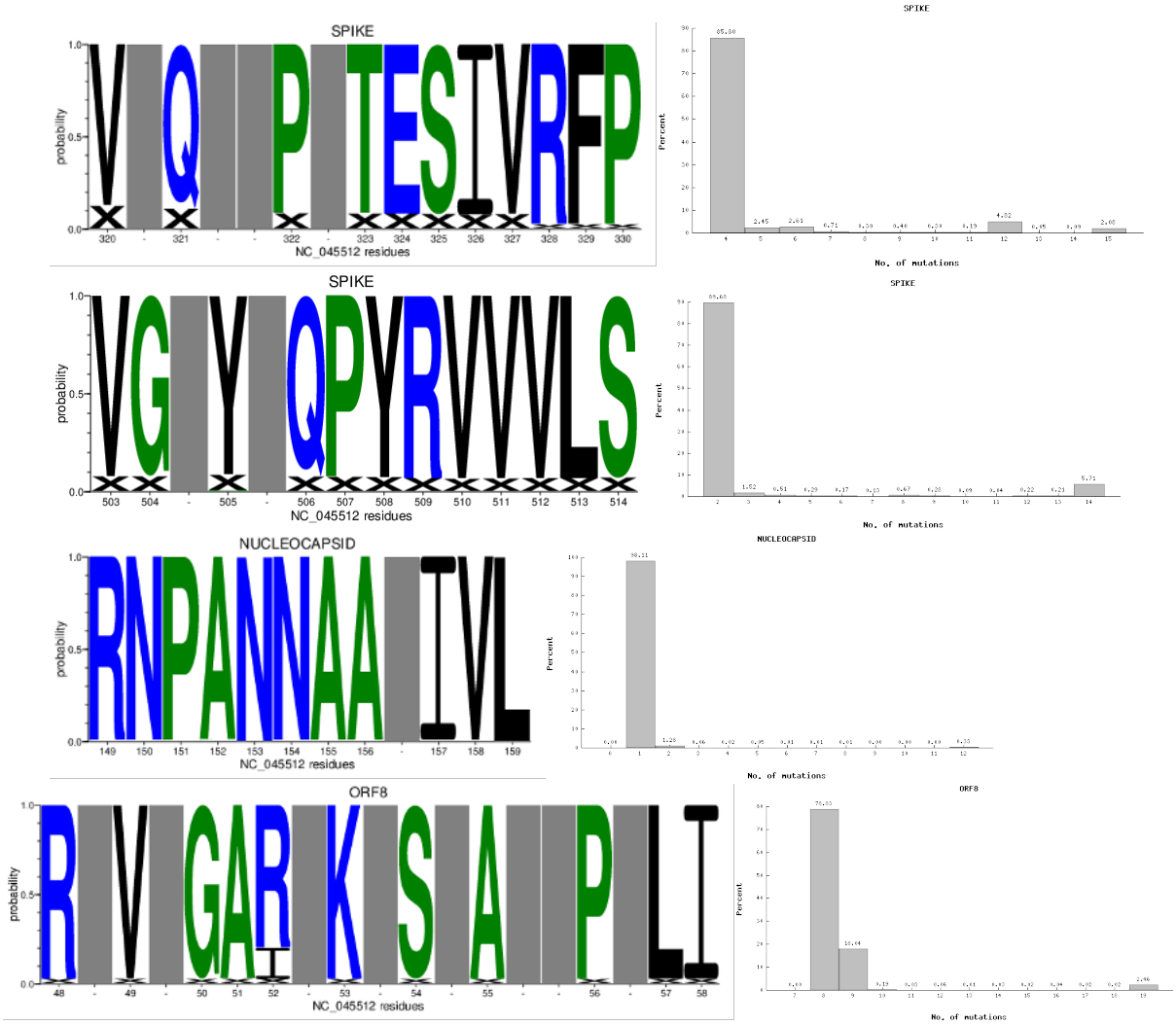

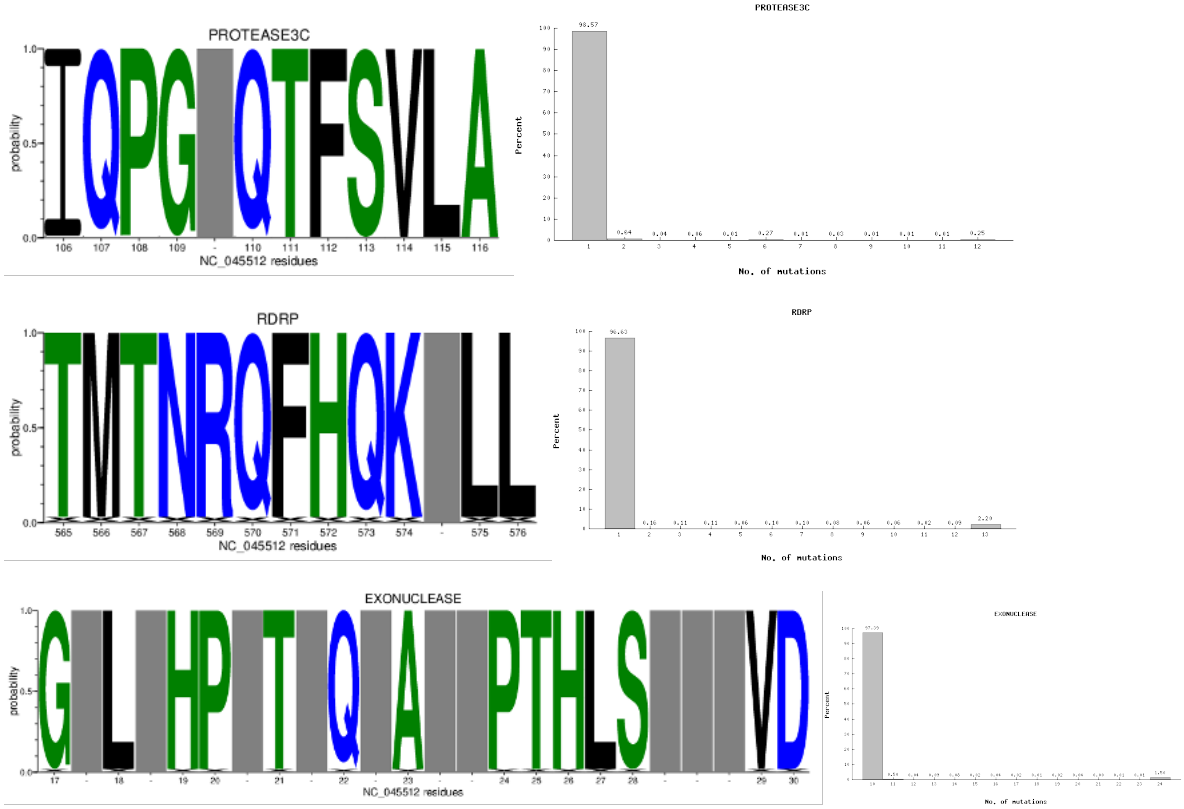
PROTEASE3C
probability
NC_045512 residues
Percent
No. of mutations
RDRP
probability
NC_045512 residues
Percent
No. of mutations
EXONUCLEASE
probability
NC_045512 residues
Percent
No. of mutations

**B. JN.1**

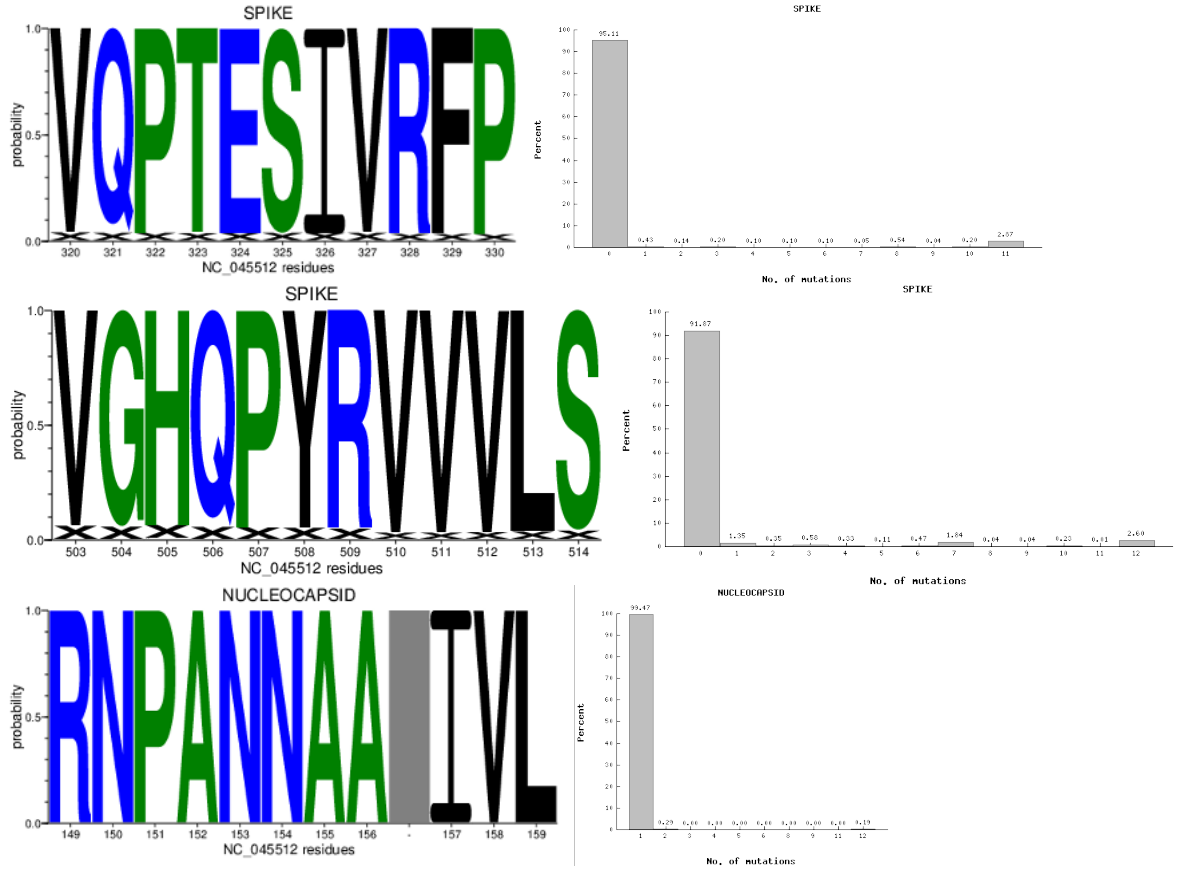
SPIKE
probability
NC_045512 residues
Percent
No. of mutations
SPIKE
probability
NC_045512 residues
Percent
No. of mutations
NUCLEOCAPSID
probability
NC_045512 residues
Percent
No. of mutations

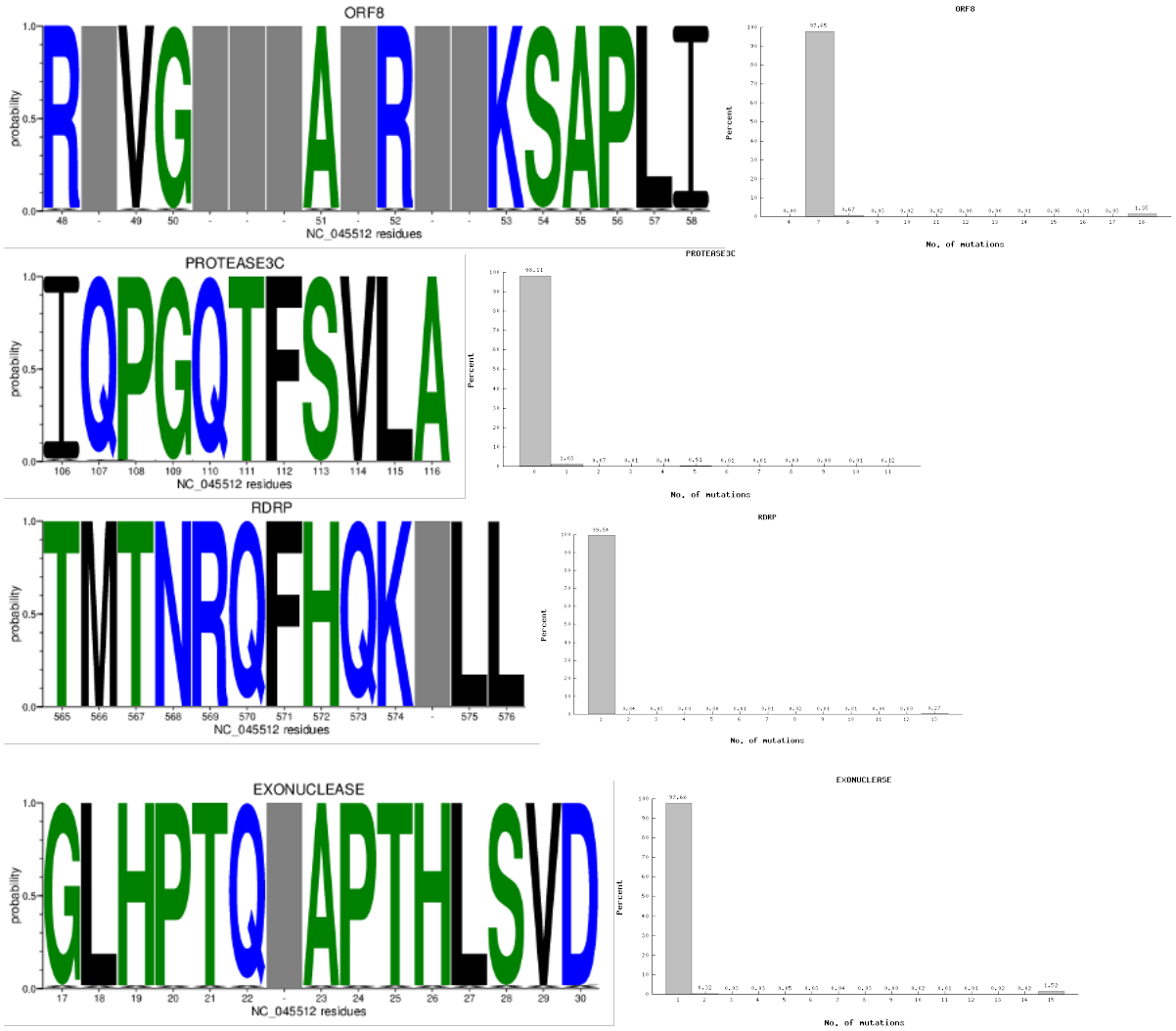


**Figure 6. This figure highlights the Logo diagrams of each epitope sequence of seven HLA-E binding SARS-CoV-2 peptides.**

These were checked and analyzed using the Los Alamos AnalyseAlign tool against more than 400,000 sequences collected between (A) June 15, 2021, and February 6, 2025 for all main SARS-CoV-2 variants, including Alpha (B.1.1.7), Beta (B.1.351), Gamma (P.1), Delta (B.1.617.2), Omicron (B.1.1.529), and (B) over 90,000 sequences collected from December 1, 2021, to February 6, 2025, for the JN.1 lineage. All epitopes demonstrated significant conservation of amino acid sequences across the main SARS-CoV-2 variants. The gray boxes in the logos indicate deletions. The colors of each amino acid are categorized based on their hydrophobicity: Hydrophilic (RKDENQ, Blue), Neutral (SGHTAP, Green), and Hydrophobic (YVMCLFIW, Black).

## 4.4 HLA-E–restricted SARS-CoV-2-specific CD8$^+$ T cell cytokine responses in convalescent and hospitalised COVID-19 patients

To evaluate the effector functions of HLA-E–restricted SARS-CoV-2-specific CD8$^+$ T cells, we directly stimulated PBMCs from 44 samples with a pool of HLA-E-binding peptides and

measured the response by assessing the frequency of IFN-γ, TNF-α, and IL-2 production by $CD8^+$T cells. A commercially available peptide pool derived from the entire Spike sequence (PepTivator) was used as a response control.

In convalescent patients, HLA-E restricted $CD8^+$ T cells mainly expressed TNF-α and, although to a lesser extent, IFN-γ (Figure 7A, left and centre) upon stimulation with the pool of HLA-E-binding SARS-CoV-2 peptides. The results were statistically significant compared to non-stimulated cells within each sample group. $CD8^+$ T cells also produced IL-2 after stimulation with the HLA-E-binding peptide pool compared to unstimulated PBMCs, but the result did not reach statistical significance (Figure 7A, right). Notably, stimulating PBMCs with PepTivator caused limited expression of IFN-γ, TNF-α, and IL-2, with cytokine levels lower than those promoted by the HLA-E-binding peptide pool, and these differences were not statistically significant from the cytokine response of unstimulated PBMCs.

We then compared the HLA-E-restricted $CD8^+$ T cell response in 22 convalescent patients with a cohort of 22 hospitalized patients with severe COVID-19. Compared to $CD8^+$ T cells from convalescent individuals, $CD8^+$ T cells from hospitalized COVID-19 patients produced significantly less TNF-α and IFN-γ (Figure 7B, left and center) after stimulation with the pool of HLA-E-binding peptides, while IL-2 production showed no difference between the $CD8^+$ T cells from both groups (Figure 7B, right). Notably, production of IFN-γ by $CD8^+$ T cells from hospitalized patients with severe COVID-19 in response to HLA-E-binding peptides was nearly absent (Figure 7B, left). Furthermore, there was no statistically significant difference in the production of IFN-γ, TNF-α, and IL-2 in response to PepTivator between $CD8^+$ T cells from convalescent and severe COVID-19 hospitalized patients.

Collectively, these results clearly demonstrate that HLA-E-restricted $CD8^+$ T cells that preferentially produce TNF-α and IFN-γ form a distinct yet significant population of the SARS-CoV-2-specific $CD8^+$ repertoire in convalescent COVID-19 patients; however, they are poorly represented in hospitalised patients with severe disease.

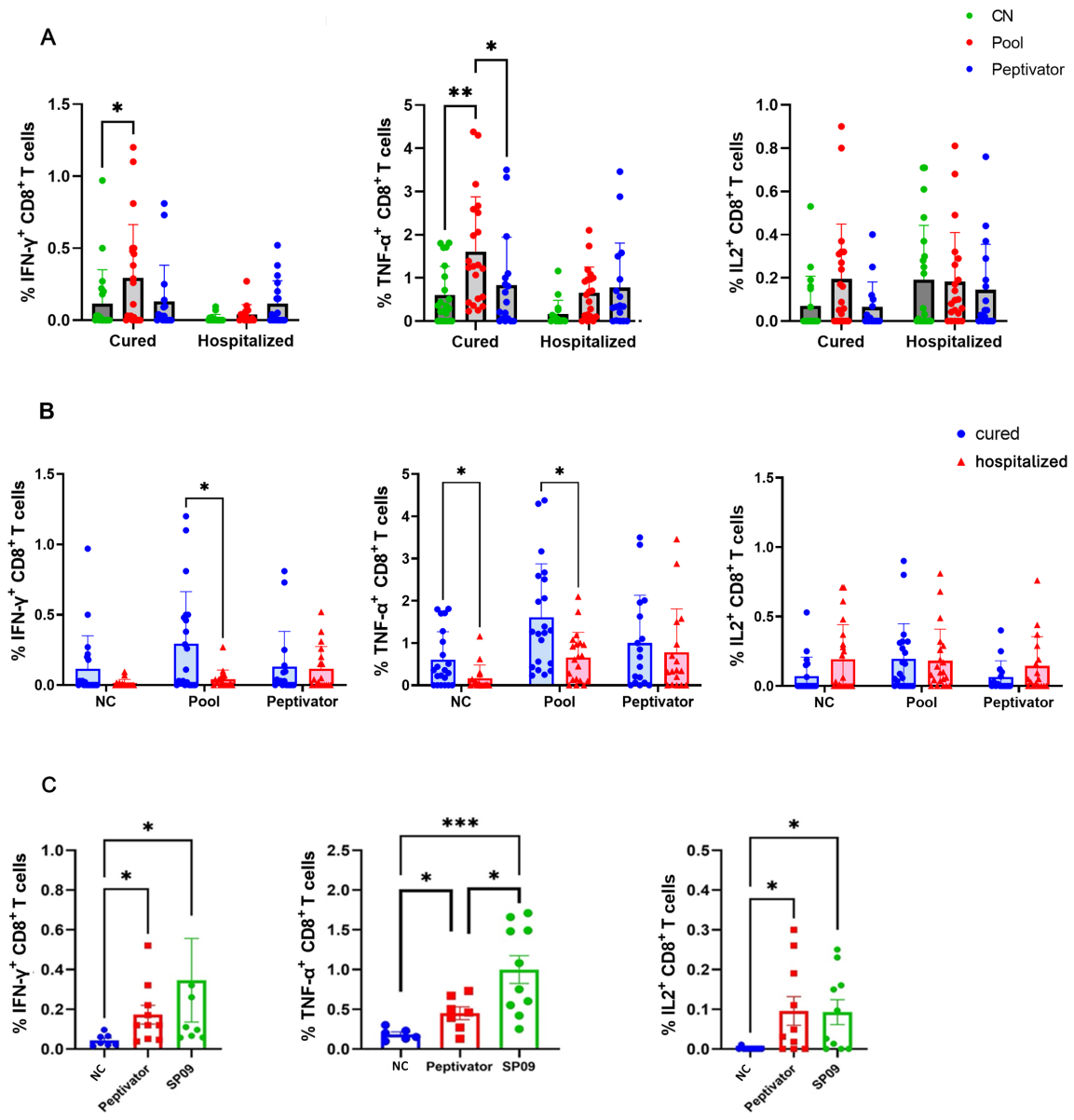


**Figure 7. Frequencies of HLA-E/SARS-CoV-2 peptide-specific CD8$^+$ T cells in convalescent and hospitalized severe COVID-19 patients.**

A) Frequency of IFN-γ, TNF-α, and IL-2 positive CD8$^+$ T cells in convalescent (n.=21) and hospitalized severe COVID-19 patients (n.=17) upon stimulation with the pool of SARS-CoV-2 peptides. Unstimulated cells were used as a negative control (NC), while the cells stimulated with PepTivator® were considered a positive control of SARS-CoV-2-specific response. The graph represents the median and the error bars. Two-way ANOVA or mixed models were used to compare the three experimental points. *p<0,05; **p<0,01.

B) Frequency of IFN-γ, TNF-α and IL-2 positive CD8$^+$ T cells in convalescent and hospitalized severe COVID-19 patients upon stimulation with the pool of SARS-CoV-2 peptides. Unstimulated cells were used as a negative control (NC), while the cells stimulated with PepTivator® were considered as a positive control of SARS-CoV-2-specific response. The graph represents the median and the error bars. Two-way ANOVA or mixed models were used to compare the three experimental points. *p<0.05.

C) Frequency of IFN-γ, TNF-α and IL-2 positive $CD8^+$ T cells in vaccinated subjects (n.=10) upon stimulation with SP09 peptide. The graph represents the median and the error bars. The Kruskal-Wallis test was used to compare the values of the groups. *$p \leq 0.05$, ***$p \leq 0.001$.

## 4.5 Vaccination increases cytokine production by HLA-E-restricted Spike peptide-specific $CD8^+$ T cells

We investigated the impact of vaccination on the HLA-E-restricted and SARS-CoV-2-specific $CD8^+$ T cells. First, we assessed the $CD8^+$ T cell response in a cohort of 25 healthy individuals who received two or three doses of the Pfizer/BioNTech BNT162b2 mRNA vaccine. PBMCs were collected from vaccinated donors, on average, 21 days after the second or third dose, and were stimulated with the HLA-E-restricted Spike-derived peptide SP09 or with PepTivator as a positive control. As shown in Figure 8C, $CD8^+$ T cell responses to the HLA-E-restricted peptide SP09 increased significantly after vaccination, with significantly higher levels of IFN-γ, TNF-α, and IL-2 compared to unstimulated controls. A similar cytokine profile was observed in response to PepTivator. Of particular interest, cytokine expression in response to SP09 was higher than that elicited by PepTivator, although the differences reached statistical significance only for TNF-α.

To study the impact of vaccine doses on the development of the HLA-E-restricted $CD8^+$ T cell response, we analysed cytokine production in response to SP09 in 15 individuals who had received two doses and 10 individuals who had received three doses. As shown in Figure 8A, the IFN-γ, TNF-α, and IL-2 $CD8^+$ T cell responses to SP09 peptide stimulation were statistically significantly lower in donors who had received a second dose compared to those who had received three doses, indicating a dose-dependent increase in the HLA-E-restricted immune response, in terms of cytokine production.

We further evaluated the combined impact of vaccination and natural SARS-CoV-2 infection on the HLA-E–restricted $CD8^+$ T cell response. To this aim, we measured cytokine production in response to the SP09 peptide in healthy donors who received three doses of the BNT162b2 vaccine (Figure 8A). The TNF-α and IFN-γ $CD8^+$ T cell responses to SP09 peptide stimulation were significantly higher in donors who received three vaccine doses and had been infected with SARS-CoV-2, compared to non-infected, vaccinated individuals (Figure 8B). These results clearly demonstrate that natural SARS-CoV-2 infection boosts HLA-restricted $CD8^+$ T

cell responses in vaccinated individuals, suggesting that this HLA-E-restricted response may contribute to protection.

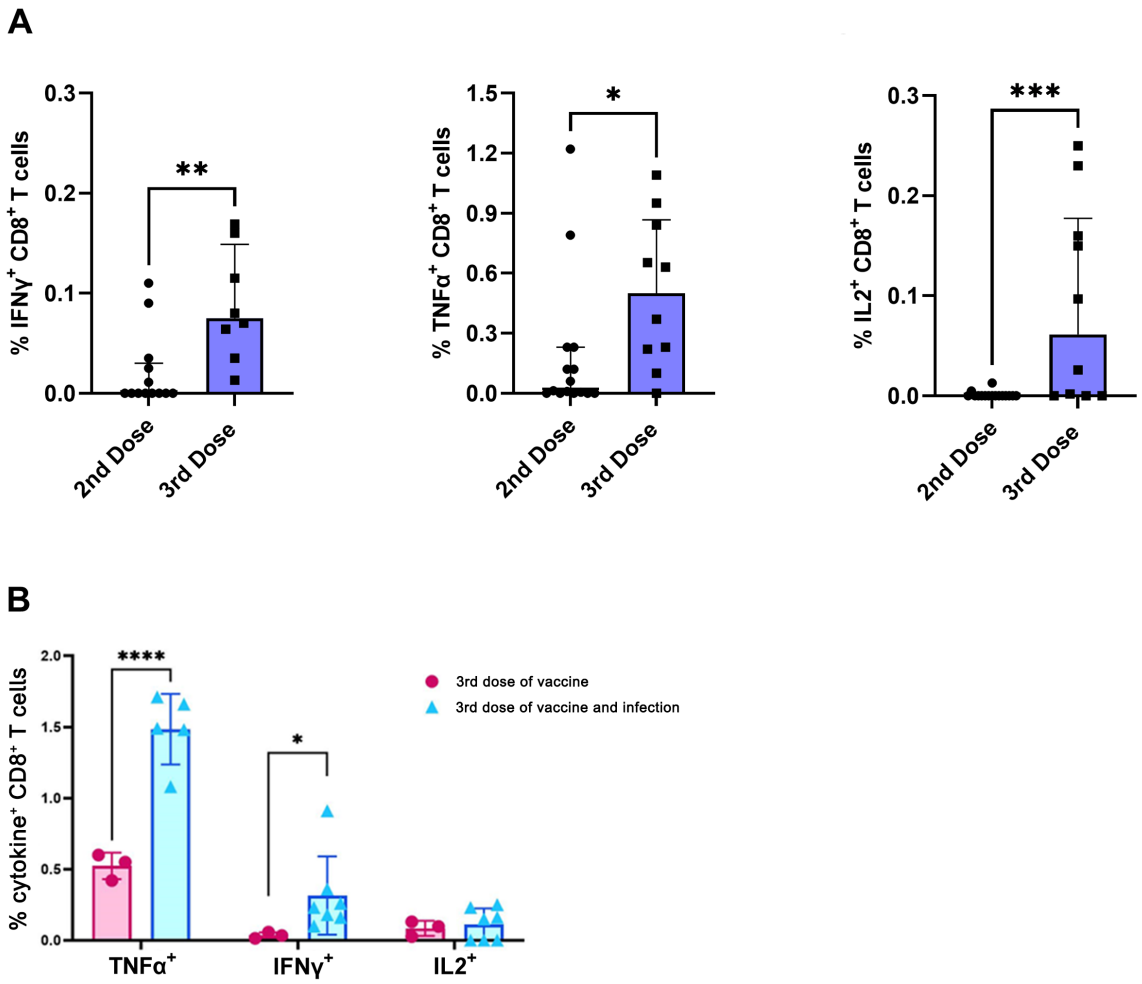


**Figure 8. Cytokine responses of $CD8^+$ T cells stimulated with peptide SP09, in vaccinated individuals, with or without subsequent infection.**

A) Frequency of IFN-γ, TNF-α, and IL-2 positive $CD8^+$ T cells after subtraction of the respective NC in 15 vaccinated subjects with two doses, and 10 with three doses. The graph represents the median and the error bars. The Mann-Whitney test was used to compare the values of the groups. *$p \leq 0.05$, ** $p \leq 0.01$, *** $p \leq 0.001$.

B) Comparison between healthy individuals vaccinated with three doses (n.=3) of the mRNA BNT162b2 vaccine without infection and individuals vaccinated with three vaccine doses who got infected with SARS-CoV-2 (n.=7). The Mann-Whitney test was used to compare the values of the groups *$p \leq 0.05$, ****$p \leq 0.0001$

# Chapter 5. Discussion

The advent of SARS-CoV-2 vaccines has significantly reduced the incidence of severe COVID-19 cases and reduced the mortality rate worldwide [132]. Despite this progress, a comprehensive understanding of the adaptive immune response, particularly the role of $CD8^+$ T cells, remains essential for optimising vaccine strategies and improving long-term protection. In this study, we identified a set of HLA-E–restricted epitopes derived from multiple SARS-CoV-2 proteins, including ORF1ab, Spike, ORF8a, and Nucleoprotein. These epitopes were selected based on their predicted binding affinity to HLA-E and their potential to elicit broad $CD8^+$ T cell responses, thereby expanding the scope of non-classical T cell-mediated immunity in SARS-CoV-2 infection.

We demonstrated the presence of HLA-E–restricted, peptide-specific $CD8^+$ T cells in PBMCs from convalescent individuals, hospitalised patients with severe COVID-19, and vaccinated donors. These findings align with previous studies describing classical HLA-Ia–restricted $CD8^+$ T cell responses in SARS-CoV-2 infection and vaccination [136,138,139,145]. Furthermore, using blocking monoclonal antibodies (mAbs) targeting TCR αβ and HLA-E molecules, we show that HLA-E/TCR recognition mediates the activation of HLA-E–restricted $CD8^+$ T cells upon stimulation with SARS-CoV-2 peptides. Previous research has highlighted the crucial role of classical $CD8^+$ T cell response in SARS-CoV-2 infection and post-vaccination immunity [136,138,146]. Although the number of patients tested was limited in our analysis, accumulating evidence from a few studies [76,146,147], in addition to our data, demonstrates that peptides derived from different components of SARS-CoV-2 protein antigens can induce HLA-E-restricted and peptide-specific $CD8^+$ T cell responses. Additionally, these peptides exhibit a high conservation rate, enabling them to retain their immunogenic potential across the most prevalent SARS-CoV-2 variants.

Interestingly, the characterization of SARS-CoV-2-specific $CD8^+$ T cells utilising a stimulation assay and flow cytometry revealed either an absence or a significant reduction of cytokine production (IFN-γ, TNF-α, and IL-2) upon stimulation with the pool of HLA-E-binding peptides during acute, severe, and critical COVID-19 disease among hospitalised patients.

Due to the low polymorphism of HLA-E molecules in the human population, exploring epitopes that bind to HLA-E could be incredibly valuable for developing universal vaccines

and/or immunotherapeutic. HLA-E–restricted T cells are detected in the blood in bacterial and viral infections [17,120,148].

$CD8^+$ T cells expressing HLA-E have been observed in viral infections, but their role in the immune response to SARS-CoV-2 remains underestimated. Yang et al. have recently reported HLA-E–restricted $CD8^+$ T cells in individuals recovering from SARS-CoV-2, which were at levels comparable to conventional HLA-Ia–restricted T cells. More importantly, they showed that, unlike classical HLA-class I molecules, HLA-E was not down-regulated by SARS-CoV-2 infection, and these HLA-E-restricted $CD8^+$ T cells were able to suppress SARS-CoV-2 infection in Calu-3 cells *in vitro* [76]. This suggests that SARS-CoV-2-specific HLA-E-restricted $CD8^+$ T cells could be beneficial when conventional T cell responses are compromised during SARS-CoV-2 infection. As presented in this study, HLA-E-restricted peptides can induce an even more potent response when compared to cells stimulated with other, non-HLA-E-binding peptides. Moreover, considering that the HLA-E-restricted $CD8^+$ T cell response is greater in convalescent patients and vaccinated subjects than in hospitalised patients with severe disease, we can hypothesise that the HLA-E response is associated with protection from the disease.

Our study also highlights robust immunity to the HLA-E-restricted Spike-derived peptide, as evidenced by the detection of $CD8^+$ T cell responses in the blood of donors following receipt of an mRNA vaccine booster. During the COVID-19 pandemic, vaccines have significantly reduced the link between SARS-CoV-2 infections and hospitalizations and deaths [149]. Despite the continuous evolution of viral variants and their ability to evade the antibody response to varying degrees [58], emerging evidence shows that T cells may play a protective role against COVID-19 [76,144,145]. Memory T cells induced by SARS-CoV-2 vaccines maintain the ability to recognize viral particles [150]. These classical $CD8^+$ T cells are detectable in 41-65% of individuals six months after the second dose, indicating sustained immunity [151]. Notably, Spike-specific classical $CD8^+$ T cell responses are observed in 70-90% of individuals weeks after a second dose mRNA COVID-19 vaccine regimen [150,152,153]. A study in Finnish healthcare workers (HCWs) vaccinated with three doses of COVID-19 mRNA vaccines showed that the levels of Spike-specific $CD8^+$ T cells remain relatively stable and are detected in 71% of HCWs [154]. Furthermore, there was a significant increase in SARS-CoV-2 spike-specific $CD4^+$ and $CD8^+$ T cell responses after the third vaccine dose [155]. These findings underscore the potential value of vaccines, explicitly highlighting the repeated boosting effect of vaccines on T cell immunity. Although non-classical HLA-

specific $CD8^+$ T cell responses in vaccinated individuals have been less explored, the peptides studied here are conserved across the most widespread SARS-CoV-2 variants; considering that HLA-E is also highly conserved, these peptides can also be promising candidates for vaccine formulations targeting T cell immunity.

In the current study, HLA-E-restricted $CD8^+$ T cells exhibit multiple cytokine production at 3-4 weeks post-third vaccine dose, hence retaining a broad memory function spectrum. Notably, there was a significant increase in SARS-CoV-2 spike-specific $CD8^+$ T cell responses after the third dose. The production of TNF-α among Spike-specific $CD8^+$ T cells linked to HLA-E-restricted peptides suggests a potential mechanism for enhanced antiviral responses. Moreover, patients with a good immune response have been observed to have durable protection from severe disease [156], indicating that long-term immunological memory could play a key role. We also assessed the frequencies and functional qualities of HLA-E-restricted SARS-CoV-2-specific $CD8^+$ T cells in donors with a history of SARS-CoV-2 infection after mRNA vaccination compared to those who had not been naturally infected. We found that natural infection additionally boosts the HLA-E-restricted Spike-specific $CD8^+$ T cell response in vaccinated subjects. Therefore, and similar to the classical T cell responses, HLA-E-restricted SARS-CoV-2 peptide-specific $CD8^+$ T cell responses are also well maintained over time, especially in those with an induced immunity due to the combination of vaccination and infection, and, as such, may contribute to sustained protection against severe disease.

In conclusion, we propose that HLA-E, given its ubiquity as an HLA allele locus, represents a promising target for developing peptide-based immunotherapeutics or vaccines. Vaccines focused on universally presented epitopes that induce HLA-E-restricted $CD8^+$ T cell responses could pave the way for more specific and effective vaccine strategies, offering broad protection across different populations and viral variants.

# Chapter 6. Conclusions

HLA-E serves a dual role at the intersection of innate and adaptive immunity. This non-classical MHC class I molecule exhibits remarkably low polymorphism and is relatively resistant to downregulation by viruses, such as SARS-CoV-2, thereby enhancing its appeal as a vaccine target in both infectious disease and oncology contexts. Robust $CD8^+$ T cell subsets restricted by HLA-E have been identified in infections such as SARS-CoV-2, CMV, HIV, EBV, HCV, and *M. tuberculosis*, often with significant antigen-specific expansion. Peptide-presenting capacity spans canonical leader peptides and pathogen or stress-derived noncanonical epitopes, potentially enabling a broad T cell response from limited peptide sets. Functional diversity includes cytotoxic, microbicidal, regulatory, and immunomodulatory activities; however, phenotypic exhaustion (e.g., in HIV/TB coinfection) may limit efficacy unless modulated. Key knowledge gaps persist regarding *in vivo* prevalence, functional biomarkers, and longitudinal contributions to immunity in natural infections and tumor control. Quantifying frequencies of HLA-E-restricted $CD8^+$ T cells across diverse pathogen models, although these unconventional T cells show diverse functions, ranging from cytotoxic activity and intracellular pathogen inhibition to immunosuppressive or regulatory roles, the frequency and *in vivo* relevance of HLA-E-restricted $CD8^+$ T cells in most infectious and tumor settings remain incompletely characterized. Therefore, future studies characterizing functional phenotypes-e.g. cytokine profiles, exhaustion markers, cytotoxic potential, in various clinical contexts are necessary. Finally, exploring vaccination strategies that leverage minimal peptide sets capable of inducing robust HLA-E-restricted T cell responses, potentially combining with checkpoint modulation (e.g., anti-PD-1) to reverse exhaustion.

# 7. References


[1] Peters B, Nielsen M, Sette A. T Cell Epitope Predictions. Annu Rev Immunol 2020;38:123–45. https://doi.org/10.1146/annurev-immunol-082119-124838.

[2] Wooldridge L, Ekeruche-Makinde J, van den Berg HA, Skowera A, Miles JJ, Tan MP, et al. A Single Autoimmune T Cell Receptor Recognizes More Than a Million Different Peptides. Journal of Biological Chemistry 2012;287:1168–77. https://doi.org/10.1074/jbc.M111.289488.

[3] Blum JS, Wearsch PA, Cresswell P. Pathways of Antigen Processing. Annu Rev Immunol 2013;31:443–73. https://doi.org/10.1146/annurev-immunol-032712-095910.

[4] Sauter J, Putke K, Schefzyk D, Pruschke J, Solloch UV, Bernas SN, et al. HLA-E typing of more than 2.5 million potential hematopoietic stem cell donors: Methods and population-specific allele frequencies. Hum Immunol 2021;82:541–7. https://doi.org/10.1016/j.humimm.2020.12.008.

[5] Paech C, Albrecht V, Putke K, Schöfl G, Schöne B, Schmidt AH, et al. <scp> *HLA-E* </scp> diversity unfolded: Identification and characterization of 170 novel <scp> *HLA-E* </scp> alleles. HLA 2021;97:389–98. https://doi.org/10.1111/tan.14195.

[6] Robinson J, Barker DJ, Georgiou X, Cooper MA, Flicek P, Marsh SGE. IPD-IMGT/HLA Database. Nucleic Acids Res 2019. https://doi.org/10.1093/nar/gkz950.

[7] Robinson J, Halliwell JA, Hayhurst JD, Flicek P, Parham P, Marsh SGE. The IPD and IMGT/HLA database: allele variant databases. Nucleic Acids Res 2015;43:D423–31. https://doi.org/10.1093/nar/gku1161.

[8] Immuno Polymorphism Database. Https://WwwEbiAcUk/Ipd/ 2025.

[9] Strong RK, Holmes MA, Li P, Braun L, Lee N, Geraghty DE. HLA-E Allelic Variants. Journal of Biological Chemistry 2003;278:5082–90. https://doi.org/10.1074/jbc.M208268200.

[10] Kanevskiy L, Erokhina S, Kobyzeva P, Streltsova M, Sapozhnikov A, Kovalenko E. Dimorphism of HLA-E and Its Disease Association. Int J Mol Sci 2019;20:5496. https://doi.org/10.3390/ijms20215496.

[11] Strong RK, Holmes MA, Li P, Braun L, Lee N, Geraghty DE. HLA-E Allelic Variants. Journal of Biological Chemistry 2003;278:5082–90. https://doi.org/10.1074/jbc.M208268200.

[12] Braud VM, Allan DSJ, O'Callaghan CA, Söderström K, D'Andrea A, Ogg GS, et al. HLA-E binds to natural killer cell receptors CD94/NKG2A, B and C. Nature 1998;391:795–9. https://doi.org/10.1038/35869.

[13] André P, Denis C, Soulas C, Bourbon-Caillet C, Lopez J, Arnoux T, et al. Anti-NKG2A mAb Is a Checkpoint Inhibitor that Promotes Anti-tumor Immunity by Unleashing Both

T and NK Cells. Cell 2018;175:1731-1743.e13. https://doi.org/10.1016/j.cell.2018.10.014.

[14] Sullivan LC, Nguyen THO, Harpur CM, Stankovic S, Kanagarajah AR, Koutsakos M, et al. Natural killer cell receptors regulate responses of HLA-E–restricted T cells. Sci Immunol 2021;6. https://doi.org/10.1126/sciimmunol.abe9057.

[15] Pump WC, Kraemer T, Huyton T, Hò G-GT, Blasczyk R, Bade-Doeding C. Between Innate and Adaptive Immune Responses: NKG2A, NKG2C, and CD8+ T Cell Recognition of HLA-E Restricted Self-Peptides Acquired in the Absence of HLA-Ia. Int J Mol Sci 2019;20:1454. https://doi.org/10.3390/ijms20061454.

[16] La Manna MP, Orlando V, Prezzemolo T, Di Carlo P, Cascio A, Delogu G, et al. HLA-E–restricted CD8 $^{+}$ T Lymphocytes Efficiently Control *Mycobacterium tuberculosis* and HIV-1 Coinfection. Am J Respir Cell Mol Biol 2020;62:430–9. https://doi.org/10.1165/rcmb.2019-0261OC.

[17] Caccamo N, Pietra G, Sullivan LC, Brooks AG, Prezzemolo T, La Manna MP, et al. Human CD8 T lymphocytes recognize *Mycobacterium tuberculosis* antigens presented by HLA-E during active tuberculosis and express type 2 cytokines. Eur J Immunol 2015;45:1069–81. https://doi.org/10.1002/eji.201445193.

[18] Mazzarino P, Pietra G, Vacca P, Falco M, Colau D, Coulie P, et al. Identification of effector-memory CMV-specific T lymphocytes that kill CMV-infected target cells in an HLA-E-restricted fashion. Eur J Immunol 2005;35:3240–7. https://doi.org/10.1002/eji.200535343.

[19] Sullivan LC, Walpole NG, Farenc C, Pietra G, Sum MJW, Clements CS, et al. A conserved energetic footprint underpins recognition of human leukocyte antigen-E by two distinct αβ T cell receptors. Journal of Biological Chemistry 2017;292:21149–58. https://doi.org/10.1074/jbc.M117.807719.

[20] Hansen SG, Wu HL, Burwitz BJ, Hughes CM, Hammond KB, Ventura AB, et al. Broadly targeted CD8 $^{+}$ T cell responses restricted by major histocompatibility complex E. Science (1979) 2016;351:714–20. https://doi.org/10.1126/science.aac9475.

[21] Malouli D, Hansen SG, Hancock MH, Hughes CM, Ford JC, Gilbride RM, et al. Cytomegaloviral determinants of CD8 $^{+}$ T cell programming and RhCMV/SIV vaccine efficacy. Sci Immunol 2021;6. https://doi.org/10.1126/sciimmunol.abg5413.

[22] Yang H, Rei M, Brackenridge S, Brenna E, Sun H, Abdulhaqq S, et al. HLA-E–restricted, Gag-specific CD8 $^{+}$ T cells can suppress HIV-1 infection, offering vaccine opportunities. Sci Immunol 2021;6. https://doi.org/10.1126/sciimmunol.abg1703.

[23] Bortolotti D, Gentili V, Rizzo S, Rotola A, Rizzo R. SARS-CoV-2 Spike 1 Protein Controls Natural Killer Cell Activation via the HLA-E/NKG2A Pathway. Cells 2020;9:1975. https://doi.org/10.3390/cells9091975.

[24] Maucourant C, Filipovic I, Ponzetta A, Aleman S, Cornillet M, Hertwig L, et al. Natural killer cell immunotypes related to COVID-19 disease severity. Sci Immunol 2020;5. https://doi.org/10.1126/sciimmunol.abd6832.

[25] Hammer Q, Dunst J, Christ W, Picarazzi F, Wendorff M, Momayyezi P, et al. SARS-CoV-2 Nsp13 encodes for an HLA-E-stabilizing peptide that abrogates inhibition of NKG2A-expressing NK cells. Cell Rep 2022;38:110503. https://doi.org/10.1016/j.celrep.2022.110503.

[26] Vietzen H, Zoufaly A, Traugott M, Aberle J, Aberle SW, Puchhammer-Stöckl E. Deletion of the NKG2C receptor encoding KLRC2 gene and HLA-E variants are risk factors for severe COVID-19. Genetics in Medicine 2021;23:963–7. https://doi.org/10.1038/s41436-020-01077-7.

[27] Hansen SG, Ford JC, Lewis MS, Ventura AB, Hughes CM, Coyne-Johnson L, et al. Profound early control of highly pathogenic SIV by an effector memory T-cell vaccine. Nature 2011;473:523–7. https://doi.org/10.1038/nature10003.

[28] Walters LC, McMichael AJ, Gillespie GM. Detailed and atypical HLA-E peptide binding motifs revealed by a novel peptide exchange binding assay. Eur J Immunol 2020;50:2075–91. https://doi.org/10.1002/eji.202048719.

[29] Walters LC, Harlos K, Brackenridge S, Rozbesky D, Barrett JR, Jain V, et al. Pathogen-derived HLA-E bound epitopes reveal broad primary anchor pocket tolerability and conformationally malleable peptide binding. Nat Commun 2018;9:3137. https://doi.org/10.1038/s41467-018-05459-z.

[30] Ruibal P, Franken KLMC, van Meijgaarden KE, van Loon JJF, van der Steen D, Heemskerk MHM, et al. Peptide Binding to HLA-E Molecules in Humans, Nonhuman Primates, and Mice Reveals Unique Binding Peptides but Remarkably Conserved Anchor Residues. The Journal of Immunology 2020;205:2861–72. https://doi.org/10.4049/jimmunol.2000810.

[31] Huisman BD, Guan N, Rückert T, Garner L, Singh NK, McMichael AJ, et al. High-throughput characterization of HLA-E-presented CD94/NKG2x ligands reveals peptides which modulate NK cell activation. Nat Commun 2023;14:4809. https://doi.org/10.1038/s41467-023-40220-1.

[32] Tomasec P, Braud VM, Rickards C, Powell MB, McSharry BP, Gadola S, et al. Surface Expression of HLA-E, an Inhibitor of Natural Killer Cells, Enhanced by Human Cytomegalovirus gpUL40. Science (1979) 2000;287:1031–3. https://doi.org/10.1126/science.287.5455.1031.

[33] Muntasell A, Vilches C, Angulo A, López-Botet M. Adaptive reconfiguration of the human NK-cell compartment in response to cytomegalovirus: A different perspective of the host-pathogen interaction. Eur J Immunol 2013;43:1133–41. https://doi.org/10.1002/eji.201243117.

[34] Zou H-M, Huang Z-F, Yang Y, Luo W-W, Wang S-Y, Luo M-H, et al. Human Cytomegalovirus Protein UL94 Targets MITA to Evade the Antiviral Immune Response. J Virol 2020;94. https://doi.org/10.1128/JVI.00022-20.

[35] Yuan Q, Fan Z, Huang W, Huo X, Yang X, Ran Y, et al. Human cytomegalovirus UL23 exploits PD-L1 inhibitory signaling pathway to evade T cell-mediated cytotoxicity. MBio 2024;15. https://doi.org/10.1128/mbio.01191-24.

[36] Heatley SL, Pietra G, Lin J, Widjaja JML, Harpur CM, Lester S, et al. Polymorphism in Human Cytomegalovirus UL40 Impacts on Recognition of Human Leukocyte Antigen-E (HLA-E) by Natural Killer Cells. Journal of Biological Chemistry 2013;288:8679–90. https://doi.org/10.1074/jbc.M112.409672.

[37] Hassan N, Eldershaw S, Stephens C, Kinsella F, Craddock C, Malladi R, et al. CMV reactivation initiates long-term expansion and differentiation of the NK cell repertoire. Front Immunol 2022;13. https://doi.org/10.3389/fimmu.2022.935949.

[38] Kobyzeva PA, Streltsova MA, Erokhina SA, Kanevskiy LM, Telford WG, Sapozhnikov AM, et al. CD56dimCD57−NKG2C+ NK cells retaining proliferative potential are possible precursors of CD57+NKG2C+ memory-like NK cells. J Leukoc Biol 2020;108:1379–95. https://doi.org/10.1002/JLB.1MA0720-654RR.

[39] Joosten SA, Sullivan LC, Ottenhoff THM. Characteristics of HLA-E Restricted T-Cell Responses and Their Role in Infectious Diseases. J Immunol Res 2016;2016:1–11. https://doi.org/10.1155/2016/2695396.

[40] Lin Z, Bashirova AA, Viard M, Garner L, Quastel M, Beiersdorfer M, et al. HLA class I signal peptide polymorphism determines the level of CD94/NKG2–HLA-E-mediated regulation of effector cell responses. Nat Immunol 2023;24:1087–97. https://doi.org/10.1038/s41590-023-01523-z.

[41] Fulkerson HL, Nogalski MT, Collins-McMillen D, Yurochko AD. Overview of Human Cytomegalovirus Pathogenesis, 2021, p. 1–18. https://doi.org/10.1007/978-1-0716-1111-1_1.

[42] García P, Llano M, Heredia AB de, Willberg CB, Caparrós E, Aparicio P, et al. Human T cell receptor-mediated recognition of HLA-E. Eur J Immunol 2002;32:936–44. https://doi.org/10.1002/1521-4141(200204)32:4<936::AID-IMMU936>3.0.CO;2-M.

[43] Romagnani C, Pietra G, Falco M, Mazzarino P, Moretta L, Mingari MC. HLA-E–restricted recognition of human cytomegalovirus by a subset of cytolytic T lymphocytes. Hum Immunol 2004;65:437–45. https://doi.org/10.1016/j.humimm.2004.02.001.

[44] Pietra G, Romagnani C, Mazzarino P, Falco M, Millo E, Moretta A, et al. HLA-E-restricted recognition of cytomegalovirus-derived peptides by human CD8 $^{+}$ cytolytic T lymphocytes. Proceedings of the National Academy of Sciences 2003;100:10896–901. https://doi.org/10.1073/pnas.1834449100.

[45] Hoare HL, Sullivan LC, Pietra G, Clements CS, Lee EJ, Ely LK, et al. Structural basis for a major histocompatibility complex class Ib–restricted T cell response. Nat Immunol 2006;7:256–64. https://doi.org/10.1038/ni1312.

[46] Tarragó D, González I, González-Escribano MF. HLA-E restricted cytomegalovirus UL40 peptide polymorphism may represent a risk factor following congenital infection. BMC Genomics 2022;23:455. https://doi.org/10.1186/s12864-022-08689-0.

[47] Martín Almazán N, Sala BM, Sandalova T, Sun Y, Resink T, Cichocki F, et al. Non-classical HLA-E restricted CMV 15-mer peptides are recognized by adaptive NK cells

and induce memory responses. Front Immunol 2023;14. https://doi.org/10.3389/fimmu.2023.1230718.

[48] Voogd L, Ruibal P, Ottenhoff THM, Joosten SA. Antigen presentation by MHC-E: a putative target for vaccination? Trends Immunol 2022;43:355–65. https://doi.org/10.1016/j.it.2022.03.002.

[49] Malouli D, Hansen SG, Hancock MH, Hughes CM, Ford JC, Gilbride RM, et al. Cytomegaloviral determinants of CD8 $^{+}$ T cell programming and RhCMV/SIV vaccine efficacy. Sci Immunol 2021;6. https://doi.org/10.1126/sciimmunol.abg5413.

[50] Smail SW, Saeed M, Twana alkasalias, Khudhur ZO, Younus DA, Rajab MF, et al. Inflammation, immunity and potential target therapy of SARS-COV-2: A total scale analysis review. Food and Chemical Toxicology 2021;150:112087. https://doi.org/10.1016/j.fct.2021.112087.

[51] Machhi J, Herskovitz J, Senan AM, Dutta D, Nath B, Oleynikov MD, et al. The Natural History, Pathobiology, and Clinical Manifestations of SARS-CoV-2 Infections. Journal of Neuroimmune Pharmacology 2020;15:359–86. https://doi.org/10.1007/s11481-020-09944-5.

[52] Wiersinga WJ, Rhodes A, Cheng AC, Peacock SJ, Prescott HC. Pathophysiology, Transmission, Diagnosis, and Treatment of Coronavirus Disease 2019 (COVID-19). JAMA 2020;324:782. https://doi.org/10.1001/jama.2020.12839.

[53] Jackson LA, Anderson EJ, Rouphael NG, Roberts PC, Makhene M, Coler RN, et al. An mRNA Vaccine against SARS-CoV-2 — Preliminary Report. New England Journal of Medicine 2020;383:1920–31. https://doi.org/10.1056/NEJMoa2022483.

[54] Tregoning JS, Flight KE, Higham SL, Wang Z, Pierce BF. Progress of the COVID-19 vaccine effort: viruses, vaccines and variants versus efficacy, effectiveness and escape. Nat Rev Immunol 2021;21:626–36. https://doi.org/10.1038/s41577-021-00592-1.

[55] Rodda LB, Netland J, Shehata L, Pruner KB, Morawski PA, Thouvenel CD, et al. Functional SARS-CoV-2-Specific Immune Memory Persists after Mild COVID-19. Cell 2021;184:169-183.e17. https://doi.org/10.1016/j.cell.2020.11.029.

[56] Dan JM, Mateus J, Kato Y, Hastie KM, Yu ED, Faliti CE, et al. Immunological memory to SARS-CoV-2 assessed for up to 8 months after infection. Science (1979) 2021;371. https://doi.org/10.1126/science.abf4063.

[57] Krause PR, Fleming TR, Longini IM, Peto R, Briand S, Heymann DL, et al. SARS-CoV-2 Variants and Vaccines. New England Journal of Medicine 2021;385:179–86. https://doi.org/10.1056/NEJMsr2105280.

[58] Harvey WT, Carabelli AM, Jackson B, Gupta RK, Thomson EC, Harrison EM, et al. SARS-CoV-2 variants, spike mutations and immune escape. Nat Rev Microbiol 2021;19:409–24. https://doi.org/10.1038/s41579-021-00573-0.

[59] Ao D, Lan T, He X, Liu J, Chen L, Baptista-Hon DT, et al. SARS-CoV-2 Omicron variant: Immune escape and vaccine development. MedComm (Beijing) 2022;3. https://doi.org/10.1002/mco2.126.

[60] Mlcochova P, Kemp SA, Dhar MS, Papa G, Meng B, Ferreira IATM, et al. SARS-CoV-2 B.1.617.2 Delta variant replication and immune evasion. Nature 2021;599:114–9. https://doi.org/10.1038/s41586-021-03944-y.

[61] Fan Y, Li X, Zhang L, Wan S, Zhang L, Zhou F. SARS-CoV-2 Omicron variant: recent progress and future perspectives. Signal Transduct Target Ther 2022;7:141. https://doi.org/10.1038/s41392-022-00997-x.

[62] Lee MJ, Leong MW, Rustagi A, Beck A, Zeng L, Holmes S, et al. SARS-CoV-2 escapes direct NK cell killing through Nsp1-mediated downregulation of ligands for NKG2D. Cell Rep 2022;41:111892. https://doi.org/10.1016/j.celrep.2022.111892.

[63] Brodin P. Immune determinants of COVID-19 disease presentation and severity. Nat Med 2021;27:28–33. https://doi.org/10.1038/s41591-020-01202-8.

[64] Ovsyannikova IG, Haralambieva IH, Crooke SN, Poland GA, Kennedy RB. The role of host genetics in the immune response to SARS-CoV-2 and COVID-19 susceptibility and severity. Immunol Rev 2020;296:205–19. https://doi.org/10.1111/imr.12897.

[65] Langton DJ, Bourke SC, Lie BA, Reiff G, Natu S, Darlay R, et al. The influence of HLA genotype on the severity of COVID-19 infection. HLA 2021;98:14–22. https://doi.org/10.1111/tan.14284.

[66] Aguiar VRC, Augusto DG, Castelli EC, Hollenbach JA, Meyer D, Nunes K, et al. An immunogenetic view of COVID-19. Genet Mol Biol 2021;44. https://doi.org/10.1590/1678-4685-gmb-2021-0036.

[67] Augusto DG, Hollenbach JA. HLA variation and antigen presentation in COVID-19 and SARS-CoV-2 infection. Curr Opin Immunol 2022;76:102178. https://doi.org/10.1016/j.coi.2022.102178.

[68] Anzurez A, Naka I, Miki S, Nakayama-Hosoya K, Isshiki M, Watanabe Y, et al. Association of *HLA- <scp>DRB1</scp> *09:01* with severe <scp>COVID</scp> -19. HLA 2021;98:37–42. https://doi.org/10.1111/tan.14256.

[69] Schindler E, Dribus M, Duffy BF, Hock K, Farnsworth CW, Gragert L, et al. <scp>HLA</scp> genetic polymorphism in patients with Coronavirus Disease 2019 in Midwestern United States. HLA 2021;98:370–9. https://doi.org/10.1111/tan.14387.

[70] Ebrahimi S, Ghasemi-Basir HR, Majzoobi MM, Rasouli-Saravani A, Hajilooi M, Solgi G. HLA-DRB1*04 may predict the severity of disease in a group of Iranian COVID-19 patients. Hum Immunol 2021;82:719–25. https://doi.org/10.1016/j.humimm.2021.07.004.

[71] Langton DJ, Bourke SC, Lie BA, Reiff G, Natu S, Darlay R, et al. The influence of HLA genotype on the severity of COVID-19 infection. HLA 2021;98:14–22. https://doi.org/10.1111/tan.14284.

[72] Weiner J, Suwalski P, Holtgrewe M, Rakitko A, Thibeault C, Müller M, et al. Increased risk of severe clinical course of COVID-19 in carriers of HLA-C*04:01. EClinicalMedicine 2021;40:101099. https://doi.org/10.1016/j.eclinm.2021.101099.

[73] Lee MJ, Blish CA. Defining the role of natural killer cells in COVID-19. Nat Immunol 2023;24:1628–38. https://doi.org/10.1038/s41590-023-01560-8.

[74] Bortolotti D, Gentili V, Rizzo S, Rotola A, Rizzo R. SARS-CoV-2 Spike 1 Protein Controls Natural Killer Cell Activation via the HLA-E/NKG2A Pathway. Cells 2020;9:1975. https://doi.org/10.3390/cells9091975.

[75] Hammer Q, Dunst J, Christ W, Picarazzi F, Wendorff M, Momayyezi P, et al. SARS-CoV-2 Nsp13 encodes for an HLA-E-stabilizing peptide that abrogates inhibition of NKG2A-expressing NK cells. Cell Rep 2022;38:110503. https://doi.org/10.1016/j.celrep.2022.110503.

[76] Yang H, Sun H, Brackenridge S, Zhuang X, Wing PAC, Quastel M, et al. HLA-E–restricted SARS-CoV-2–specific T cells from convalescent COVID-19 patients suppress virus replication despite HLA class Ia down-regulation. Sci Immunol 2023;8. https://doi.org/10.1126/sciimmunol.abl8881.

[77] Yuen M-F, Chen D-S, Dusheiko GM, Janssen HLA, Lau DTY, Locarnini SA, et al. Hepatitis B virus infection. Nat Rev Dis Primers 2018;4:18035. https://doi.org/10.1038/nrdp.2018.35.

[78] Wu J-F, Chang M-H. Natural history of chronic hepatitis B virus infection from infancy to adult life -the mechanism of inflammation triggering and long-term impacts. J Biomed Sci 2015;22:92. https://doi.org/10.1186/s12929-015-0199-y.

[79] Udompap P, Kim WR. Development of Hepatocellular Carcinoma in Patients With Suppressed Viral Replication: Changes in Risk Over Time. Clin Liver Dis (Hoboken) 2020;15:85–90. https://doi.org/10.1002/cld.904.

[80] WHO. Hepatitis B. https://www.who.int/news-room/fact-sheets/ detail/hepatitis-b 2024.

[81] Guidotti LG, Inverso D, Sironi L, Di Lucia P, Fioravanti J, Ganzer L, et al. Immunosurveillance of the Liver by Intravascular Effector CD8 + T Cells. Cell 2015;161:486–500. https://doi.org/10.1016/j.cell.2015.03.005.

[82] Bertoletti A, Ferrari C. Adaptive immunity in HBV infection. J Hepatol 2016;64:S71–83. https://doi.org/10.1016/j.jhep.2016.01.026.

[83] Fisicaro P, Barili V, Rossi M, Montali I, Vecchi A, Acerbi G, et al. Pathogenetic Mechanisms of T Cell Dysfunction in Chronic HBV Infection and Related Therapeutic Approaches. Front Immunol 2020;11. https://doi.org/10.3389/fimmu.2020.00849.

[84] Jeng W-J, Lok ASF. What will it take to cure hepatitis B? Hepatol Commun 2023;7. https://doi.org/10.1097/HC9.0000000000000084.

[85] Tan AT, Loggi E, Boni C, Chia A, Gehring AJ, Sastry KSR, et al. Host Ethnicity and Virus Genotype Shape the Hepatitis B Virus-Specific T-Cell Repertoire. J Virol 2008;82:10986–97. https://doi.org/10.1128/JVI.01124-08.

[86] Murugesan G, Paterson RL, Kulkarni R, Ilkow V, Suckling RJ, Connolly MM, et al. Viral sequence determines HLA-E-restricted T cell recognition of hepatitis B surface antigen. Nat Commun 2024;15:10126. https://doi.org/10.1038/s41467-024-54378-9.

[87] Sun Y, Yu H, Li F, Lan L, He D, Zhao H, et al. Identification of Hub Genes and Potential Molecular Mechanisms in Patients with HBV-Associated Acute Liver Failure. Evol Bioinform Online 2020;16:1176934320943901. https://doi.org/10.1177/1176934320943901.

[88] Laaribi AB, Mehri A, Chaouch H, Babay W, Jbir I, Ouzari H-I, et al. Association of HLA-Ib (HLA-G, HLA-E and HLA-F) with spontaneous HBV clearance. Infect Dis (Lond) 2025:1–11. https://doi.org/10.1080/23744235.2025.2487254.

[89] Saag MS, Gandhi RT, Hoy JF, Landovitz RJ, Thompson MA, Sax PE, et al. Antiretroviral Drugs for Treatment and Prevention of HIV Infection in Adults. JAMA 2020;324:1651. https://doi.org/10.1001/jama.2020.17025.

[90] van Schalkwyk C, Mahy M, Johnson LF, Imai-Eaton JW. Updated Data and Methods for the 2023 UNAIDS HIV Estimates. JAIDS Journal of Acquired Immune Deficiency Syndromes 2024;95:e1–4. https://doi.org/10.1097/QAI.0000000000003344.

[91] Xu Y, Abad M, Warren JA, Clutton G, Goonetilleke N. CD8+ T cell-mediated inhibition of HIV-1. The Journal of Immunology 2018;200:125.23-125.23. https://doi.org/10.4049/jimmunol.200.Supp.125.23.

[92] van Stigt Thans T, Akko JI, Niehrs A, Garcia-Beltran WF, Richert L, Stürzel CM, et al. Primary HIV-1 Strains Use Nef To Downmodulate HLA-E Surface Expression. J Virol 2019;93. https://doi.org/10.1128/JVI.00719-19.

[93] Wallace Z, Heunis T, Paterson RL, Suckling RJ, Grant T, Dembek M, et al. Instability of the HLA-E peptidome of HIV presents a major barrier to therapeutic targeting. Molecular Therapy 2024;32:678–88. https://doi.org/10.1016/j.ymthe.2024.01.010.

[94] Bansal A, Gehre MN, Qin K, Sterrett S, Ali A, Dang Y, et al. HLA-E–restricted HIV-1–specific CD8+ T cell responses in natural infection. Journal of Clinical Investigation 2021;131. https://doi.org/10.1172/JCI148979.

[95] Hannoun Z, Lin Z, Brackenridge S, Kuse N, Akahoshi T, Borthwick N, et al. Identification of novel HIV-1-derived HLA-E-binding peptides. Immunol Lett 2018;202:65–72. https://doi.org/10.1016/j.imlet.2018.08.005.

[96] Davis ZB, Cogswell A, Scott H, Mertsching A, Boucau J, Wambua D, et al. A Conserved HIV-1-Derived Peptide Presented by HLA-E Renders Infected T-cells Highly Susceptible to Attack by NKG2A/CD94-Bearing Natural Killer Cells. PLoS Pathog 2016;12:e1005421. https://doi.org/10.1371/journal.ppat.1005421.

[97] Nattermann J, Nischalke HD, Hofmeister V, Kupfer B, Ahlenstiel G, Feldmann G, et al. HIV-1 Infection Leads to Increased HLA-E Expression Resulting in Impaired Function of Natural Killer Cells. Antivir Ther 2005;10:95–107. https://doi.org/10.1177/135965350501000107.

[98] Jost S, Lucar O, Lee E, Yoder T, Kroll K, Sugawara S, et al. Antigen-specific memory NK cell responses against HIV and influenza use the NKG2/HLA-E axis. Sci Immunol 2023;8:eadi3974. https://doi.org/10.1126/sciimmunol.adi3974.

[99] Alrubayyi A, Hassan AS, Hare J, Hsieh A, Gilmour J, Price MA, et al. An early functional adaptive NK cell signature drives optimal CD8 $^{+}$ T-cell activation and

predicts sustained HIV-1 viral control 2025. https://doi.org/10.1101/2025.03.17.643703.

[100] Hammer Q, Rückert T, Romagnani C. Natural killer cell specificity for viral infections. Nat Immunol 2018;19:800–8. https://doi.org/10.1038/s41590-018-0163-6.

[101] Ugrinovic S, Brooks CG, Robson J, Blacklaws BA, Hormaeche CE, Robinson JH. H2-M3 Major Histocompatibility Complex Class Ib-Restricted CD8 T Cells Induced by *Salmonella enterica* Serovar Typhimurium Infection Recognize Proteins Released by *Salmonella* Serovar Typhimurium. Infect Immun 2005;73:8002–8. https://doi.org/10.1128/IAI.73.12.8002-8008.2005.

[102] Fresnay S, McArthur MA, Magder L, Darton TC, Jones C, Waddington CS, et al. Salmonella Typhi-specific multifunctional CD8+ T cells play a dominant role in protection from typhoid fever in humans. J Transl Med 2016;14:62. https://doi.org/10.1186/s12967-016-0819-7.

[103] Heinzel AS, Grotzke JE, Lines RA, Lewinsohn DA, McNabb AL, Streblow DN, et al. HLA-E–dependent Presentation of Mtb-derived Antigen to Human CD8+ T Cells. J Exp Med 2002;196:1473–81. https://doi.org/10.1084/jem.20020609.

[104] Rudolph ME, McArthur MA, Magder LS, Barnes RS, Chen WH, Sztein MB. Age-Associated Heterogeneity of Ty21a-Induced T Cell Responses to HLA-E Restricted Salmonella Typhi Antigen Presentation. Front Immunol 2019;10. https://doi.org/10.3389/fimmu.2019.00257.

[105] Salerno-Goncalves R, Wahid R, Sztein MB. *Ex Vivo* Kinetics of Early and Long-Term Multifunctional Human Leukocyte Antigen E-Specific CD8 $^{+}$ Cells in Volunteers Immunized with the Ty21a Typhoid Vaccine. Clinical and Vaccine Immunology 2010;17:1305–14. https://doi.org/10.1128/CVI.00234-10.

[106] Salerno-Gonçalves R, Fernandez-Viña M, Lewinsohn DM, Sztein MB. Identification of a Human HLA-E-Restricted CD8+ T Cell Subset in Volunteers Immunized with *Salmonella enterica* Serovar Typhi Strain Ty21a Typhoid Vaccine. The Journal of Immunology 2004;173:5852–62. https://doi.org/10.4049/jimmunol.173.9.5852.

[107] World Health Organization. Global tuberculosis report 2024. Https://WwwWhoInt/Publications/i/Item/9789240101531 2024.

[108] Ernst JD. Mechanisms of M. tuberculosis Immune Evasion as Challenges to TB Vaccine Design. Cell Host Microbe 2018;24:34–42. https://doi.org/10.1016/j.chom.2018.06.004.

[109] Grotzke JE, Harriff MJ, Siler AC, Nolt D, Delepine J, Lewinsohn DA, et al. The Mycobacterium tuberculosis Phagosome Is a HLA-I Processing Competent Organelle. PLoS Pathog 2009;5:e1000374. https://doi.org/10.1371/journal.ppat.1000374.

[110] Lewinsohn DM, Alderson MR, Briden AL, Riddell SR, Reed SG, Grabstein KH. Characterization of Human CD8+ T Cells Reactive with *Mycobacterium tuberculosis* –infected Antigen-presenting Cells. J Exp Med 1998;187:1633–40. https://doi.org/10.1084/jem.187.10.1633.

[111] Joosten SA, van Meijgaarden KE, van Weeren PC, Kazi F, Geluk A, Savage NDL, et al. Mycobacterium tuberculosis Peptides Presented by HLA-E Molecules Are Targets for Human CD8+ T-Cells with Cytotoxic as well as Regulatory Activity. PLoS Pathog 2010;6:e1000782. https://doi.org/10.1371/journal.ppat.1000782.

[112] Voogd L, van Wolfswinkel M, Satti I, White A, Dijkman K, Gela A, et al. Mtb-Specific HLA-E-Restricted T Cells Are Induced during Mtb Infection but Not after BCG Administration in Non-Human Primates and Humans. Vaccines (Basel) 2024;12:1129. https://doi.org/10.3390/vaccines12101129.

[113] van Meijgaarden KE, Haks MC, Caccamo N, Dieli F, Ottenhoff THM, Joosten SA. Human CD8+ T-cells Recognizing Peptides from Mycobacterium tuberculosis (Mtb) Presented by HLA-E Have an Unorthodox Th2-like, Multifunctional, Mtb Inhibitory Phenotype and Represent a Novel Human T-cell Subset. PLoS Pathog 2015;11:e1004671. https://doi.org/10.1371/journal.ppat.1004671.

[114] McMurtrey C, Harriff MJ, Swarbrick GM, Duncan A, Cansler M, Null M, et al. T cell recognition of Mycobacterium tuberculosis peptides presented by HLA-E derived from infected human cells. PLoS One 2017;12:e0188288. https://doi.org/10.1371/journal.pone.0188288.

[115] Harriff MJ, Wolfe LM, Swarbrick G, Null M, Cansler ME, Canfield ET, et al. HLA-E Presents Glycopeptides from the Mycobacterium tuberculosis Protein MPT32 to Human CD8+ T cells. Sci Rep 2017;7:4622. https://doi.org/10.1038/s41598-017-04894-0.

[116] Voogd L, Riou C, Scriba TJ, van Wolfswinkel M, van Meijgaarden KE, Franken KLMC, et al. HLA-E/Mtb specific CD4+ and CD8+ T cells have a memory phenotype in individuals with TB infection. Front Immunol 2024;15:1505329. https://doi.org/10.3389/fimmu.2024.1505329.

[117] Barber C, De Souza VA, Paterson RL, Martin-Urdiroz M, Mulakkal NC, Srikannathasan V, et al. Structure-guided stabilization of pathogen-derived peptide-HLA-E complexes using non-natural amino acids conserves native TCR recognition. Eur J Immunol 2022;52:618–32. https://doi.org/10.1002/eji.202149745.

[118] Nguyen AT, McSorley SJ. Fighting the enemy within: Systemic immune defense against mucosal Salmonella infection. Immunol Lett 2024;270:106930. https://doi.org/10.1016/j.imlet.2024.106930.

[119] Ruibal P, Franken KLMC, van Meijgaarden KE, van Wolfswinkel M, Derksen I, Scheeren FA, et al. Identification of HLA-E Binding *Mycobacterium tuberculosis* – Derived Epitopes through Improved Prediction Models. The Journal of Immunology 2022;209:1555–65. https://doi.org/10.4049/jimmunol.2200122.

[120] Badami GD, La Manna MP, Di Carlo P, Stanek O, Linhartova I, Caccamo N, et al. Delivery of Mycobacterium tuberculosis epitopes by Bordetella pertussis adenylate cyclase toxoid expands HLA-E-restricted cytotoxic CD8+ T cells. Front Immunol 2023;14. https://doi.org/10.3389/fimmu.2023.1289212.

[121] Paterson RL, La Manna MP, Arena De Souza V, Walker A, Gibbs-Howe D, Kulkarni R, et al. An HLA-E-targeted TCR bispecific molecule redirects T cell immunity against

Mycobacterium tuberculosis. Proceedings of the National Academy of Sciences 2024;121. https://doi.org/10.1073/pnas.2318003121.

[122] Verweij MC, Hansen SG, Iyer R, John N, Malouli D, Morrow D, et al. Modulation of MHC-E transport by viral decoy ligands is required for RhCMV/SIV vaccine efficacy. Science (1979) 2021;372. https://doi.org/10.1126/science.abe9233.

[123] Malouli D, Gilbride RM, Wu HL, Hwang JM, Maier N, Hughes CM, et al. Cytomegalovirus-vaccine-induced unconventional T cell priming and control of SIV replication is conserved between primate species. Cell Host Microbe 2022;30:1207-1218.e7. https://doi.org/10.1016/j.chom.2022.07.013.

[124] Picker LJ, Lifson JD, Gale M, Hansen SG, Früh K. Programming cytomegalovirus as an HIV vaccine. Trends Immunol 2023;44:287–304. https://doi.org/10.1016/j.it.2023.02.001.

[125] De Louche CD, Roghanian A. Human inhibitory leukocyte Ig-like receptors: from immunotolerance to immunotherapy. JCI Insight 2022;7. https://doi.org/10.1172/jci.insight.151553.

[126] Malouli D, Taher H, Mansouri M, Iyer RF, Reed J, Papen C, et al. Human cytomegalovirus UL18 prevents priming of MHC-E– and MHC-II–restricted CD8 $^{+}$ T cells. Sci Immunol 2024;9. https://doi.org/10.1126/sciimmunol.adp5216.

[127] Hansen SG, Hancock MH, Malouli D, Marshall EE, Hughes CM, Randall KT, et al. Myeloid cell tropism enables MHC-E-restricted CD8+ T cell priming and vaccine efficacy by the RhCMV/SIV vaccine. Sci Immunol 2022;7:eabn9301. https://doi.org/10.1126/sciimmunol.abn9301.

[128] Hansen SG, Schell JB, Marshall EE, Ojha S, Feltham S, Morrow D, et al. Glycoprotein L–deleted single-cycle rhesus cytomegalovirus vectors elicit MHC-E–restricted CD8+ T cells that protect against SIV. The Journal of Immunology 2025. https://doi.org/10.1093/jimmun/vkaf104.

[129] Coppola J, Parren M, Bastidas R, Saye K, Malvin J, Jardine JG, et al. Combining a rhesus cytomegalovirus/SIV vaccine with a neutralizing antibody to protect against SIV challenges in rhesus macaques. Front Microbiol 2025;16. https://doi.org/10.3389/fmicb.2025.1592647.

[130] Maldini CR, Coholan LJ, Karaca C. Hypoimmunogenic HLA-E Single Chain Inhibits Alloreactive Immune Responses. The Journal of Immunology 2024;213:1799–810. https://doi.org/10.4049/jimmunol.2400491.

[131] Fergusson JR, Wallace Z, Connolly MM, Woon AP, Suckling RJ, Hine DW, et al. Immune-Mobilizing Monoclonal T Cell Receptors Mediate Specific and Rapid Elimination of Hepatitis B–Infected Cells. Hepatology 2020;72:1528–40. https://doi.org/10.1002/hep.31503.

[132] Ciotti M, Ciccozzi M, Terrinoni A, Jiang W-C, Wang C-B, Bernardini S. The COVID-19 pandemic. Crit Rev Clin Lab Sci 2020;57:365–88. https://doi.org/10.1080/10408363.2020.1783198.

[133] Weingarten-Gabbay S, Klaeger S, Sarkizova S, Pearlman LR, Chen D-Y, Gallagher KME, et al. Profiling SARS-CoV-2 HLA-I peptidome reveals T cell epitopes from out-of-frame ORFs. Cell 2021;184:3962-3980.e17. https://doi.org/10.1016/j.cell.2021.05.046.

[134] Prather AA, Dutcher EG, Robinson J, Lin J, Blackburn E, Hecht FM, et al. Predictors of long-term neutralizing antibody titers following COVID-19 vaccination by three vaccine types: the BOOST study. Sci Rep 2023;13:6505. https://doi.org/10.1038/s41598-023-33320-x.

[135] da Silva Antunes R, Fajardo-Rosas V, Yu ED, Gálvez RI, Abawi A, Escarrega EA, et al. Evolution of SARS-CoV-2 T cell responses as a function of multiple COVID-19 boosters. Cell Rep 2025;44:115907. https://doi.org/10.1016/j.celrep.2025.115907.

[136] Cai C, Gao Y, Adamo S, Rivera-Ballesteros O, Hansson L, Österborg A, et al. SARS-CoV-2 vaccination enhances the effector qualities of spike-specific T cells induced by COVID-19. Sci Immunol 2023;8. https://doi.org/10.1126/sciimmunol.adh0687.

[137] Sette A, Sidney J, Crotty S. T Cell Responses to SARS-CoV-2. Annu Rev Immunol 2023;41:343–73. https://doi.org/10.1146/annurev-immunol-101721-061120.

[138] Kared H, Redd AD, Bloch EM, Bonny TS, Sumatoh H, Kairi F, et al. SARS-CoV-2–specific CD8+ T cell responses in convalescent COVID-19 individuals. Journal of Clinical Investigation 2021;131. https://doi.org/10.1172/JCI145476.

[139] Peng Y, Mentzer AJ, Liu G, Yao X, Yin Z, Dong D, et al. Broad and strong memory CD4+ and CD8+ T cells induced by SARS-CoV-2 in UK convalescent individuals following COVID-19. Nat Immunol 2020;21:1336–45. https://doi.org/10.1038/s41590-020-0782-6.

[140] Dobrijević Z, Gligorijević N, Šunderić M, Penezić A, Miljuš G, Tomić S, et al. The association of human leucocyte antigen (HLA) alleles with COVID-19 severity: A systematic review and meta-analysis. Rev Med Virol 2023;33. https://doi.org/10.1002/rmv.2378.

[141] Zhang Y, Chen Y, Li Y, Huang F, Luo B, Yuan Y, et al. The ORF8 protein of SARS-CoV-2 mediates immune evasion through down-regulating MHC-I. Proceedings of the National Academy of Sciences 2021;118. https://doi.org/10.1073/pnas.2024202118.

[142] La Manna MP, Orlando V, Li Donni P, Sireci G, Di Carlo P, Cascio A, et al. Identification of plasma biomarkers for discrimination between tuberculosis infection/disease and pulmonary non tuberculosis disease. PLoS One 2018;13:e0192664. https://doi.org/10.1371/journal.pone.0192664.

[143] Korber B, Fischer WM, Gnanakaran S, Yoon H, Theiler J, Abfalterer W, et al. Tracking Changes in SARS-CoV-2 Spike: Evidence that D614G Increases Infectivity of the COVID-19 Virus. Cell 2020;182:812-827.e19. https://doi.org/10.1016/j.cell.2020.06.043.

[144] Watson OJ, Barnsley G, Toor J, Hogan AB, Winskill P, Ghani AC. Global impact of the first year of COVID-19 vaccination: a mathematical modelling study. Lancet Infect Dis 2022;22:1293–302. https://doi.org/10.1016/S1473-3099(22)00320-6.

[145] Ferretti AP, Kula T, Wang Y, Nguyen DMV, Weinheimer A, Dunlap GS, et al. Unbiased Screens Show CD8+ T Cells of COVID-19 Patients Recognize Shared Epitopes in SARS-CoV-2 that Largely Reside outside the Spike Protein. Immunity 2020;53:1095-1107.e3. https://doi.org/10.1016/j.immuni.2020.10.006.

[146] Wang Y, Yang L, Tang K, Zhang Y, Zhang C, Zhang Y, et al. Ad5-nCoV Vaccination Could Induce HLA-E Restricted CD8+ T Cell Responses Specific for Epitopes on Severe Acute Respiratory Syndrome Coronavirus 2 Spike Protein. Viruses 2023;16:52. https://doi.org/10.3390/v16010052.

[147] Caccamo N, Sullivan LC, Brooks AG, Dieli F. Harnessing HLA-E-restricted CD8 T lymphocytes for adoptive cell therapy of patients with severe COVID-19. Br J Haematol 2020;190. https://doi.org/10.1111/bjh.16895.

[148] Prezzemolo T, van Meijgaarden KE, Franken KLMC, Caccamo N, Dieli F, Ottenhoff THM, et al. Detailed characterization of human *Mycobacterium tuberculosis* specific HLA-E restricted CD8 $^{+}$ T cells. Eur J Immunol 2018;48:293–305. https://doi.org/10.1002/eji.201747184.

[149] Moore SC, Kronsteiner B, Longet S, Adele S, Deeks AS, Liu C, et al. Evolution of long-term vaccine-induced and hybrid immunity in healthcare workers after different COVID-19 vaccine regimens. Med 2023;4:191-215.e9. https://doi.org/10.1016/j.medj.2023.02.004.

[150] Tarke A, Coelho CH, Zhang Z, Dan JM, Yu ED, Methot N, et al. SARS-CoV-2 vaccination induces immunological T cell memory able to cross-recognize variants from Alpha to Omicron. Cell 2022;185:847-859.e11. https://doi.org/10.1016/j.cell.2022.01.015.

[151] Goel RR, Painter MM, Apostolidis SA, Mathew D, Meng W, Rosenfeld AM, et al. mRNA vaccines induce durable immune memory to SARS-CoV-2 and variants of concern. Science (1979) 2021;374. https://doi.org/10.1126/science.abm0829.

[152] Guerrera G, Picozza M, D'Orso S, Placido R, Pirronello M, Verdiani A, et al. BNT162b2 vaccination induces durable SARS-CoV-2–specific T cells with a stem cell memory phenotype. Sci Immunol 2021;6. https://doi.org/10.1126/sciimmunol.abl5344.

[153] Zhang Z, Mateus J, Coelho CH, Dan JM, Moderbacher CR, Gálvez RI, et al. Humoral and cellular immune memory to four COVID-19 vaccines. Cell 2022;185:2434-2451.e17. https://doi.org/10.1016/j.cell.2022.05.022.

[154] Belik M, Liedes O, Vara S, Haveri A, Pöysti S, Kolehmainen P, et al. Persistent T cell-mediated immune responses against Omicron variants after the third COVID-19 mRNA vaccine dose. Front Immunol 2023;14. https://doi.org/10.3389/fimmu.2023.1099246.

[155] Juhl AK, Dietz LL, Søgaard OS, Reekie J, Nielsen H, Johansen IS, et al. Longitudinal Evaluation of Severe Acute Respiratory Syndrome Coronavirus 2 T-Cell Immunity Over 2 Years Following Vaccination and Infection. J Infect Dis 2024. https://doi.org/10.1093/infdis/jiae215.

[156] Bobrovitz N, Ware H, Ma X, Li Z, Hosseini R, Cao C, et al. Protective effectiveness of previous SARS-CoV-2 infection and hybrid immunity against the omicron variant and

severe disease: a systematic review and meta-regression. Lancet Infect Dis 2023;23:556–67. https://doi.org/10.1016/S1473-3099(22)00801-5.

# 8. Appendices

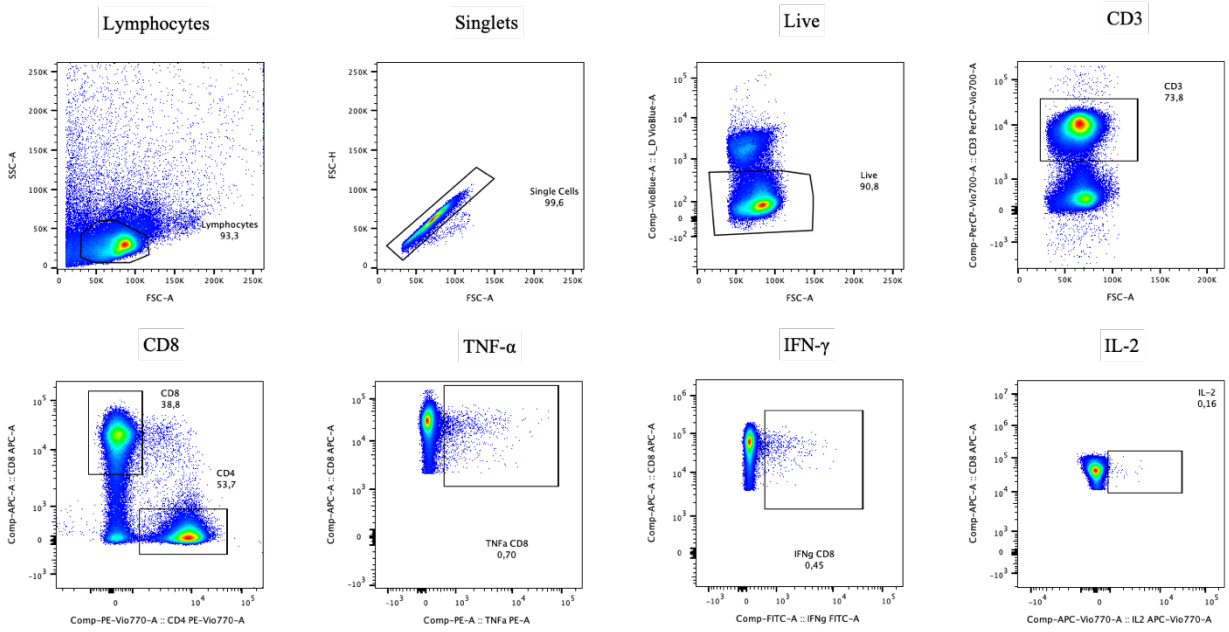


**Figure S1. Gating strategy for cytokine-producing CD8⁺ T cells.**

PBMCs were isolated from patients and vaccinated individuals, stimulated with designed peptides, and stained for surface and intracellular markers. Lymphocytes were first gated based on forward scatter (FSC) and side scatter (SSC) properties, followed by singlet selection to exclude doublets. Viable cells were identified using viability dye, and $CD3^+$ T cells were gated within this population. $CD8^+$ T cells were selected as $CD3^+CD8^+CD4^-$, and their cytokine expression (TNF-α, IFN-γ, IL-2) was analyzed.

**Data Sheet S1. Logo frequency by the position for Spike, Nucleocapsid, ORF8, and ORF1ab Proteins.**

**A. <u>Alpha (B.1.1.7), Beta (B.1.351), Gamma (P.1), Delta (B.1.617.2), and Omicron (B.1.1.529) variants.</u>**

SP09 / SPIKE

| | Percentage and raw count of non-gap | Non-gap/total (percentage) | Gap/total (percentage) |
|---|---|---|---|
| 320 | V: 87.54% (339285); X: 12.44% (48227); F: 0.01% (38); I: 0.00% (10); D: 0.00% (3); A: 0.00% (1); G: 0.00% (1); T: 0.00% (1) | 387566/387636 (99.98%) | 70/387636 (0.02%) |
| - | X: 100.00% (4) | 4/387636 (0.00%) | 387632/387636 (100.00%) |
| 321 | Q: 89.14% (345484); X: 10.84% (42015); L: 0.00% (19); P: 0.00% (14); E: 0.00% (8); K: 0.00% (7); H: 0.00% (5); R: 0.00% (2) | 387554/387636 (99.98%) | 82/387636 (0.02%) |
| - | X: 92.86% (13); W: 7.14% (1) | 14/387636 (0.00%) | 387622/387636 (100.00%) |
| - | X: 88.89% (8); L: 11.11% (1) | 9/387636 (0.00%) | 387627/387636 (100.00%) |
| 322 | P: 91.48% (354581); X: 8.49% (32917); S: 0.02% (83); L: 0.00% (2); T: 0.00% (2); A: 0.00% (1); R: 0.00% (1) | 387587/387636 (99.99%) | 49/387636 (0.01%) |
| - | X: 80.00% (4); K: 20.00% (1) | 5/387636 (0.00%) | 387631/387636 (100.00%) |
| 323 | T: 91.44% (354426); X: 8.25% (31993); I: 0.29% (1114); R: 0.01% (43); K: 0.00% (6); A: 0.00% (2); L: 0.00% (1) | 387585/387636 (99.99%) | 51/387636 (0.01%) |
| 324 | E: 91.73% (355519); X: 8.25% (31982); Q: 0.02% (64); G: 0.00% (6); D: 0.00% (5); A: 0.00% (4); K: 0.00% (4); V: 0.00% (1) | 387585/387636 (99.99%) | 51/387636 (0.01%) |
| 325 | S: 91.97% (356476); X: 8.02% (31083); F: 0.00% (11); Y: 0.00% (10); T: 0.00% (2); A: 0.00% (1); R: 0.00% (1) | 387584/387636 (99.99%) | 52/387636 (0.01%) |
| 326 | I: 92.26% (357611); X: 7.73% (29965); V: 0.00% (12); T: 0.00% (2); F: 0.00% (1); L: 0.00% (1) | 387592/387636 (99.99%) | 44/387636 (0.01%) |
| 327 | V: 92.07% (356863); X: 7.91% (30651); I: 0.02% (66); A: 0.00% (1); D: 0.00% (1); G: 0.00% (1) | 387583/387636 (99.99%) | 53/387636 (0.01%) |

| | | | |
|---|---|---|---|
| 328 | R: 97.58% (378235); X: 2.42% (9367); K: 0.00% (6); D: 0.00% (1); G: 0.00% (1); I: 0.00% (1); S: 0.00% (1); V: 0.00% (1) | 387613/387636 (99.99%) | 23/387636 (0.01%) |
| 329 | F: 97.45% (377741); X: 2.55% (9865); S: 0.00% (10); L: 0.00% (2); I: 0.00% (1); V: 0.00% (1) | 387620/387636 (100.00%) | 16/387636 (0.00%) |
| 330 | P: 97.48% (377869); X: 2.46% (9529); S: 0.05% (191); L: 0.01% (22); T: 0.00% (3); A: 0.00% (1); D: 0.00% (1); F: 0.00% (1); G: 0.00% (1); H: 0.00% (1) | 387619/387636 (100.00%) | 17/387636 (0.00%) |

NP02 / NUCLEOCAPSID

| | **Percentage and raw count of non-gap** | **Non-gap/total (percentage)** | **Gap/total (percentage)** |
|---|---|---|---|
| 149 | R: 99.51% (371997); X: 0.48% (1793); L: 0.01% (48); C: 0.00% (1)T: 0.00% (1) | 373840/373840 (100.00%) | 0/373840 (0.00%) |
| 150 | N: 99.52% (372043); X: 0.48% (1785); S: 0.00% (6); K: 0.00% (2); Y: 0.00% (2); G: 0.00% (1)T: 0.00% (1) | 373840/373840 (100.00%) | 0/373840 (0.00%) |
| 151 | P: 99.32% (371306); X: 0.44% (1627); L: 0.16% (614); S: 0.07% (273); H: 0.00% (18); A: 0.00% (1)T: 0.00% (1) | 373840/373840 (100.00%) | 0/373840 (0.00%) |
| 152 | A: 99.04% (370237); S: 0.51% (1905); X: 0.42% (1557); V: 0.03% (124); T: 0.00% (9); D: 0.00% (4); F: 0.00% (2); G: 0.00% (1)P: 0.00% (1) | 373840/373840 (100.00%) | 0/373840 (0.00%) |
| 153 | N: 99.64% (372495); X: 0.36% (1336); S: 0.00% (3); E: 0.00% (1); G: 0.00% (1); I: 0.00% (1); K: 0.00% (1); T: 0.00% (1)Y: 0.00% (1) | 373840/373840 (100.00%) | 0/373840 (0.00%) |
| 154 | N: 99.49% (371929); X: 0.36% (1333); D: 0.13% (486); S: 0.02% (73); Y: 0.00% (11); I: 0.00% (3); G: 0.00% (1) | 373836/373840 (100.00%) | 4/373840 (0.00%) |
| 155 | A: 99.52% (372060); X: 0.36% (1343); V: 0.06% (222); S: 0.05% (196); D: 0.00% (8); T: 0.00% (5); P: 0.00% (4); F: 0.00% (1)L: 0.00% (1) | 373840/373840 (100.00%) | 0/373840 (0.00%) |
| 156 | A: 99.47% (371856); X: 0.37% (1395); S: 0.15% (575); G: 0.00% (5); V: 0.00% (3); P: 0.00% (2); E: 0.00% (1); F: 0.00% (1); K: 0.00% (1) | 373839/373840 (100.00%) | 1/373840 (0.00%) |
| - | A: 50.00% (1); V: 50.00% (1) | 2/373840 (0.00%) | 373838/373840 (100.00%) |
| 157 | I: 99.51% (371997); X: 0.48% (1780); T: 0.01% (36); L: 0.01% (22); V: 0.00% (4) | 373839/373840 (100.00%) | 1/373840 (0.00%) |

| | | | |
|---|---|---|---|
| 158 | V: 99.55% (372141); X: 0.44% (1634); L: 0.02% (62); A: 0.00% (2)E: 0.00% (1) | 373840/373840 (100.00%) | 0/373840 (0.00%) |
| 159 | L: 99.59% (372312); X: 0.41% (1518); I: 0.00% (5); V: 0.00% (2); A: 0.00% (1); M: 0.00% (1)P: 0.00% (1) | 373840/373840 (100.00%) | 0/373840 (0.00%) |

PP02 / PROTEASE3C 3C-like_PROTEASE

| | **Percentage and raw count of non-gap** | **Non-gap/total (percentage)** | **Gap/total (percentage)** |
|---|---|---|---|
| 106 | I: 99.24% (377855); X: 0.76% (2879); V: 0.00% (7); F: 0.00% (2); M: 0.00% (2); *: 0.00% (1); D: 0.00% (1); H: 0.00% (1); T: 0.00% (1) | 380749/380754 (100.00%) | 5/380754 (0.00%) |
| 107 | Q: 99.35% (378284); X: 0.64% (2453); R: 0.00% (7); C: 0.00% (2); E: 0.00% (1); K: 0.00% (1); L: 0.00% (1) | 380749/380754 (100.00%) | 5/380754 (0.00%) |
| 108 | P: 98.93% (376683); X: 0.63% (2404); S: 0.35% (1335); L: 0.07% (263); R: 0.01% (38); T: 0.00% (13); Q: 0.00% (10); *: 0.00% (1); A: 0.00% (1); C: 0.00% (1); K: 0.00% (1) | 380750/380754 (100.00%) | 4/380754 (0.00%) |
| 109 | G: 99.39% (378410); X: 0.61% (2334); R: 0.00% (4); E: 0.00% (2); S: 0.00% (1) | 380751/380754 (100.00%) | 3/380754 (0.00%) |
| - | V: 50.00% (1); X: 50.00% (1) | 2/380754 (0.00%) | 380752/380754 (100.00%) |
| 110 | Q: 99.39% (378432); X: 0.61% (2306); H: 0.00% (7); *: 0.00% (2); L: 0.00% (2); Y: 0.00% (1) | 380750/380754 (100.00%) | 4/380754 (0.00%) |
| 111 | T: 99.61% (379281); X: 0.38% (1464); N: 0.00% (2); E: 0.00% (1); F: 0.00% (1); K: 0.00% (1) | 380750/380754 (100.00%) | 4/380754 (0.00%) |
| 112 | F: 99.67% (379491); X: 0.33% (1257); E: 0.00% (1); P: 0.00% (1) | 380750/380754 (100.00%) | 4/380754 (0.00%) |
| 113 | S: 99.69% (379571); X: 0.31% (1172); L: 0.00% (8); P: 0.00% (1) | 380752/380754 (100.00%) | 2/380754 (0.00%) |
| 114 | V: 99.65% (379401); X: 0.35% (1325); M: 0.00% (11); L: 0.00% (9); A: 0.00% (3); G: 0.00% (1); K: 0.00% (1) | 380751/380754 (100.00%) | 3/380754 (0.00%) |
| 115 | L: 99.64% (379371); X: 0.36% (1377); *: 0.00% (1); Q: 0.00% (1); S: 0.00% (1); V: 0.00% (1) | 380752/380754 (100.00%) | 2/380754 (0.00%) |

| | | | |
|---|---|---|---|
| 116 | A: 99.63% (379341); X: 0.35% (1342); V: 0.01% (53); S: 0.00% (6); P: 0.00% (3); T: 0.00% (2); D: 0.00% (1); I: 0.00% (1); Q: 0.00% (1) | 380750/380754 (100.00%) | 4/380754 (0.00%) |

PP06 / RDRP_RNA-dependent_RNA_polymerase

| | **Percentage and raw count of non-gap** | **Non-gap/total (percentage)** | **Gap/total (percentage)** |
|---|---|---|---|
| 565 | T: 97.33% (369681); X: 2.67% (10144); I: 0.00% (3); A: 0.00% (1); P: 0.00% (1) | 379830/379837 (100.00%) | 7/379837 (0.00%) |
| 566 | M: 97.21% (369223); X: 2.78% (10573); I: 0.01% (28); V: 0.00% (3); T: 0.00% (1) | 379828/379837 (100.00%) | 9/379837 (0.00%) |
| 567 | T: 97.23% (369307); X: 2.77% (10517); D: 0.00% (3); K: 0.00% (2) | 379829/379837 (100.00%) | 8/379837 (0.00%) |
| 568 | N: 97.26% (369434); X: 2.74% (10392); D: 0.00% (1); H: 0.00% (1) | 379828/379837 (100.00%) | 9/379837 (0.00%) |
| 569 | R: 97.28% (369491); X: 2.72% (10334); *: 0.00% (1); D: 0.00% (1); I: 0.00% (1); K: 0.00% (1) | 379829/379837 (100.00%) | 8/379837 (0.00%) |
| 570 | Q: 97.30% (369585); X: 2.69% (10236); H: 0.00% (5); R: 0.00% (2); L: 0.00% (1) | 379829/379837 (100.00%) | 8/379837 (0.00%) |
| 571 | F: 97.27% (369473); X: 2.73% (10351); V: 0.00% (2); L: 0.00% (1); S: 0.00% (1) | 379828/379837 (100.00%) | 9/379837 (0.00%) |
| 572 | H: 97.27% (369463); X: 2.72% (10348); Y: 0.00% (11); N: 0.00% (3); P: 0.00% (1); Q: 0.00% (1) | 379827/379837 (100.00%) | 10/379837 (0.00%) |
| 573 | Q: 97.32% (369644); X: 2.68% (10172); K: 0.00% (5); *: 0.00% (3); H: 0.00% (2); P: 0.00% (1) | 379827/379837 (100.00%) | 10/379837 (0.00%) |
| 574 | K: 97.36% (369812); X: 2.63% (10008); N: 0.00% (3); E: 0.00% (1); M: 0.00% (1); Q: 0.00% (1); R: 0.00% (1) | 379827/379837 (100.00%) | 10/379837 (0.00%) |
| - | K: 66.67% (2); X: 33.33% (1) | 3/379837 (0.00%) | 379834/379837 (100.00%) |
| 575 | L: 97.31% (369618); X: 2.69% (10204); F: 0.00% (3); I: 0.00% (1); S: 0.00% (1); T: 0.00% (1) | 379828/379837 (100.00%) | 9/379837 (0.00%) |

| | | | |
|---|---|---|---|
| 576 | L: 97.36% (369783); X: 2.64% (10024); F: 0.00% (13); *: 0.00% (2); G: 0.00% (2); M: 0.00% (2); W: 0.00% (1) | 379827/379837 (100.00%) | 10/379837 (0.00%) |

PP17 / EXONUCLEASE

| | **Percentage and raw count of non-gap** | **Non-gap/total (percentage)** | **Gap/total (percentage)** |
|---|---|---|---|
| 17 | G: 98.22% (374027); X: 1.76% (6711); P: 0.01% (22); R: 0.00% (12); W: 0.00% (8); Y: 0.00% (4); K: 0.00% (2); L: 0.00% (2); V: 0.00% (2); H: 0.00% (1); N: 0.00% (1); S: 0.00% (1); T: 0.00% (1) | 380794/380802 (100.00%) | 8/380802 (0.00%) |
| - | I: 66.67% (2); X: 33.33% (1) | 3/380802 (0.00%) | 380799/380802 (100.00%) |
| 18 | L: 98.23% (374056); X: 1.76% (6708); Y: 0.01% (23); E: 0.00% (4); V: 0.00% (2); A: 0.00% (1); C: 0.00% (1); D: 0.00% (1); F: 0.00% (1); N: 0.00% (1); W: 0.00% (1) | 380799/380802 (100.00%) | 3/380802 (0.00%) |
| - | *: 33.33% (1); K: 33.33% (1); T: 33.33% (1) | 3/380802 (0.00%) | 380799/380802 (100.00%) |
| 19 | H: 98.20% (373935); X: 1.79% (6830); N: 0.01% (26); C: 0.00% (2); K: 0.00% (2); Q: 0.00% (2); D: 0.00% (1); F: 0.00% (1); L: 0.00% (1); V: 0.00% (1) | 380801/380802 (100.00%) | 1/380802 (0.00%) |
| 20 | P: 98.19% (373918); X: 1.80% (6840); S: 0.01% (25); I: 0.00% (5); Y: 0.00% (4); F: 0.00% (2); N: 0.00% (2); D: 0.00% (1); H: 0.00% (1); R: 0.00% (1) | 380799/380802 (100.00%) | 3/380802 (0.00%) |
| - | K: 33.33% (1); S: 33.33% (1); X: 33.33% (1) | 3/380802 (0.00%) | 380799/380802 (100.00%) |
| 21 | T: 98.28% (374243); X: 1.71% (6514); L: 0.00% (4); R: 0.00% (4); A: 0.00% (3); M: 0.00% (3); I: 0.00% (2); E: 0.00% (1); H: 0.00% (1); S: 0.00% (1); V: 0.00% (1) | 380777/380802 (99.99%) | 25/380802 (0.01%) |
| - | K: 40.00% (2); L: 20.00% (1); N: 20.00% (1); X: 20.00% (1) | 5/380802 (0.00%) | 380797/380802 (100.00%) |
| 22 | Q: 98.17% (373836); X: 1.73% (6584); H: 0.09% (358); S: 0.00% (8); K: 0.00% (3); L: 0.00% (3); R: 0.00% (3); P: 0.00% (2); *: 0.00% (1); V: 0.00% (1) | 380799/380802 (100.00%) | 3/380802 (0.00%) |
| - | N: 95.65% (22); S: 4.35% (1) | 23/380802 (0.01%) | 380779/380802 (99.99%) |

| | | | |
|---|---|---|---|
| 23 | A: 98.30% (374338); X: 1.67% (6359); S: 0.02% (80); L: 0.00% (4); R: 0.00% (4); T: 0.00% (4); D: 0.00% (2); V: 0.00% (2); *: 0.00% (1); E: 0.00% (1); K: 0.00% (1); Q: 0.00% (1); Y: 0.00% (1) | 380798/380802 (100.00%) | 4/380802 (0.00%) |
| - | H: 100.00% (4) | 4/380802 (0.00%) | 380798/380802 (100.00%) |
| - | V: 100.00% (4) | 4/380802 (0.00%) | 380798/380802 (100.00%) |
| 24 | P: 98.35% (374499); X: 1.64% (6240); V: 0.01% (22); L: 0.00% (13); T: 0.00% (6); H: 0.00% (4); R: 0.00% (3); S: 0.00% (3); C: 0.00% (2); N: 0.00% (2); *: 0.00% (1); A: 0.00% (1); I: 0.00% (1) | 380797/380802 (100.00%) | 5/380802 (0.00%) |
| 25 | T: 98.32% (374416); X: 1.67% (6365); D: 0.00% (4); R: 0.00% (4); A: 0.00% (2); I: 0.00% (2); E: 0.00% (1); G: 0.00% (1); Q: 0.00% (1); S: 0.00% (1); V: 0.00% (1); Y: 0.00% (1) | 380799/380802 (100.00%) | 3/380802 (0.00%) |
| 26 | H: 98.13% (373657); X: 1.71% (6495); Y: 0.13% (503); Q: 0.02% (87); N: 0.01% (22); R: 0.00% (8); E: 0.00% (1); V: 0.00% (1) | 380774/380802 (99.99%) | 28/380802 (0.01%) |
| 27 | L: 98.27% (374216); X: 1.71% (6495); I: 0.01% (38); F: 0.01% (25); R: 0.00% (12); H: 0.00% (5); C: 0.00% (2); P: 0.00% (2); *: 0.00% (1); K: 0.00% (1); N: 0.00% (1); V: 0.00% (1); Y: 0.00% (1) | 380800/380802 (100.00%) | 2/380802 (0.00%) |
| 28 | S: 98.17% (373812); X: 1.77% (6730); I: 0.03% (104); G: 0.02% (94); C: 0.01% (28); K: 0.01% (22); N: 0.00% (2); Y: 0.00% (2); A: 0.00% (1); F: 0.00% (1); L: 0.00% (1); Q: 0.00% (1); R: 0.00% (1) | 380799/380802 (100.00%) | 3/380802 (0.00%) |
| - | Q: 100.00% (1) | 1/380802 (0.00%) | 380801/380802 (100.00%) |
| - | N: 100.00% (1) | 1/380802 (0.00%) | 380801/380802 (100.00%) |
| - | G: 80.00% (4); A: 20.00% (1) | 5/380802 (0.00%) | 380797/380802 (100.00%) |
| 29 | V: 98.23% (374028); X: 1.77% (6736); A: 0.00% (3); I: 0.00% (1); L: 0.00% (1); Q: 0.00% (1); R: 0.00% (1); T: 0.00% (1); W: 0.00% (1) | 380773/380802 (99.99%) | 29/380802 (0.01%) |
| 30 | D: 98.13% (373674); X: 1.87% (7102); E: 0.00% (6); V: 0.00% (4); G: 0.00% (3); M: 0.00% (2); N: 0.00% (2); A: 0.00% (1); L: 0.00% (1); P: 0.00% (1); Q: 0.00% (1); Y: 0.00% (1) | 380798/380802 (100.00%) | 4/380802 (0.00%) |

## B. JN.1 variant.

SP09 / SPIKE

| | Percentage and raw count of non-gap | Non-gap/total (percentage) | Gap/total (percentage) |
|---|---|---|---|
| 320 | V: 95.92% (87612); X: 4.07% (3719); F: 0.01% (5); I: 0.00% (3); L: 0.00% (1) | 91340/91343 (100.00%) | 3/91343 (0.00%) |
| 321 | Q: 96.00% (87683); X: 3.97% (3625); L: 0.02% (18); R: 0.01% (8); K: 0.00% (4); I: 0.00% (1); P: 0.00% (1) | 91340/91343 (100.00%) | 3/91343 (0.00%) |
| 322 | P: 96.11% (87786); X: 3.89% (3553); I: 0.00% (1); S: 0.00% (1) | 91341/91343 (100.00%) | 2/91343 (0.00%) |
| 323 | T: 95.98% (87667); X: 3.90% (3559); I: 0.12% (109); K: 0.01% (6); L: 0.00% (1) | 91342/91343 (100.00%) | 1/91343 (0.00%) |
| 324 | E: 96.08% (87761); X: 3.91% (3573); D: 0.00% (2); Q: 0.00% (2); A: 0.00% (1); I: 0.00% (1); V: 0.00% (1) | 91341/91343 (100.00%) | 2/91343 (0.00%) |
| 325 | S: 96.09% (87766); X: 3.91% (3574) | 91340/91343 (100.00%) | 3/91343 (0.00%) |
| 326 | I: 96.08% (87757); X: 3.92% (3578); V: 0.01% (5) | 91340/91343 (100.00%) | 3/91343 (0.00%) |
| 327 | V: 95.99% (87675); X: 4.01% (3664); F: 0.00% (1) | 91340/91343 (100.00%) | 3/91343 (0.00%) |
| 328 | R: 96.51% (88152); X: 3.49% (3188) | 91340/91343 (100.00%) | 3/91343 (0.00%) |
| 329 | F: 96.55% (88185); X: 3.44% (3146); C: 0.01% (5); L: 0.00% (3) | 91339/91343 (100.00%) | 4/91343 (0.00%) |
| 330 | P: 96.74% (88359); X: 3.25% (2973); S: 0.00% (4); L: 0.00% (3) | 91339/91343 (100.00%) | 4/91343 (0.00%) |

NP02 / NUCLEOCAPSID

| | Percentage and raw count of non-gap | Non-gap/total (percentage) | Gap/total (percentage) |
|---|---|---|---|
| 149 | R: 99.79% (90117)X: 0.21% (188) | 90305/90305 (100.00%) | 0/90305 (0.00%) |
| 150 | N: 99.79% (90116); X: 0.20% (185); I: 0.00% (3)K: 0.00% (1) | 90305/90305 (100.00%) | 0/90305 (0.00%) |
| 151 | P: 99.72% (90049); X: 0.20% (183); L: 0.04% (38); S: 0.03% (28)H: 0.01% (7) | 90305/90305 (100.00%) | 0/90305 (0.00%) |
| 152 | A: 99.73% (90063); X: 0.20% (184); V: 0.04% (32); T: 0.02% (14); S: 0.01% (10)D: 0.00% (2) | 90305/90305 (100.00%) | 0/90305 (0.00%) |
| 153 | N: 99.80% (90120)X: 0.20% (185) | 90305/90305 (100.00%) | 0/90305 (0.00%) |
| 154 | N: 99.78% (90105); X: 0.21% (188); S: 0.01% (7); Y: 0.00% (3); D: 0.00% (1)I: 0.00% (1) | 90305/90305 (100.00%) | 0/90305 (0.00%) |
| 155 | A: 99.70% (90032); X: 0.21% (188); V: 0.07% (61); S: 0.02% (19)T: 0.01% (5) | 90305/90305 (100.00%) | 0/90305 (0.00%) |
| 156 | A: 99.79% (90111); X: 0.21% (187)S: 0.01% (7) | 90305/90305 (100.00%) | 0/90305 (0.00%) |
| - | X: 100.00% (1) | 1/90305 (0.00%) | 90304/90305 (100.00%) |
| 157 | I: 99.78% (90104); X: 0.22% (195)T: 0.01% (6) | 90305/90305 (100.00%) | 0/90305 (0.00%) |
| 158 | V: 99.79% (90114)X: 0.21% (191) | 90305/90305 (100.00%) | 0/90305 (0.00%) |
| 159 | L: 99.78% (90109); X: 0.21% (192); V: 0.00% (2); E: 0.00% (1)I: 0.00% (1) | 90305/90305 (100.00%) | 0/90305 (0.00%) |

| 8A01 / ORF8 | | | |
|---|---|---|---|
| | **Percentage and raw count of non-gap** | **Non-gap/total (percentage)** | **Gap/total (percentage)** |
| 48 | R: 98.55% (89550); X: 1.43% (1302); K: 0.01% (11); L: 0.00% (4); S: 0.00% (2) | 90869/90878 (99.99%) | 9/90878 (0.01%) |
| - | S: 100.00% (2) | 2/90878 (0.00%) | 90876/90878 (100.00%) |
| 49 | V: 98.55% (89550); X: 1.44% (1309); I: 0.00% (4); L: 0.00% (3); F: 0.00% (1); S: 0.00% (1); T: 0.00% (1) | 90869/90878 (99.99%) | 9/90878 (0.01%) |
| 50 | G: 98.54% (89545); X: 1.43% (1303); E: 0.01% (6); R: 0.01% (6); *: 0.00% (4); V: 0.00% (2); C: 0.00% (1); H: 0.00% (1); L: 0.00% (1) | 90869/90878 (99.99%) | 9/90878 (0.01%) |
| - | T: 100.00% (1) | 1/90878 (0.00%) | 90877/90878 (100.00%) |
| - | *: 100.00% (1) | 1/90878 (0.00%) | 90877/90878 (100.00%) |
| - | T: 100.00% (1) | 1/90878 (0.00%) | 90877/90878 (100.00%) |
| 51 | A: 98.37% (89388); X: 1.51% (1370); V: 0.11% (97); D: 0.01% (5); S: 0.00% (3); T: 0.00% (3); C: 0.00% (1) | 90867/90878 (99.99%) | 11/90878 (0.01%) |
| - | F: 50.00% (1); X: 50.00% (1) | 2/90878 (0.00%) | 90876/90878 (100.00%) |
| 52 | R: 98.40% (89414); X: 1.55% (1411); I: 0.02% (22); *: 0.01% (7); S: 0.01% (6); K: 0.00% (4) | 90864/90878 (99.98%) | 14/90878 (0.02%) |
| - | X: 100.00% (1) | 1/90878 (0.00%) | 90877/90878 (100.00%) |
| - | R: 100.00% (1) | 1/90878 (0.00%) | 90877/90878 (100.00%) |
| 53 | K: 98.49% (89485); X: 1.51% (1369); *: 0.00% (4); I: 0.00% (2); M: 0.00% (1) | 90861/90878 (99.98%) | 17/90878 (0.02%) |

| | | | |
|---|---|---|---|
| 54 | S: 98.32% (89335); X: 1.50% (1359); L: 0.15% (133); P: 0.03% (29); T: 0.00% (4); *: 0.00% (2); R: 0.00% (1) | 90863/90878 (99.98%) | 15/90878 (0.02%) |
| 55 | A: 98.36% (89366); X: 1.53% (1388); V: 0.10% (92); T: 0.01% (8); S: 0.00% (3) | 90857/90878 (99.98%) | 21/90878 (0.02%) |
| 56 | P: 98.43% (89431); X: 1.51% (1372); S: 0.05% (43); L: 0.01% (5); H: 0.00% (4); K: 0.00% (1); T: 0.00% (1) | 90857/90878 (99.98%) | 21/90878 (0.02%) |
| 57 | L: 98.45% (89453); X: 1.54% (1395); S: 0.01% (12); F: 0.00% (2); R: 0.00% (1); T: 0.00% (1) | 90864/90878 (99.98%) | 14/90878 (0.02%) |
| 58 | I: 98.45% (89433); X: 1.53% (1391); T: 0.01% (10); F: 0.00% (4); M: 0.00% (2); *: 0.00% (1); P: 0.00% (1); S: 0.00% (1) | 90843/90878 (99.96%) | 35/90878 (0.04%) |

PP02 / PROTEASE3C 3C-like_PROTEASE

| | **Percentage and raw count of non-gap** | **Non-gap/total (percentage)** | **Gap/total (percentage)** |
|---|---|---|---|
| 106 | I: 98.36% (89262); X: 1.64% (1484); S: 0.00% (1); V: 0.00% (1); Y: 0.00% (1) | 90749/90750 (100.00%) | 1/90750 (0.00%) |
| 107 | Q: 99.22% (90038); X: 0.78% (710)R: 0.00% (2) | 90750/90750 (100.00%) | 0/90750 (0.00%) |
| 108 | P: 99.09% (89925); X: 0.74% (669); S: 0.17% (151); L: 0.00% (4)T: 0.00% (1) | 90750/90750 (100.00%) | 0/90750 (0.00%) |
| 109 | G: 99.28% (90098); X: 0.72% (649); M: 0.00% (1); P: 0.00% (1)R: 0.00% (1) | 90750/90750 (100.00%) | 0/90750 (0.00%) |
| 110 | Q: 99.31% (90123); X: 0.69% (626)V: 0.00% (1) | 90750/90750 (100.00%) | 0/90750 (0.00%) |
| 111 | T: 99.82% (90588); X: 0.18% (161)I: 0.00% (1) | 90750/90750 (100.00%) | 0/90750 (0.00%) |
| 112 | F: 99.84% (90607); X: 0.16% (141); L: 0.00% (1) | 90749/90750 (100.00%) | 1/90750 (0.00%) |
| 113 | S: 99.84% (90608); X: 0.16% (141)L: 0.00% (1) | 90750/90750 (100.00%) | 0/90750 (0.00%) |

| | | | |
|---|---|---|---|
| 114 | V: 99.84% (90609); X: 0.15% (139); I: 0.00% (1)L: 0.00% (1) | 90750/90750 (100.00%) | 0/90750 (0.00%) |
| 115 | L: 99.84% (90602); X: 0.16% (147)T: 0.00% (1) | 90750/90750 (100.00%) | 0/90750 (0.00%) |
| 116 | A: 99.84% (90602); X: 0.16% (142); V: 0.01% (5): 0.00% (1) | 90750/90750 (100.00%) | 0/90750 (0.00%) |

PP06 / RDRP_RNA-dependent_RNA_polymerase

| | **Percentage and raw count of non-gap** | **Non-gap/total (percentage)** | **Gap/total (percentage)** |
|---|---|---|---|
| 565 | T: 99.67% (90824)X: 0.33% (300) | 91124/91124 (100.00%) | 0/91124 (0.00%) |
| 566 | M: 99.68% (90831); X: 0.32% (292)I: 0.00% (1) | 91124/91124 (100.00%) | 0/91124 (0.00%) |
| 567 | T: 99.70% (90851)X: 0.30% (273) | 91124/91124 (100.00%) | 0/91124 (0.00%) |
| 568 | N: 99.70% (90847)X: 0.30% (277) | 91124/91124 (100.00%) | 0/91124 (0.00%) |
| 569 | R: 99.69% (90843)X: 0.31% (281) | 91124/91124 (100.00%) | 0/91124 (0.00%) |
| 570 | Q: 99.66% (90813); X: 0.34% (310)*: 0.00% (1) | 91124/91124 (100.00%) | 0/91124 (0.00%) |
| 571 | F: 99.65% (90808)X: 0.35% (316) | 91124/91124 (100.00%) | 0/91124 (0.00%) |
| 572 | H: 99.64% (90799); X: 0.36% (324)Y: 0.00% (1) | 91124/91124 (100.00%) | 0/91124 (0.00%) |
| 573 | Q: 99.62% (90781)X: 0.38% (343) | 91124/91124 (100.00%) | 0/91124 (0.00%) |
| 574 | K: 99.66% (90811); X: 0.34% (310); R: 0.00% (2)Q: 0.00% (1) | 91124/91124 (100.00%) | 0/91124 (0.00%) |

| | | | |
|---|---|---|---|
| - | K: 100.00% (1) | 1/91124 (0.00%) | 91123/91124 (100.00%) |
| 575 | L: 99.65% (90802)X: 0.35% (322) | 91124/91124 (100.00%) | 0/91124 (0.00%) |
| 576 | L: 99.65% (90802)X: 0.35% (322) | 91124/91124 (100.00%) | 0/91124 (0.00%) |

PP17 / EXONUCLEASE

| | **Percentage and raw count of non-gap** | **Non-gap/total (percentage)** | **Gap/total (percentage)** |
|---|---|---|---|
| 17 | G: 98.23% (90032); X: 1.76% (1611); W: 0.01% (7); R: 0.01% (6); E: 0.00% (1)P: 0.00% (1) | 91658/91658 (100.00%) | 0/91658 (0.00%) |
| 18 | L: 98.24% (90044); X: 1.76% (1611); S: 0.00% (2)Y: 0.00% (1) | 91658/91658 (100.00%) | 0/91658 (0.00%) |
| 19 | H: 98.25% (90051); X: 1.75% (1604); Y: 0.00% (2)N: 0.00% (1) | 91658/91658 (100.00%) | 0/91658 (0.00%) |
| 20 | P: 98.26% (90061); X: 1.74% (1593); R: 0.00% (2); H: 0.00% (1)S: 0.00% (1) | 91658/91658 (100.00%) | 0/91658 (0.00%) |
| 21 | T: 98.27% (90074); X: 1.72% (1579); A: 0.00% (1); I: 0.00% (1); K: 0.00% (1); S: 0.00% (1) | 91657/91658 (100.00%) | 1/91658 (0.00%) |
| 22 | Q: 98.23% (90037); X: 1.75% (1606); H: 0.02% (14)P: 0.00% (1) | 91658/91658 (100.00%) | 0/91658 (0.00%) |
| - | N: 100.00% (1) | 1/91658 (0.00%) | 91657/91658 (100.00%) |
| 23 | A: 98.22% (90026); X: 1.73% (1589); S: 0.04% (41); I: 0.00% (1)T: 0.00% (1) | 91658/91658 (100.00%) | 0/91658 (0.00%) |
| 24 | P: 98.26% (90059); X: 1.69% (1549); L: 0.03% (30); S: 0.01% (10); H: 0.01% (7); T: 0.00% (1); V: 0.00% (1)W: 0.00% (1) | 91658/91658 (100.00%) | 0/91658 (0.00%) |
| 25 | T: 98.28% (90086)X: 1.72% (1572) | 91658/91658 (100.00%) | 0/91658 (0.00%) |

| | | | |
|---|---|---|---|
| 26 | H: 98.20% (90003); X: 1.75% (1605); Y: 0.05% (46); N: 0.00% (2); L: 0.00% (1) | 91657/91658 (100.00%) | 1/91658 (0.00%) |
| 27 | L: 98.23% (90032); X: 1.77% (1618); F: 0.01% (5); I: 0.00% (2)H: 0.00% (1) | 91658/91658 (100.00%) | 0/91658 (0.00%) |
| 28 | S: 98.20% (90008); X: 1.79% (1641); G: 0.00% (2); I: 0.00% (2); N: 0.00% (2); C: 0.00% (1); K: 0.00% (1)L: 0.00% (1) | 91658/91658 (100.00%) | 0/91658 (0.00%) |
| 29 | V: 98.22% (90021); X: 1.78% (1632); A: 0.00% (4) | 91657/91658 (100.00%) | 1/91658 (0.00%) |
| 30 | D: 98.13% (89940); X: 1.86% (1706); E: 0.01% (6); Y: 0.00% (2); G: 0.00% (1); H: 0.00% (1); N: 0.00% (1) | 91657/91658 (100.00%) | 1/91658 (0.00%) |

**Table S1. Key resources table.**

| REAGENT OR RESOURCE | COMPANY | IDENTIFIER |
|---|---|---|
| **Commercial reagents used** | | |
| PepTivator®SARS-CoV-2 Prot_S Complete – research grade | Miltenyi Biotec | Cat# 130-127-951 |
| PepTivator®SARS-CoV-2 Prot_S+ – research grade | Miltenyi Biotec | Cat# 130-127-311 |
| PepTivator®SARS-CoV-2 Prot_S1 – research grade | Miltenyi Biotec | Cat# 130-127-041 |
| CytoStim (TM), Human | Miltenyi Biotec | Cat# 130-092-172 |
| eBioscience™ IC Fixation Buffer | eBioscience | Cat# 00-8222-49 |
| Intracellular Staining Permeabilization Wash Buffer (10X) | BioLegend | Cat# 421002 |
| TexMACS™ Medium | Miltenyi Biotec | Cat# 130-097-196 |
| RPMI | Euroclone | Cat# ECB9006L |
| Lympholyte®-H Cell Separation Media | CEDARLANE | Cat# CL5020 |
| Fetal bovine serum (FBS) | SIGMA life science | Cat# F9665 |
| Trypan Blue 0.5 % | Euroclone | Cat# ECM0990D |
| Turk's reagent | CARLO ERBA | Cat# 490451 |
| Dulbecco's Phosphate Buffered Saline (PBS) | Euroclone | Cat#ECB4004L |
| Penicillin-streptomycin solution 100x | Euroclone | Cat# ECB3001D |
| HEPES | Euroclone | Ca3# ECM0180D |
| Dimethyl sulfoxide | Merck KGaA | Cat# 472301 |
| **Deposited Data** | | |
| GISAID | | https://gisaid.org/ |
| NCBI Protein Database | | https://www.ncbi.nlm.nih.gov/protein/ |
| **Experimental Models: Cell Lines** | | |
| RMA-S/HLA-E | ATCC | Provided by J. E. Coligan, Laboratory of Immunogenetics, NIAID, Rockville, MD, USA |

| **Software and Equipments** | | |
|---|---|---|
| FlowJo® software v10.9 | BD Biosciences | https://www.flowjo.com/solutions/flowjo |
| GraphPad Prism 9 | GraphPad Software, Inc | https://www.graphpad.com/ |
| Los Alamos National Lab SARS-CoV-2 Analysis Pipeline: AnalyzeAlign | | https://cov.lanl.gov/content/sequence/ANALYZEALIGN/analyze_align.html |
| NetMHC4.0 | | https://www.iedb.org/ |
| Thermo Scientific™ Mr. Frosty™ Freezing Container | Thermo Scientific™ | Cat# 15-350-50 |
| VACUETTE® TUBE 3 ml heparin tubes | Greiner bio-one | Cat# 484511 |
| FACSLyric® flow cytometer | BD Biosciences | FACSLyric® flow cytometer |

**Table S2. List of commercial antibodies used for flow cytometry.**

| ANTIBODY | COMPANY | CATALOGUE NUMBER | RRID OR CLONE |
|---|---|---|---|
| Anti-human CD3-PerCP-Vio 700 | Miltenyi Biotec | 130-113-141 | REA613 |
| Anti-human CD8-APC | Miltenyi Biotec | 130-110-679 | REA734 |
| Anti-human CD4-PE- Vio 770 | Miltenyi Biotec | 130-113-227 | REA623 |
| Anti-human TNF-a -PE | Miltenyi Biotec | 130-118-974 | REA656 |
| Anti-human IFN-γ-FITC | Miltenyi Biotec | 130-113-497 | REA600 |
| Anti-human IL-2-APC Vio 770 | Miltenyi Biotec | 130-111-306 | REA689 |
| Viobility 405/452 Fixable Dye | Miltenyi Biotec | 130-130-403 | - |
| Anti-human TCR ab unconiugated | eBioscience | 14-9986-82 | IP26 |
| Anti-human HLA-E unconiugated | eBioscience | 14-9953-82 | 3D12HLA-E |
| Mouse IgG1 kappa Isotype Control | eBioscience | 14-4714-82 | P3.6.2.8.1 |
| Anti-human HLA-E-PE | Miltenyi Biotec | 130-117-401 | REA1031 |